

UC Berkeley

SEMM Reports Series

Title

Basic Mechanics Study for Computer Evaluation of Automobile Barrier Systems

Permalink

<https://escholarship.org/uc/item/0qn2671c>

Authors

Kelly, James

Tseng, Wen

El-Kasrawy, Tamim

Publication Date

1969-09-01

Report No. 69-10

Structures and Materials Research
Department of Civil Engineering
Division of Structural Engineering
and
Structural Mechanics

Basic Mechanics Study for
Computer Evaluation of Automobile
Barrier Systems

by

James M. Kelly
Associate Professor of Civil Engineering

Wen-Shou Tseng
Tamim El-Kasrawy
Graduate Students, Department of Civil Engineering

to

U.S. Department of Commerce
Bureau of Public Roads
Under Contract CPRL-6059

College of Engineering
University of California
Berkeley, California

September 1, 1969

TABLE OF CONTENTS

	Page
Abstract	iv
Acknowledgments	vii
1. INTRODUCTION	1
2. CONSTITUTIVE EQUATIONS OF DYNAMIC PLASTIC BEHAVIOR	3
2.1 Rate Independent Plastic Behavior	3
(i) Perfectly Plastic Materials	3
(ii) Work Hardening Plastic Equations	8
2.2 Rate Dependent Plastic Behavior	14
(i) Uniaxial Constitutive Equations	15
(ii) Multiaxial Constitutive Equations	22
(iii) Extension by use of hereditary integrals	25
2.3 Delayed Yield Phenomenon	29
3. IMPULSIVE LOADING ON STRUCTURAL SYSTEMS	33
3.1 Moving Mass Impact on Elastic Beams	33
3.2 Normal Impact of a Moving Mass on a Rigid Plastic System	37
(i) Basic Assumptions and Method of Solution	38
(ii) Numerical Examples	48
(iii) Notation for Section 3.2	52
(iv) Figures for Section 3.2	53
3.3 Oblique impact of a Moving Mass on a Rigid-Plastic System	57
(i) Analytical Approach	57
(ii) Numerical examples	68
(iii) Notation for Section 3.3	72
(iv) Figures for Section 3.3	74

	Page
3.4 Combined Loading in Rigid Perfectly Plastic Beams . . .	79
(i) Interaction Effects due to Shear and Axial Forces	79
(ii) Moving Mass Impact on a Rigid Perfectly Plastic Beam with Axial Force Interaction	88
(iii) Figures for Section 3.4	108
3.5 Influence of Delay Time on Mass Impact on Beams	113
4. IMPULSIVE LOADING ON RATE DEPENDENT STRUCTURAL SYSTEMS . . .	117
4.1 Combined Loading on Viscoplastic Beams	117
(i) The Generalized Constitutive Equation for the Pure Bending of Viscoplastic Beams	117
(ii) The Generalized Constitutive Equation for Combined Bending and Extension	124
(iii) The Dynamic Yield Surface for Combined Bending and Extension	135
(iv) Figures for Section 4.1	138
4.2 Direct Methods for the Study of Impulsive Loading on Elastic Viscoplastic Beams	145
(i) Transformation of the Uniaxial Constitutive Equation into an Incremental Form	145
(ii) Incremental Constitutive Equation for a Beam of Rectangular Section	151
(iii) Dynamic Equilibrium Equations for Beam Element in Incremental Form	155
(iv) Figure for Section 4.2	170
4.3 Numerical Examples of Impulsive Loading Problems in Elastic Viscoplastic Beams	171
(i) Figures for Section 4.3	175
5. CONCLUDING REMARKS, AREA OF FURTHER STUDY	182
6. BIBLIOGRAPHY	183

ABSTRACT

This report presents a summary of some of the results of the basic mechanics study performed in conjunction with the development of a general computer program for the analysis of highway protective systems. In the course of these studies several areas of interest were identified and efforts were made to obtain results in some depth in these areas.

It was found that theories and methods of solution using plasticity to represent material and structural behavior were not readily available. Much of the work on the subject related to particular types of dynamic material testing and has been found to be relevant to the present problem, providing that it be reinterpreted from the point of view of design for dynamic and impulsive loading. Furthermore methods for the inclusion of rate effects have, in the past, used only the idea of an arbitrarily increased yield point in a bilinear material model. These results indicate that it would be useful to collect a reinterpretation of much of the existing published research in dynamic plasticity from the point of view of design for impulsive loading.

The report begins with a study of uniaxial and multiaxial constitutive equations for strain rate insensitive and strain rate sensitive plastic materials developed in this way. The constitutive theories for dynamic plastic behavior which are included have been developed in a way which allows their incorporation into any numerical solution technique using an incremental method for integration in the time domain. In addition there has been an attempt to include the delayed yield phenomenon, a characteristic of the dynamic loading of mild steel, into a design problem for dynamic loadings.

In the third chapter of the report a series of solutions for rate independent systems are presented. The first deals with the response of a laterally supported beam subjected to normal impact by a moving object. The problem may be considered to be a model of the collision of an automobile with a highway impact protective system. The problem is idealized by assuming the beam to be rigid perfectly plastic and carried on a rigid perfectly plastic support. The impacting object is also taken to be rigid perfectly plastic in that it can sustain only a limited force in contact with the barrier. Closed form solutions are found for a number of specific examples, and estimates of the vehicle damage are given.

The second is concerned with the oblique impact of a moving deformable mass on a beam laterally supported by some kind of energy absorbing material. As before the problem is idealized by assuming the beam to be rigid perfectly plastic and backed by a rigid-perfectly plastic support material, and the impacting mass is taken as rigid-perfectly plastic in that it can sustain only a limited force in contact with barrier. The solution includes the determination of the contact force between mass and barrier and includes variable mass velocity parallel to the barrier and also includes convective terms which arise out of the rate of change of slope of the beam at the point of contact of beam and mass. Inclusion of this term allows the determination of the speed and the angle of the vehicle as it leaves the deformed barrier. Closed form solutions are no longer possible for this problem but a fairly simple numerical integration procedure is developed and solutions for particular examples are obtained.

The question of how this has to be modified when the effect of axial forces on the yield condition is included is then taken up and an approach to this case is developed.

In the fourth chapter a general method of finding the dynamic plastic response of some structural elements of rate sensitive materials under impulsive loading is developed.

The uniaxial constitutive equation is extended to a beam element in terms of generalized forces, generalized deformations and generalized rates. Also a dynamic yield surface which changes with rate was established.

A finite element approach is used to form dynamic equilibrium equations of general beam. The differential constitutive equation was transformed into an incremental one. The solution was carried out in a step by step numerical integration. A computer program was developed for this purpose and some problems involving cantilever beams were solved.

Acknowledgment

This investigation was sponsored by the U.S. Department of Transportation, Bureau of Public Roads, under Contract No. CPRL1-6059. The opinions, findings and conclusions expressed in this report are those of the authors and not necessarily those of the Bureau of Public Roads.

1. INTRODUCTION

This report presents a summary of some of the results of the basic mechanics study performed in conjunction with the development of a general computer program for the analysis of highway protective systems. In the course of these studies several areas of interest were identified and efforts were made to obtain results of some depth in these areas.

During this study it was found that with respect to elastic and bilinear theories of behavior the essential features of the appropriate theories and the techniques needed for the solution of impact problems were well understood. On the other hand, it was found that corresponding theories and methods of solution using plasticity to represent material and structural behavior were not so readily available. There has been, however, an extensive amount of work on the subject related to particular forms of dynamic material testing and much of this work has been found to be relevant to the present problem, providing that it be interpreted from the point of view of design for dynamic and impulsive loading. For example, there has been no systematic attempt to include the delayed yield phenomenon, which is a characteristic of the dynamic loading of mild steel, into a design problem for dynamic loadings. An approach in this direction has been worked out in the basic mechanics study under this contract. Further methods for the inclusion of rate effects have, in the past, used only the idea of an arbitrarily increased yield point in a bilinear material model. These results indicate that it would be useful to collect the results of the present study and a reinterpretation of much of the existing published research in dynamic plasticity, from the point of view of design for impulsive loading, in the form of a summary report to the Bureau; and hence this constitutes the second part of the present final report.

Much of the work reported here, in particular the solutions obtained for moving mass impact on laterally backed beams and the approach for rate sensitive structures, is original to this study. On the other hand, some of the material presented here has appeared in other contexts but has been reinterpreted from the point of view of its application to structural impact problems. For example, the constitutive theories for dynamic plastic behavior which are included have been developed in a way which allows their incorporation into any numerical solution technique using an incremental method for integration in the time domain.

2. CONSTITUTIVE EQUATIONS OF DYNAMIC PLASTIC BEHAVIOR

2.1 Rate Independent Plastic Behavior

The classical theory of plasticity as developed, for example, in the text books by Hill [2.1] or Prager and Hodge [2.2] is a theory which does not admit the influence of rate effects by virtue of the fact that the constitutive equations are homogeneous in time. The classical theory extends to multiaxial states of stress the main features of plastic behavior which are characterized by the uniaxial stress strain curve of a material, usually expressed in the simple form:

$$\sigma = f(\varepsilon)$$

where σ represents either an engineering stress or a true stress and ε some suitable measure of the strain. Included with this is the notion of irreversibility, in that unloading occurs elastically, leaving a permanent plastic deformation.

The generalization to multiaxial states of stress leads to systems of equations which are well known; and in giving them here, the purpose is to present them in a form particularly suitable for incorporation into numerical solutions of structural problems. These resulting equations take significantly different forms when the material is assumed to be perfectly plastic and when it is assumed to work harden, and it is useful to consider these separately.

(i) Perfectly Plastic Materials

In what follows we denote the stress tensor by σ_{ij} , and the total infinitesimal strain tensor by ε_{ij} , and assume that it can be divided into an elastic part ε_{ij}^e , and a plastic part ε_{ij}^p . For yield to occur and continue in a perfectly plastic material, it is necessary that

the stresses satisfy a yield condition of the form:

$$f(\sigma_{ij}) = 0 \quad (2.1.1)$$

When $f < 0$ the behavior is elastic and $f > 0$ is not possible. The flow rule, which, as a consequence of the principle of maximum plastic work enunciated by Drucker [2.3], identifies the potential of the plastic strain rates with the yield function f , leads to the equation:

$$\dot{\epsilon}_{ij}^p = \lambda \partial f / \partial \sigma_{ij} \quad (2.1.2)$$

where λ is a positive factor of proportionality. The elastic part of the strain rate may be obtained by assuming that the instantaneous elastic compliances μ_{ijkl} are independent of the plastic strain, thus:

$$\dot{\epsilon}_{ij}^e = \mu_{ijkl} \dot{\sigma}_{kl}$$

Eliminating λ from this equation by contracting with σ_{ij} , leads to:

$$\dot{\epsilon}_{ij} = \mu_{ijkl} \dot{\sigma}_{ij} + \frac{\sigma_{pq} \dot{\epsilon}_{pq} - \mu_{pqrs} \dot{\sigma}_{pq} \sigma_{rs}}{nf} \partial f / \partial \sigma_{ij} \quad (2.1.3)$$

where it has been assumed that $f(\sigma_{ij})$ is homogeneous of order n .

This may be written in a form particularly suitable for incorporation into incremental numerical approaches, as follows:

$$\left(\delta_{pi} \delta_{qj} - \frac{\sigma_{pq}}{nf} \right) \dot{\epsilon}_{pq} = \left(\mu_{ijpq} - \frac{\partial f}{\partial \sigma_{ij}} \frac{\mu_{pqrs} \sigma_{rs}}{nf} \right) \dot{\sigma}_{pq} \quad (2.1.4)$$

where δ_{ij} is the Kronecker delta.

Taking the 6 independent components of ϵ_{ij} as a vector $\underline{\underline{E}}$ and the components of σ_{ij} as a vector $\underline{\underline{S}}$ these equations take the matrix form:

$$\underline{\underline{A}}(\underline{\underline{S}}) \underline{\underline{E}} = (\underline{\underline{M}} + \underline{\underline{B}}(\underline{\underline{S}})) \dot{\underline{\underline{S}}} \quad (2.1.5)$$

where \underline{A} and \underline{B} are matrices dependent on the instantaneous stress state and \underline{M} is a constant matrix.

For an isotropic material, in the case where the yield function does not depend on the pressure and the plastic strains are equivoluminal, certain simplifications result. When the Mises yield condition is used, the stress strain relations reduce to the Prandtl-Reuss equations:

$$\dot{e}_{ij} = \dot{s}_{ij}/2G + \lambda s_{ij}, \quad \dot{\epsilon}_{kk} = \dot{\sigma}_{kk}/3K \quad (2.1.6)$$

where G is the shear modulus and K the bulk modulus of the material, and

$$e_{ij} = \epsilon_{ij} - \epsilon_{kk}/3 \delta_{ij} \quad (2.1.7)$$

and

$$s_{ij} = \sigma_{ij} - \sigma_{kk}/3 \delta_{ij} \quad (2.1.8)$$

are the strain and stress deviation tensors. The factor λ in this case becomes:

$$\lambda = s_{ij} \dot{e}_{ij} / 2k^2$$

and the matrix form of equations reduces to:

$$2G(\underline{I} - \underline{B}(\underline{S}))\underline{\dot{E}} = \underline{\dot{S}} \quad (2.1.9)$$

To illustrate the convenience of this type of representation for incremental methods of solution we may consider the propagation of elastic plastic waves of combined stress. The simplest problem of this kind involves the propagation of combined shear waves in a half space. Taking the half space to be $\dot{x}_3 \geq 0$ these waves may be generated by impulsive

shear loadings t_1 and t_2 in directions x_1, x_2 independent of x_1, x_2 , on $x_3 = 0$. For this problem, the equations of motion for small displacements, namely:

$$\sigma_{ij,j} = \rho v_{i,t}$$

where ρ is the density of the material and v_i the velocity vector, take the form:

$$\partial \sigma_{13} / \partial x_3 = \rho \partial v_1 / \partial t, \quad \partial \sigma_{23} / \partial x_3 = \rho \partial v_2 / \partial t$$

and the strain displacement relations for infinitesimal theory reduce to:

$$\partial \epsilon_{13} / \partial t = 1/2 \partial v_1 / \partial x_3$$

$$\partial \epsilon_{23} / \partial t = 1/2 \partial v_2 / \partial x_3$$

The constitutive equation (2.1.9) takes the form:

$$\begin{bmatrix} 1 - \sigma_{13}^2/k^2, & -\sigma_{23}\sigma_{13}/k^2 \\ -\sigma_{23}\sigma_{13}/k^2, & 1 - \sigma_{23}^2/k^2 \end{bmatrix} \begin{Bmatrix} \dot{\epsilon}_{13} \\ \dot{\epsilon}_{23} \end{Bmatrix} = \frac{1}{2G} \begin{Bmatrix} \dot{\sigma}_{13} \\ \dot{\sigma}_{23} \end{Bmatrix} \quad (2.1.10)$$

and the complete formulation of the problem is:

$$\underline{\underline{C}} \underline{\underline{W}},_t + \underline{\underline{D}} \underline{\underline{W}},_x = 0$$

where x indicates x_3 , $\underline{\underline{W}}$ is the vector

$$\underline{\underline{W}} = \begin{Bmatrix} v_1 \\ \sigma_{13} \\ v_2 \\ \sigma_{23} \end{Bmatrix}$$

and \underline{C} and \underline{D} are the symmetric matrices given by:

$$\underline{C} = \begin{bmatrix} 0, & -1, & 0, & 0 \\ -1, & 0, & 0, & 0 \\ 0, & 0, & 0, & -1 \\ 0, & 0, & -1, & 0 \end{bmatrix}$$

and

$$\underline{D} = \begin{bmatrix} G(1 - \sigma_{13}^2/k^2), & 0, & -G\sigma_{23}\sigma_{13}/k^2, & 0 \\ 0, & 1/\rho, & 0 & 0 \\ -G\sigma_{23}\sigma_{13}/k^2, & 0, & G(1 - \sigma_{23}^2/k^2), & 0 \\ 0, & 0, & 0, & 1/\rho \end{bmatrix}$$

This constitutes a set of quasi-linear partial differential equations of the first order for which there exists an extensive body of knowledge on their solution by the method of characteristics.

Detailed discussion of the technique can be found in Courant and Hilbert [2.4] or Jeffrey and Taniuti [2.5]. It is enough to note here that the characteristic wave speeds are given by roots of the equation:

$$\det (\lambda \underline{C} - \underline{D}) = 0$$

and for the real symmetric matrices which appear here these speeds are real. In the particular case above there are four roots, but two of these coalesce to zero and the system of equations is not wholly hyperbolic. However, the yield condition supplies an algebraic relationship between the two stress components, and thus three characteristics are adequate for a solution. The characteristics of the problem are not

known a priori and are in general curved in the (x_3, t) plane. This, however, presents no serious difficulty if the solution is to be obtained by an incremental technique based on difference equations in the characteristic directions.

(ii) Work Hardening Plastic Equations

The introduction of work hardening into the material description increases the complexity of the theory, and there is at the present time no generally accepted constitutive theory which includes the very wide range of physical behavior experienced in any real material. This complexity is clear when we consider that at any plastic state of stress the current yield surface depends on the entire history of the loading process up to that time. Thus a proper description of the plastic deformation should be based on functional representations, as is done for general viscoelastic materials. Some work along these lines has appeared, for example, by Rivlin and Pipkin [2.6] but has led to no development along these lines suitable for application to problems of the kind we are interested in here.

To overcome the complexities of the functional approach the usual process is to represent the change in the current yield surface in terms of current level of plastic strain and the current plastic work. Reference may be made to the textbook by Fung [2.7] for the details of this approach.

The yield condition is taken to be:

$$f(\sigma_{ij}, \epsilon_{ij}^p, q_\alpha) = 0$$

where now the q_α are scalar parameters which may influence the expansion of the yield condition. Typical examples of q_α are the plastic work:

$$q_1 = W^p = \int_0^t \sigma_{ij} \dot{\epsilon}_{ij}^p dt \quad (2.1.11)$$

or the equivalent plastic strain:

$$q_2 = E^p = \int_0^t (\dot{\epsilon}_{ij}^p \dot{\epsilon}_{ij}^p)^{1/2} dt \quad (2.1.12)$$

As before, the flow rule applies that:

$$\dot{\epsilon}_{ij} = \lambda \partial f / \partial \sigma_{ij}$$

where λ is a positive factor of proportionality.

Since $f = 0$ is the condition for continued plastic behavior, we must have:

$$\dot{f} = \partial f / \partial \sigma_{ij} \dot{\sigma}_{ij} + \partial f / \partial \epsilon_{ij}^p \dot{\epsilon}_{ij}^p + \partial f / \partial q_\alpha \dot{q}_\alpha \quad (2.1.13)$$

From this we can eliminate λ , as before, obtaining:

$$\dot{\epsilon}_{ij}^p = - \frac{\partial f / \partial \sigma_{ij} \partial f / \partial \sigma_{kl} \dot{\sigma}_{kl}}{(\partial f / \partial \epsilon_{mn}^p + \partial f / \partial q_\alpha \partial q_\alpha / \partial \epsilon_{mn}^p) \partial f / \partial \sigma_{mn}} \quad (2.1.14)$$

To complete the specification of the material response it is necessary to know the quantities $\partial f / \partial \epsilon_{mn}^p$ and $\partial f / \partial q_\alpha$.

Two fairly simple one parameter models have been developed which enable the necessary information to be obtained from uniaxial stress strain curves. The first, known as kinematic hardening, assumes that in stress space the yield condition remains fixed in shape but translates in this space. Thus the yield condition may be written in the form:

$$f(\sigma_{ij} - \alpha_{ij}) = 0, \quad \alpha_{ij} = \alpha_{ij}(q) \quad (2.1.15)$$

where α_{ij} represents the translation of the center of the yield surface and q may be either the plastic work or the total equivalent plastic strain. If it is assumed that the center translates instantaneously in the direction of the plastic strain rate, we have:

$$\dot{\alpha}_{ij} = C(q)\dot{\epsilon}_{ij}^p$$

Taking C to be a constant generalizes the bilinear law of uniaxial behavior, and using as before equations (2.1.14) and (2.1.15), we obtain:

$$\lambda = \frac{1}{C} \frac{(\partial f / \partial \sigma_{ij}) \dot{\sigma}_{ij}}{\partial f / \partial \sigma_{kl} \partial f / \partial \sigma_{kl}}$$

An alternative assumption is that the center translates with the direction of the vector joining the instantaneous center with the stress point, thus giving:

$$\dot{\alpha}_{ij} = C(q)(\sigma_{ij} - \alpha_{ij})$$

The second one parameter hardening law is known as isotropic hardening. According to this hypothesis, the yield condition in stress space is a surface which retains its shape but uniformly expands.

A typical yield condition of this kind is:

$$f(\sigma_{ij}) - C(q) = 0$$

or

$$(2.1.16)$$

$$f(\sigma_{ij}) = k^n$$

where in the second form f is a homogeneous function of order n and $k = k(q)$ is a characteristic stress. When the quantity q is identified with the plastic work or the equivalent plastic strain, as in

equations (2.1.11) or (2.1.12), the information needed to construct $k(q)$ can be obtained from a tension test.

For example, if q is the plastic work then inverting the relationship $k = k(W^D)$ to give $W^D = W^D(k)$, we have:

$$W^D = \frac{dW^D}{dk} k \quad (2.1.17)$$

From the yield condition we have:

$$\partial f / \partial \sigma_{kl} \dot{\sigma}_{kl} = nk^{n-1} \dot{k}$$

and from the flow rule we have:

$$\begin{aligned} W^D &= \lambda \partial f / \partial \sigma_{ij} \sigma_{ij} \\ &= \lambda n f \end{aligned}$$

since f is homogeneous of order n in σ_{ij} .

Thus the expression for λ takes the form:

$$\lambda = \frac{dW^D/dk}{n^2 k^{2n-1}} \partial f / \partial \sigma_{kl} \dot{\sigma}_{kl} \quad (2.1.18)$$

which when isotropic elastic stress strain relations as used leads to:

$$\dot{\epsilon}_{ij} = \frac{1+\nu}{E} \dot{\sigma}_{ij} - \frac{\nu}{E} \delta_{ij} \dot{\sigma}_{kk} + G(k) \partial f / \partial \sigma_{kl} \partial f / \partial \sigma_{ij} \dot{\sigma}_{kl} \quad (2.1.19)$$

where:

$$G(k) = dW^D/dk n^{-2} k^{-2n+1}$$

The function $G(k)$ is a scalar function of k , and through the yield condition (2.1.16), of the stress σ_{ij} . This system of equations can, as before, be put into a matrix form particularly suited to incorporation into incremental numerical methods of solutions, in this case taking the form:

$$\dot{\underline{\underline{E}}} = (\underline{\underline{K}} + \underline{\underline{A}}(\underline{\underline{S}}))\dot{\underline{\underline{S}}}$$

where $\underline{\underline{K}}$ is an elastic matrix and $\underline{\underline{A}}$ is a matrix dependent on the current stress vector $\underline{\underline{S}}$.

If we are given the uniaxial stress strain curve for the material in the form:

$$\sigma = f(\varepsilon)$$

then using:

$$\varepsilon^p = \varepsilon - \varepsilon/E$$

it is possible to construct a curve

$$\varepsilon^p = g(\sigma)$$

From this the rate of plastic work \dot{W}^p is:

$$\dot{W}^p = \sigma g'(\sigma) \dot{\sigma} = (\sigma^2/2) \dot{g}'(\sigma)$$

Thus:

$$dW^p/d(\sigma^2) = \frac{1}{2} g'(\sigma)$$

and if the material obeys the Mises yield condition, then:

$$\sigma^2 = 3k^2$$

and

$$dW^p/d(k^2) = \frac{2}{3} g' \left(\frac{k}{\sqrt{3}} \right)$$

which, when inserted into equation (2.1.19), with $n = 2$ for the Mises condition, leads to:

$$G(k) = \frac{1}{3} g' \left(\frac{f^{1/2}(\sigma_{ij})}{\sqrt{3}} \right) \frac{1}{f(\sigma_{ij})}$$

This particular set of constitutive equations has been applied to the problem of the propagation of plastic wave of combined tension and torsion by Clifton [2.8], using the method of characteristics as the solution technique.

Neither of the two simple one parameter hardening models given here reflects accurately the physical behavior of a real material. If, however, the state of stress is such that the stress point in stress space remains in a fairly small neighborhood, the isotropic hardening model is likely to be accurate and fairly easy to use. On the other hand, if stress reversals take place it is likely that the kinematic hardening law, although more difficult to use due to the presence of the additional six quantities α_{ij} , is likely to be the most accurate.

2.2 Rate Dependent Plastic Behavior

The equations of the classical plasticity theory are homogeneous in time and are as a consequence insensitive to strain rate effects. This particular mathematical form for these equations was sought precisely to reflect the observed physical response of ductile metals in the range of loading rates normally encountered in the technical situations to which the plasticity theory was directed. As an idea of the strain rates involved, a standard tension test on a steel specimen usually incurs strain rates of the order of 10^{-3} to 10^{-4} per sec. It is generally accepted that plastic deformation results from the generation and movement of dislocation lines of various kinds throughout the crystal lattice of metal being deformed. The characteristic times associated with the propagation of a dislocation line across a grain are generally of the order of milliseecs so that under the usual rates of loading the times associated with the loading process are very much greater than those associated with the plastic deformation, which may then be considered to be rate independent.

However, at even the moderate strain rates experience by dynamically loaded structures (in the range 10^0 to 10^2 per sec, for example), the times associated with the loading become comparable to those of the dislocation motion, and the observed physical behavior of the metal becomes quite different from that observed in quasi-static experiments. This type of behavior is generally referred to in the literature as strain rate sensitivity.

A large amount of experimental work has been published on strain rate sensitivity, indicating that it varies widely from metal to metal and for a single metal, for example, mild steel it depends on grain

size, chemical composition and heat treatment. Often different measures of rate sensitivity are obtained on nominally the same material when tested using different experimental techniques. Also, specimens cut from the same stock show differences in sensitivity when cut parallel to the direction of rolling and when cut transverse to it. A complete summary of the experimental information is not possible here. Data up to 1960 are given in the book by Goldsmith [2.9].

(1) Uniaxial Constitutive Equations

It is customary to present experiment results on the strain rate sensitivity of a metal in the form of plot of stress σ as a function of strain ϵ and strain rate $\dot{\epsilon}$ by means of an isometric diagram (see for example Marsh and Campbell [2.10]). The surface which results in the $\sigma, \epsilon, \dot{\epsilon}$ space is in a sense an equation of state for the material, $f(\sigma, \epsilon, \dot{\epsilon}) = 0$, and such a relationship cannot be strictly correct since it assumes that one of the three quantities is known when the other two are specified. It is obvious that for such materials the stress depends on the strain history experienced by the material, and thus the equation of state representation is only approximate. It is a convenient one, however, and it appears from the results of Marsh and Campbell [2.10] that the same diagram results for mild steel when tested in constant stress tests and in constant strain rate tests, indicating that strain history effects are not serious.

To a certain extent the strain history can be incorporated into the constitutive equation of the material if the equation of state of the material is rewritten in the form:

$$\dot{\epsilon}^p = g(\sigma, \epsilon)$$

indicating that the current plastic strain rate, $\dot{\epsilon}^p$, depends on the current stress and strain.

Since

$$\dot{\epsilon}^p = \dot{\epsilon} - \dot{\sigma}/E$$

where E is the Young's modulus, this equation becomes:

$$E\dot{\epsilon} = \dot{\sigma} + g(\sigma, \epsilon) \quad (2.2.1)$$

An equation of this type was introduced by Malvern [2.11]. Since we are interested in plastic materials, i.e. materials which exhibit an elastic range given, say, for static loading by a stress curve $\sigma = f^+(\epsilon)$ when σ, ϵ are tensile and $\sigma = f^-(\epsilon)$ when compressive, the function $g(\sigma, \epsilon)$ should be interpreted as follows:

$$g(\sigma, \epsilon) > 0, \quad \sigma > f^+(\epsilon) > 0$$

$$g(\sigma, \epsilon) = 0, \quad f^+(\epsilon) > \sigma > f^-(\epsilon)$$

$$g(\sigma, \epsilon) < 0, \quad f^-(\epsilon) > \sigma$$

Also, to incorporate the irreversibility implicit in plastic behavior, the constitutive equation should be the elastic law:

$$E\dot{\epsilon} = \dot{\sigma}$$

whenever $\dot{\epsilon} < 0$ and $\sigma > f^+(\epsilon)$

or $\dot{\epsilon} > 0$ and $\sigma < f^-(\epsilon)$

It is thus possible to have a loading situation when the stress and stress rate are opposite in sign, for example, in a relaxation test where $\dot{\epsilon} = 0$ but $\dot{\epsilon}^p \neq 0$, and if $\sigma > f^+(\epsilon)$ then $\dot{\sigma} = -E\dot{\epsilon}^p > 0$.

Several simple forms of equation (2.2.1) have been used in the study of uniaxial wave propagation problems. The earliest appears to be due to Sokolovsky [2.12], who showed that a closed form solution to the uniaxial wave problem could be obtained when the constitutive equation

$$E\dot{\epsilon} = \dot{\sigma} + \frac{1}{\tau} (\sigma - \sigma_0) \quad (2.2.2)$$

was used. In this equation σ_0 is the static yield stress and τ a time constant. Malvern [2.11], although suggesting an equation of the form (2.2.1), actually used the simpler equation:

$$E\dot{\epsilon} = \dot{\sigma} + \frac{1}{\tau} (\sigma - f(\epsilon)) \quad (2.2.3)$$

Where as before $f(\epsilon)$ is the static stress strain curve taken to be the same in tension and compression and τ a time constant. These simple equations, which indicate that the plastic strain rate is linear in the over-stress $\sigma - \sigma_0$ or $\sigma - f(\epsilon)$, are particularly convenient to use in problems but have a very limited range of applicability. If the strain is specified, equation (2.1.22) can be integrated to give:

$$\sigma = f(\epsilon) + \int_0^t (E - df/d\epsilon) e^{-(t-t')/\tau} d\epsilon(t')/dt' dt' \quad (2.2.4)$$

where $t = 0$ is chosen so that $\sigma = 0$, $\epsilon = 0$. In this form the partial incorporation of strain history effects in equation (2.2.2) is clear. It is clear from equation (2.2.4) above that it predicts the the dynamic stress strain curve is asymptotically parallel to the static curve. Tests by Hauser, Simmons and Dorn [2.13] have indicated that the asymptotic slope increases with strain rate. This type of response can be included if equation (2.2.3) is modified (see Kelly, [2.14]) to:

$$E\dot{\epsilon} = \dot{\sigma} + \frac{\mu(\epsilon)}{\tau} (\sigma - f(\epsilon)) \quad (2.2.5)$$

This equation remains linear in σ and can immediately be integrated to give:

$$\sigma(t) = f(\epsilon) + \int_0^t (E - df/d\epsilon) e^{-\frac{\xi(t)-\xi(t')}{\tau}} \frac{d\epsilon(t')}{dt'} dt'$$

where:

$$\xi(t) = \int_0^t \mu(\epsilon(t')) dt'$$

A simple form of $\mu(\epsilon)$, which gives the effect sought, is $\mu(\epsilon) = \frac{\epsilon_0}{\epsilon - \epsilon_0}$, where $\epsilon_0 < 0$ and constant. Considering the case when we take f in the simple form:

$$\begin{aligned} f(\epsilon) &= E\epsilon & \epsilon < \epsilon_y \\ &= \sigma_0 = E\epsilon_y, & \epsilon > \epsilon_y \end{aligned}$$

where ϵ_y is the yield strain, and for a constant strain rate $\dot{\epsilon} = \alpha$ this leads to

$$\sigma = \sigma_0 + \frac{E}{1 - \epsilon_0/\alpha\tau} \left[\frac{\epsilon - \epsilon_0}{\epsilon_s - \epsilon_0} - \left(\frac{\epsilon_s - \epsilon_0}{\epsilon - \epsilon_0} \right)^{-\epsilon_0/\alpha\tau} \right] (\epsilon_s - \epsilon_0)$$

which asymptotically gives curves of the form:

$$\sigma = \sigma_0 + \frac{E}{1 - \epsilon_0/\alpha\tau} (\epsilon - \epsilon_0)$$

implying an increase in slope with increasing strain rate. The same type of modification taking instead $\mu(\epsilon) = A(\epsilon + c)^{-2}$ has been discussed

recently by Lubliner and Valathur [2.15] in application to wave propagation problems.

In addition to the fact that equation (2.2.3) predicts dynamic curves parallel to the static curves, it also predicts that the over-stress is linear in the strain rate, and in fact this linear dependence is not experimentally confirmed over even moderate ranges of strain rate (say from 10^0 to 10^3 per sec). In fact, for mild steel in particular and for many other metals, the experimental results suggest a logarithm dependence. This behavior results from equation (2.2.1) if written in the form:

$$E\dot{\epsilon} = \dot{\sigma} + \sigma_c/\tau \left(e^{-\frac{\sigma-f(\epsilon)}{\sigma_c}} - 1 \right) \quad (2.2.6)$$

where σ_c is a characteristic stress. It was shown by Kelly [2.16] that this equation can be linearized in $(\sigma - f(\epsilon))$ and integrated formally for $\sigma(t)$ in terms of strain history.

In a situation in which the strain is prescribed, it is convenient to write (2.2.6) in the form:

$$\frac{d}{dt} \left\{ \frac{\sigma - f(\epsilon)}{\sigma_c} \right\} + \frac{1}{\tau} \left(e^{+\frac{\sigma-f(\epsilon)}{\sigma_c}} - 1 \right) = (E - f')/\sigma_c \, d\epsilon/dt$$

which by suitable manipulations and use of the integrating factor

$$e^{+t/\tau} \quad e^{-\frac{\sigma-f(\epsilon)}{\sigma_c}}$$

leads to the integral:

$$\sigma(t) = f(\epsilon) - \sigma_c \ln \left\{ 1 - \frac{1}{\sigma_c} \int_0^t (E - df/d\epsilon) e^{-(t-t')/\tau} e^{-E(\epsilon-\epsilon')/\sigma_c} e^{(f(\epsilon)-f(\epsilon'))/\sigma_c} \partial\epsilon'/\partial t' dt' \right\} \quad (2.2.7)$$

where $\epsilon' = \epsilon(t')$, and σ , and ϵ are taken to be zero at $t = 0$.

Since σ is always greater than or equal to the stress corresponding to the static lower yield point for all strain rates, the fact that $df/d\epsilon$ is very much less than E over most of the plastic range can be used to simplify the above result. The term $f(\epsilon) - f(\epsilon')$ is, as a consequence, negligible in comparison to $E(\epsilon - \epsilon')$, and the above result reduces to:

$$\sigma(t) = f(\epsilon) - \sigma_c \ln \left\{ 1 - \frac{E}{\sigma_c} \int_0^t e^{-(t-t')/\tau} e^{-E(\epsilon-\epsilon')/\sigma_c} \partial\epsilon'/\partial t' dt' \right\} \quad (2.2.8)$$

The representation of stress in terms of strain history thus involves a fading memory in time with a relaxation time τ (using the terminology of viscoelasticity theory) and in addition has a fading memory in strain, with the characteristic memory strain given by σ_c/E .

In the case of constant strain rate, $\dot{\epsilon} = \alpha$ the reduced form (2.2.8) becomes:

$$\sigma = f(\epsilon) - \sigma_c \ln \left\{ e^{-E\epsilon/\sigma_c} e^{-\epsilon/\alpha\tau} + \left[1 - e^{-\epsilon/\alpha\tau} e^{-E\epsilon/\sigma_c} \right] \left(1 + \frac{E\alpha\tau}{\sigma_c} \right) \right\}$$

The asymptotic form of the above equation is:

$$\sigma = f(\epsilon) + \sigma_c \ln \left(1 + \frac{E\alpha\tau}{\sigma_c} \right)$$

Curves of σ against $\log \alpha$ were given by Marsh and Campbell [2.10] for mild steel specimens of two grain sizes: one a large grain-size material with 346 grains/mm² and the other a small grain-size material have 2030 grains/mm². Using this equation and the data of Marsh and Campbell, reasonable values of σ_c and τ to be 26,000 psi and 10⁻¹ sec for both materials are obtained. It is possible to extend equation (2.2.6) further by inclusion, as in equation (2.2.5), of a term in $\mu(\epsilon)$ and in this the variable transformation from t to $\xi(t)$, as given for equation (2.2.5), can be used to obtain an integral equivalent to (2.2.7).

A wide variety of other forms for the function of $g(\sigma, \epsilon)$ are possible. On the basis of a theory of thermally activated dislocation motion a representation of the form:

$$g(\sigma, \epsilon) = \frac{\sigma_c}{\tau} \sinh ((\sigma - f(\epsilon))/\sigma_c)$$

is suggested (see for example Dorn and Mote, [2.17]). Other theories of dislocation motion have led to power law expressions involving $(\sigma - \sigma_0)^n$. On the basis of experimental results on the stress dependence of dislocation motion, Gilman [2.18] and Johnston [2.19] proposed an equation of the form:

$$g(\sigma, \epsilon) = \frac{1}{\tau} \exp \left(- \frac{D}{\sigma} \right)$$

which differs from the others in that there is no explicit elastic range.

(ii) Multiaxial Constitutive Equations

In extending the models proposed in the previous section to multiaxial states, there is very little experimental information to act as a guide, and any assumptions made must be regarded as speculative. The general approach used, for example, by Perzyna [2.20] and reviewed by Cristescu [2.21] assumes the existence of a static yield surface and assumes that this can be used as a potential for the plastic strain rates. Thus, for example, for a statically non-hardening material for which the yield condition may be

$$f(\sigma_{ij}) = k^2$$

where f is homogeneous of order n in the σ_{ij} we have:

$$\dot{\epsilon}_{ij}^p = \lambda \partial f / \partial \sigma_{ij}$$

but in contrast to equations (2.1.1) and (2.1.2), $f > k^n$ is possible and λ here is a factor of proportionality which depends on the stress state which may be outside the yield condition. It is generally assumed that

$$\lambda = \frac{1}{\tau} \Phi \left(\frac{f - k^n}{k^n} \right)$$

when, as before, τ is a time constant but Φ is a dimensionless function of the extent to which the stress state lies beyond the static yield condition. Thus the stress strain relations for the material may be written in the form:

$$\dot{\epsilon}_{ij} = \frac{1 - \nu}{E} \dot{\sigma}_{ij} - \frac{\nu}{E} \dot{\sigma}_{kk} \delta_{ij} + \frac{1}{\tau} \Phi \left(\frac{f - k^n}{k^n} \right) \partial f / \partial \sigma_{ij} \quad (2.2.9)$$

where ν is Poisson's ratio.

If the static yield surface is given by the Mises yield condition, written in the form:

$$(1/2 s_{ij}s_{ij})^{1/2} = k$$

we can obtain an extension of the linear model in the form:

$$2G \dot{e}_{ij} = \dot{s}_{ij} + \frac{1}{\tau} \frac{(1/2 s_{kl}s_{kl})^{1/2} - k}{(1/2 s_{kl}s_{kl})^{1/2}} s_{ij} \quad (2.2.10)$$

$$3k \dot{e}_{kk} = \dot{\sigma}_{kk}$$

with e_{ij} , s_{ij} defined by equations (2.1.7) and (2.1.8). This reduces the equation (2.2.3) when σ_{ij} is uniaxial.

On the other hand, the alternative extension

$$2G \dot{e}_{ij} = \dot{s}_{ij} + \frac{1}{\tau} \frac{1/2 s_{kl}s_{kl} - k^2}{k^2} s_{ij} \quad (2.2.11)$$

which results from the Mises condition when written in the form:

$$1/2 s_{ij}s_{ij} = k^2$$

does not reduce to (2.2.3) when σ_{ij} is uniaxial, but cannot be dismissed on these grounds, for in the range of small values of overstress to which the linear equation (2.2.3) applies the equation resulting from (2.2.11) is the same as that resulting from (2.2.10).

The second alternative form:

$$2G \dot{e}_{ij} = \dot{s}_{ij} + \frac{1}{\tau} \frac{1/2 s_{kl}s_{kl} - k^2}{1/2 s_{kl}s_{kl}} s_{ij} \quad (2.2.12)$$

which also does not reduce to equation (2.2.3) when σ_{ij} is uniaxial, is equally as acceptable as equation (2.2.10) or (2.2.11).

Noting that $\dot{\epsilon}_{ij}^p = \dot{\epsilon}_{ij} - \frac{\dot{s}_{ij}}{2G}$, it is obvious that these equations can be interpreted in terms of a dynamic yield condition; for taking \dot{s}_{ij} to the left side and squaring both sides gives for (2.2.9):

$$4G^2(1/2 \dot{\epsilon}_{ij}^p \dot{\epsilon}_{ij}^p) = 1/\tau^2((1/2 s_{kl} s_{kl})^{1/2} - k)^2$$

or

$$(1/2 s_{kl} s_{kl})^{1/2} = k + 2G\tau(1/2 \dot{\epsilon}_{ij}^p \dot{\epsilon}_{ij}^p)^{1/2}$$

A dynamic yield curve of the form:

$$1/2 s_{kl} s_{kl} = k^2 + 2G\tau(1/2 \dot{\epsilon}_{ij}^p \dot{\epsilon}_{ij}^p)$$

proposed by Craggs [2.22], suggests a constitutive equation of the form:

$$2G \dot{\epsilon}_{ij} = \dot{s}_{ij} + \frac{1}{\tau} \frac{(1/2 s_{kl} s_{kl} - k^2)^{1/2}}{(1/2 s_{kl} s_{kl})^{1/2}} s_{ij} \quad (2.2.13)$$

which is another way to extend the uniaxial equation.

Extensions to include isotropic work hardening of the yield condition are possible, e.g. if we write the yield condition in the form:

$$f(\sigma_{ij}) = c(q)$$

where q is the plastic work w^p or the equivalent plastic strain E^p , then:

$$\dot{\epsilon}_{ij}^p = \frac{1}{\tau} \left(\frac{f - c}{c_0} \right) \partial f / \partial \sigma_{ij}$$

and: $c = c_0 + \beta(q)$; $\beta(0) = 0$.

Extensions similar to (2.2.5) may be obtained by setting

$$\dot{\epsilon}_{ij}^p = \frac{1}{\tau} (E^p) \Phi \left(\frac{f(\sigma_{ij}) - k^n}{k^n} \right) \partial f / \partial \sigma_{ij}$$

and many obvious combinations can be derived. All of these are speculative and none are known to be the superior in any sense other than convenience to analytical solutions.

An entirely different approach to the extension of these constitutive relations which retains the linearity of relations of the type (2.2.3) and improves their correspondence with physical data by the use of hereditary integrals is given in the next section.

Regardless of which form of equation (2.2.9) is used, and independently of the choice of the function Φ , it is always possible to put the equations into a matrix form suitable for incorporation into incremental numerical solutions, and in this case the strain rate vectors and stress rate vectors are operated on by matrices which are constants. Thus the equations reduce to:

$$\dot{\underline{E}} = \underline{K}\dot{\underline{S}} + \underline{A}(\underline{S}) \quad (2.2.14)$$

(iii) Extension by Use of Hereditary Integrals

Suppose we consider the extended form of the linear law (2.2.3) as given in equation (2.2.12). Multiplying both sides of this equation by $1/2 s_{ij}$ gives:

$$1/2 s_{ij} \dot{s}_{ij} + 1/\tau (1/2 s_{ij} s_{ij} - k^2) = G s_{ij} \dot{\epsilon}_{ij}$$

which can be written in the form:

$$\frac{1}{2} \dot{J}_2 + 1/\tau (J_2 - k^2) = G\dot{w}$$

Where $J_2 = 1/2 s_{ij}s_{ij}$ is the 2nd invariant of the stress deviator and $\dot{w} = s_{ij}\dot{e}_{ij}$ is rate of work. This equation can be written immediately in the form:

$$J_2 = k^2 + 2G \int_0^t e^{-(t-t')/\tau/2} \dot{w}(t') dt'$$

where for convenience $t = 0$ is selected so that $s_{ij}(0), e_{ij}(0)$ vanish. This is an equation of the hereditary integral type with a single relaxation time $\tau/2$. However, in any real material there is no single natural time, but a large number of different times corresponding to the multiplicity of crystal grains and orientations. If we assume that instead of a single time $\tau/2$, a spectrum of natural times $0 < \tau < \infty$, then replacing G by $G\varphi(\tau)$, where $\varphi(\tau)$ is a normalized function of τ such that $\int_0^\infty \varphi(\tau) d\tau = 1$, and summing over the entire range, we obtain:

$$J_2 = k^2 + 2G \int_0^t \psi(t - t') \dot{w}(t') dt' \quad (2.2.15)$$

The function $\psi(t)$, appearing above, is a nondimensional relaxation function constructed from:

$$\psi(t) = \int_0^\infty \varphi(\tau) e^{-t/\tau/2} d\tau \quad (2.2.16)$$

and having the properties:

$$\psi(0) = 1 \quad \psi(t) \geq 0, \quad t \geq 0$$

$$\lim_{t \rightarrow \infty} \psi(t) = 0, \quad \psi'(t) \leq 0, \quad t \geq 0$$

The determination of $\psi(t)$ by experiment is possible by means of uniaxial relaxation tests. In this case, $\dot{w}(t) = \frac{\sigma^{*2}}{E} \delta(t)$ where σ^* is the instantaneous value of $\sigma(t)$ at $t = 0^+$. When $\sigma(t)$, $t > 0$ is measured, we obtain:

$$1/3 \sigma^2(t) = k^2 + \psi(t) \sigma^{*2}/3$$

Thus:

$$\psi(t) = (\sigma^2(t) - 3k^2)/\sigma^{*2}$$

Tests at constant rate of work could also provide a means for the determination of $\psi(t)$.

For a material defined in this way the complete stress strain relations become:

$$2G \dot{e}_{ij} = \dot{s}_{ij} + \lambda s_{ij}$$

where now, as in equation (2.1.2), λ is a factor of proportionality given by equation (2.2.15) for J_2 . In fact, λ takes the form:

$$\lambda = \frac{-2G \int_0^t \psi'(t-t') \dot{w}(t') dt'}{k^2 + 2G \int_0^t \psi(t-t') \dot{w}(t') dt'} \quad (2.2.17)$$

This particular form is no more involved than equation (2.2.12) when applied to incremental computations as $t = 0$ may be taken at the start of the interval, initial conditions there included explicitly and the

integral taken over the length of the increment in any approximate form consistent with the approximations used in the rest of integration procedure.

2.3 Delayed Yield Phenomenon

The rate sensitivity of the yield stress for certain metals is well known and, as indicated above, a reasonably well understood phenomenon. Another type of rate effect in certain metals which is much less well understood is that of the yield delay time. This involves a delay in the development of plastic strain when a stress in excess of yield stress is instantaneously applied. The order of magnitude of the delay time in mild steel for stresses which exceed the yield stress by about 20% is 7 millisecc. It appears, however, to be extremely sensitive to the stress level, decreasing with increasing stress. This effect gives rise to the familiar upper yield point and yield drop in simple tension tests on mild steel, but there is much controversy as to whether this is a material property or due solely to the stiffness of the machine used for the tests. There is no doubt that interaction between machine and specimen strongly influences the observed delay time in tension tests, but the phenomenon appears in wave propagation tests and in other test situations where the stiffness effects are not present.

It appears to have been first observed by Hopkinson [2.23] and has been studied experimentally by Clark and Wood [2.24], Campbell and Marsh [2.25] and Krafft and Sullivan [2.26]. These experimental results show that with increasing strain rate the upper yield point increases faster than the lower yield point, and thus the effect might become increasingly important for very rapid loading, although so far as is known no consideration of this behavior has been included in any studies of impulsively loaded structures. For statically loaded structures or for dynamically loaded structures for which the strain rates remain small (< 1 per sec.) the effect is of no importance and is always ignored.

Whether or not the effect can be ignored for dynamic loading with high strain rates is an open question and only extensive experimental and computational work could resolve this.

In the following we develop a rate sensitive constitutive theory that incorporates a delay time showing how the constitutive equations have to be modified. A method for determining the upper yield point dependence on strain rate is given. Later in the report, in the section on analysis, the constitutive equations will be applied to the problem of a dynamically loaded beam and one possible effect of the yield time will be shown.

We assume for this development that the response of the material from the unstained, unstressed state be described by the two basic equations:

$$\begin{aligned} E\dot{\epsilon} &= \dot{\sigma} , & t \leq t_d \\ E\dot{\epsilon} &= \dot{\sigma} + g(\sigma, \epsilon) , & t > t_d \end{aligned} \tag{2.3.1}$$

providing $\dot{\epsilon} \geq 0$.

To estimate t_d use will be made of published experimental data by Campbell and Marsh [2.25]. In their tests, mild steel specimens of various grain sizes were loaded dynamically in compression under constant stress. It was found that the delay time is dependent on the applied constant stress and on the grain size. The authors discussed a number of models and found that the one which best corresponds to the data is the hypothesis that macroscopic yielding can only occur when a critical fraction of the grains contain released dislocations. For uniform grain size this gives the result:

$$t_d = \frac{A}{d^3} \left(\frac{\sigma_0}{\sigma} \right)^\beta \quad (2.3.2)$$

where σ is the constant stress and σ_0 is twice the shear stress required to release a source in the absence of thermal fluctuations and d is the average grain diameter. Taking σ_0 as $2G/45$, the value of A obtained from the data was $1.2 \times 10^{-6} \text{ mm}^3 \text{ sec}$ and β was approximately 9.

In situations, as here, where the stress is not constant, the determination of the delay time can only be conjectured. It will be assumed here that the above model is valid and that the rate of release of dislocations is a function of the applied stress. Thus, if the critical fraction required for macroscopic yielding is F , then the rate R at which this critical fraction is reached under constant stress is:

$$R = F / \frac{A}{d^3} \left(\frac{\sigma_0}{\sigma} \right)^\beta \quad (2.3.3)$$

Assuming that the same formula will hold for variable stress, the delay time t_d will be given by the solution of:

$$\int_0^{t_d} \frac{d^3}{A} \left(\frac{\sigma}{\sigma_0} \right)^\beta dt = 1 \quad (2.3.4)$$

In the case of constant strain rate $\dot{\epsilon} = \alpha$, this takes the form:

$$E \alpha t_d = \sigma^* = \left\{ E(1 + \beta) A \sigma_0^\beta \alpha / d^3 \right\}^{1/1+\beta} \quad (2.3.5)$$

On this basis, the upper yield point σ^* is proportional to 1/10-th power of the strain rate. Since the lower yield point is asymptotically proportional to \ln for mild steel (see equation (2.2.8)) the upper yield point will increase more rapidly with increasing α than the lower yield point.

Substitution of the values of A, d, β for the two grain sizes given in paper by March and Campbell [2.10], gives:

$$\sigma^* = 77,000 \alpha^{1/10} \text{ (p.s.i.) for } 2030 \text{ grains/mm}^2$$

and

(2.3.6)

$$\sigma^* = 60,000 \alpha^{1/10} \text{ (p.s.i.) for } 346 \text{ grains/mm}^2$$

3. IMPULSIVE LOADING ON STRUCTURAL SYSTEMS

3.1 Moving Mass Impact on Elastic Beams

The problem of the impact of a mass on a beam is of interest in the understanding of the behavior of an automobile which collides with a highway barrier and has an intrinsic interest as a problem of structural dynamics. The total response combination of elastic and plastic behavior, in the fence and in the impacting vehicle, the initial stages of the impact, which might produce the highest decelerations on the passengers, and during which time energy dissipation due to plastic flow is still of minor importance, might be covered by an elastic approach.

To this end, a Laplace transform method of solution for the impact of a mass on an elastic beam of infinite extent, in which primary concern was with the motion of the mass after impact, was given in a recent paper by Kelly [3.1]. It was shown that the solution on the basis of simple (Bernoulli-Euler) beam theory can be given in closed form, but while this provides physically reasonable values of velocity and displacement of the mass immediately after impact, it leads to an infinite deceleration of the mass at the instant of impact.

It is well known that the Bernoulli-Euler theory of dynamic response of beams predicts that the disturbance due to a suddenly applied load propagates infinitely rapidly. However, it was shown that the impact of a mass on a tightly stretched string has a finite value of initial deceleration. It may be conjectured then that the infinite value of the deceleration is a result of the infinite wave velocity of the simple beam theory and that it may be removed by using the Timoshenko beam theory in which finite wave velocities occur. It was shown that the Timoshenko beam equations do, in fact, predict a finite value of initial deceleration.

The equation of displacement, $w(x, t)$ of a beam of cross sectional area A , moment of inertia I , density ρ and modulus of elasticity E is, on the basis of Bernoulli-Euler theory,

$$EIw_{,xxxx} + \rho Aw_{,tt} = - p(x, t) \quad (3.1.1)$$

where $p(x, t)$ is the external applied force on the beam which in this case is given by:

$$p(x, t) = - Mw_{,tt} \Big|_{x=0} \delta(x) \quad (3.1.2)$$

M being the mass (impacting at $t = 0$ at $x = 0$) and $\delta(x)$ the Dirac delta function.

The details of the Laplace transform method of solution of (3.1.1) with (3.1.2) is given in [3.1]; the solution taking the form:

$$\begin{aligned} w(0, t) &= V_0 \int_0^t e^{\alpha^2 \tau} \operatorname{erfc}(\alpha \sqrt{\tau}) d\tau, \quad \alpha = \frac{8EI K^3}{M} \\ w_{,t}(0, t) &= V_0 e^{\alpha^2 t} \operatorname{erfc}(\alpha \sqrt{t}), \quad K = \left(\frac{\rho A}{4EI} \right)^{1/4} \\ w_{,tt}(0, t) &= V_0 \left\{ \alpha^2 e^{\alpha^2 t} \operatorname{erfc}(\alpha \sqrt{t}) - \frac{1}{4} \alpha / \sqrt{t} \right\} \end{aligned} \quad (3.1.3)$$

It is clear from the last of these results that this solution, while providing reasonable velocity and displacement solution, indicates an infinite deceleration at the instant of impact. Intuitively, the reason for this result is that the slope of the beam under the point of application of the load must be continuous and thus at the moment of impact the mass engages a finite portion of the beam, this being intimately connected with the infinite wave velocity. If we look at the same problem for a string of linear density ρ and tension T in which case

the equation for displacement $w(x, t)$ is:

$$T w_{,xx} - \rho w_{,tt} = M w_{,tt} \Big|_{x=0} \delta(x) \quad (3.1.4)$$

and we obtain, by the same method, the solutions:

$$\begin{aligned} w(0, t) &= V_0 (Mc/2T) (1 - e^{-(2T/Mc)t}) \\ w_{,t}(0, t) &= V_0 e^{-(2T/Mc)t} \\ w_{,tt}(0, t) &= -V_0 (2T/Mc) e^{-(2T/Mc)t}, \quad c = \left(\frac{T}{\rho}\right)^{1/2} \end{aligned} \quad (3.1.5)$$

This shows that where a finite wave velocity exists, a finite deceleration is obtained. In fact, in this case it is clear that at the instant of impact the portion of the string carried forward by the mass has zero mass.

It was further shown that the bending moment under the point of impact, $M(0, t)$ takes the form:

$$M(0, t) = 2EI k^2 V_0 e^{\alpha^2 t} \operatorname{erfc}(\alpha \sqrt{t})$$

The result for the bending moment is a multiple of that for the velocity under the load and the formula may be taken as a physically reasonable one. The initial value of the moment, $2EI k^2 V_0$, is independent of the magnitude of the impacting mass. Since the moment decays from this initial value (for a finite impacting mass) for the impact to be elastic it is enough that $2EI k^2 V_0 < M_y$, the yield moment of the beam cross section. Since $M_y = I \sigma_y / y$ where σ_y is the yield stress and y the distance from the centroidal axis of the beam to the extreme fiber, the limiting velocity for an elastic impact is given by:

$$V_0/C_1 = (r/y)\epsilon_y$$

where $r = (I/A)^{1/2}$ is the radius of gyration of the section and $\epsilon_y = \sigma_y/E$ is the yield strain and $C_1 = (E/\rho)^{1/2}$ the velocity of longitudinal waves in the beam material.

We will make use of this result in a later section when the effect of a delay time is studied.

The corresponding solution for the elastic beam in which rotary inertia and transverse shear deformation i.e. the Timoshenko beam was also obtained in [3.1]. It was found that the initial deceleration could be expressed in the form:

$$w_{,tt}(0, 0) = - 2V_0GA_s/Mc_2$$

where G is the shear modulus, A_s the effective shear area, and $c_2 = (G/\rho)^{1/2}$ is the velocity of propagation of shear waves in the beam material.

This result for the initial deceleration is fairly simple but in fact leads to values of the initial deceleration which appear to be excessively high, and thus, while the inclusion of the propagation effects has improved the estimate, the neglect of deformability of the mass and the plastic behavior of the system prevents a realistic result. In the following section solutions which neglect wave propagation effects but include the deformability of the mass and plastic behavior will be given.

3.2 Normal Impact of a Moving Mass on a Rigid Plastic System

Many suggested barrier systems comprise beam or cable elements which are backed by an energy absorbing material such as plastic foam or metal honeycomb. The impact of a moving object against a beam backed by such a material is consequently of some interest in that its solution could lead to an increased understanding of the behavior of an automobile in collision with such a protective barrier. The response of the barrier and the vehicle are interrelated kinematically and dynamically, and in both is a complex combination of elastic and plastic behavior. This problem can only be treated directly by massive computation. The load deflection characteristics of materials such as plastic foam or metal honeycomb are fairly well approximated, for the purpose of predicting their absorbing ability, by a rigid plastic model. Thus, in order to reduce the problem to manageable proportions and to allow the identification of important parameters and features of the response, we consider here the problem of moving mass impacting a rigid perfectly plastic beam backed by a rigid perfectly plastic support. In effect, the elastic deformations are disregarded, being assumed negligible in comparison with the plastic deformations.

A considerable literature on the dynamic plastic deformation of impulsive loaded beams using rigid plastic model of deformation has developed since the original paper by Lee and Symonds [3.2], dealing with a free-free beam of finite length subject to concentrated load. Other load distributions on free-free beams were studied by Symonds [3.3], Salvadori and Dimaggio [3.4], and Seiler and Symonds [3.5], and infinite beams by Hopkins [3.6] and Conroy [3.7]. An extensive series of papers on impulsively loaded cantilever beams quoting both theoretical and

experimental results was published by Bodner and Symonds. In particular in [3.8] they concluded from experiments that the rigid perfectly plastic approximation to the material behavior is reasonable so long as the ratio of the kinetic energy input to the maximum possible elastic stored energy is at least three. This tends to limit the application of rigid perfectly plastic analysis to problems where the impulsive loading causes extensive damage to the structure, but it is precisely this damage which is of major interest in such cases.

The particular problem considered here leads to quite simple solutions, primarily as a result of the inclusion of the rigid plastic support. This leads to a simplification in the boundary conditions over that of the finite beam [3.2-3.5] or the infinite beam [3.6-3.7]. The representation of the vehicle is much more difficult to resolve, but here we have made the not unreasonable conjecture that it is rigid perfectly plastic in that the force between the vehicle and the beam has an upper bound determined by the physical characteristics of the vehicle itself.

A general solution of the problem is presented here in closed form, and particular illustrative examples are given. Approximate solutions suitable for cases where the moving object is either very massive or very rigid--these will be given precise meaning in the paper--are also described.

(i) Basic Assumptions and Method of Solution

The elementary rigid-plastic analysis used here is characterized by the following assumptions on the behavior of the beam

- a. elastic deformations are neglected
- b. no strain hardening of the material and no strain rate sensitivity

- c. equations of motion are written in the undeformed configuration
- d. axial forces in the beam are neglected
- e. the curvature of any section of the beam remains constant if the moment is below the yield moment denoted by M_0

Further, the backing material is taken to provide a continuous reaction to the beam, the beam displacement rate being zero if this reaction is below a yield value denoted by q_0 (force per unit length of beam).

The vehicle itself is taken to be rigid perfectly plastic with the yield force denoted by P_0 .

Equations of Motion

In setting up the equations of motion, it is assumed that the magnitude of the impact is sufficient to cause the formation of three hinges, one at the point of impact and the other two symmetrically placed on either side, thus creating a mechanism of deformation. It will be verified a posteriori that this assumption is sufficient to determine the solution.

The question of the behavior of the beam at a moving hinge has been studied by Lee and Symonds [3.2] and Hopkins [3.6]. It is established by Hopkins [3.6] that if the hinge is moving, then the lateral velocity of the beam is continuous across the hinge, and the acceleration may be discontinuous. If the hinge is stationary, both are continuous. In addition, the bending moment at a moving hinge is continuous as is both the spatial and temporal derivatives of the bending moment across the hinge. Since at a hinge the moment must be a maximum according to the yield criterion, it follows that the shear force must vanish if no concentrated loads act there.

Consider a beam of unlimited extent $-\infty < x < \infty$ of density m (mass per unit length) acted on by a force $P(t)$ at $x = 0$ and assume a symmetrical velocity field $v(x, t)$ of the form:

$$\begin{aligned} v(x, t) &= v_0(t) \left(1 - \frac{x}{\xi(t)}\right); & 0 \leq x \leq \xi(t) \\ &= 0 & \xi(t) \leq x \end{aligned} \quad (3.2.1)$$

Thus v_0 is the velocity of the point of impact and $\pm \xi(t)$ the location of moving hinges. This velocity field which implies that the beam is moving as a rigid body between 0 and ξ is consistent with the yield criterion which requires that the beam be rigid when the moment M is within the yield limits $\pm M_0$ for the moment is $+M_0$ at $x = 0$ and $-M_0$ at $x = \xi$ and continuous between.

If $\omega(t)$ is the angular velocity of the portion $0 < x < \xi$ and $\dot{\omega}(t)$ the angular acceleration, it is easily shown that

$$\dot{\omega}(t) = a/\xi - \omega \dot{\xi}/\xi \quad (3.2.2)$$

where $a = \dot{v}_0$ is the linear acceleration of the point $x = 0$. The equations of motion of the portion $0 < x < \xi$ as shown in Figure 3.2.1 are:

$$P/2 = q_0 \xi + m \xi \left(a - \frac{1}{2} \xi \dot{\omega} \right) \quad (3.2.3)$$

$$P\xi/4 = 2M_0 + \frac{m}{12} \xi^3 \dot{\omega} \quad (3.2.4)$$

The equation of motion of the vehicle takes the form:

$$P = -M \dot{a}_v \quad (3.2.5)$$

with M the mass and a_v the acceleration of the vehicle.

Rewriting equation (3.2.4) in the form:

$$\dot{\omega} = \frac{3P}{m\xi^2} - \frac{24M_0}{m\xi^3} \quad (3.2.6)$$

and substitution in equation (3.2.3) and then (3.2.2) leads to the more convenient equations of motion:

$$a = \frac{2P}{m\xi} - \frac{12M_0}{m\xi^2} - \frac{q_0}{m} \quad (3.2.7)$$

$$\dot{v}_0\xi = \frac{12M_0}{m\xi} - \frac{q_0\xi}{m} - \frac{P}{m} \quad (3.2.8)$$

If the mass is rigid then $a_v = a$ and the unknowns become $\xi(t)$, $a(t)$, $\dot{\omega}(t)$, and $P(t)$. On the other hand, if the mass is behaving plastically, P is then prescribed, $a_v(t)$ to be determined. In each case the equations (3.2.5) - (3.2.8) are adequate for a solution. When a rigid mass impacts a rigid beam, the contact force is instantaneously infinite. Thus, one or both of the elements must yield. Both will yield if P_0 exceeds the static yield load P_b of the beam. This static yield load P_b is given by assuming that equation (3.2.1) with constant ξ provides an incipient velocity field and minimizing the resultant collapse load with respect to ξ . It is found that

$$P_b = 4(M_0 q_0)^{1/2}$$

and the value of ξ , say $\xi = L$, for which this minimum is achieved, is

$$L = 2(M_0/q_0)^{1/2}$$

Thus P_b and L constitute a characteristic force and a characteristic length of the beam system.

It is convenient to carry out the subsequent analysis in dimensionless variables and thus, by making use of P_b and L as obtained above, the

following are defined:

$$T = \frac{t}{M_0^{1/4} m^{1/2} / q_0^{3/4}} ; \quad X = \frac{x}{2(M_0/q_0)^{1/2}}$$

$$S = \frac{\xi}{2(M_0/q_0)^{1/2}} ; \quad S' = dS/dT = \frac{\xi}{2M_0^{1/4} q_0^{1/4} / m^{1/2}}$$

$$V = \frac{v_0}{2M_0^{1/4} q_0^{1/4} / m^{1/2}} ; \quad V' = dV/dT = \frac{a}{2q_0/m}$$

The mass ratio μ and the force ratio ϕ are defined by:

$$\mu = \frac{M}{2m(M_0/q_0)^{1/2}} , \quad \phi = \frac{P_0}{4(M_0 q_0)^{1/2}}$$

The case when $\phi \leq 1$ has a trivial solution and it will be assumed that $\phi > 1$, for which case the motion has two parts. In the first stage, the contact force is given by $P = P_0$ and the beam accelerates from rest, the velocity of the beam being different from that of the mass. At a certain time the velocities are equal and subsequently the contact force drops below P_0 . The mass is then rigid and both the beam at the point of contact and the mass have the same velocity. In this stage, the motion of the beam is decelerative.

Accelerative Phase

In the first stage it is assumed that $P = P_0$, constant. The equations (3.2.5) (3.2.8) admit a unique solution with $\xi = \text{constant}$ which, after some simple algebra, takes the form:

$$a = (P_0 - 2q_0\xi)/m\xi \quad (3.2.9)$$

with:

$$\xi = \frac{(P_0^2 + 48M_0q_0)^{1/2} - P_0}{2q_0} \quad (3.2.10)$$

Thus, during this phase the beam accelerates with constant central acceleration a and fixed hinge distance ξ ; the impacting mass decelerates with acceleration $-P_0/M$. The time t^* at which the velocities are equal is given by:

$$t^* = \frac{V_0(0)}{a + P_0/M}$$

and the velocity then is v_0^* given by:

$$v_0^* = at^*$$

These quantities provide the initial conditions for the second state, which in terms of dimensionless quantities, are:

$$S(T^*) = S^* = (\phi^2 + 3)^{1/2} - \phi \quad (3.2.11)$$

$$\frac{dV}{dT}(T^*) = (\phi - S^*)/S^* \quad (3.2.12)$$

$$V(T^*) = V^* = \frac{\mu V_0(\phi - S_0^*)}{\phi S^* + \mu(\phi - S^*)} \quad (3.2.13)$$

$$T^* = \frac{\mu V_0 S^*}{\phi S^* + \mu(\phi - S^*)} \quad (3.2.14)$$

where V_0 is the dimensionless velocity at $T = 0$.

Decelerative Phase

In this phase $P(t) \leq P_0$ and $a_v = a$. Thus, using equation (3.2.5), equations (3.2.7) and (3.2.8) become, in physical quantities:

$$a = - \frac{12M_0 + q_0 \xi^2}{\xi(2M + m\xi)}$$

and

$$v_0 \xi = \frac{12(M/m\xi)M_0 + 12M_0 - 3(M/m\xi)q_0 \xi^2 - q_0 \xi^2}{2(M + m\xi)}$$

and in dimensionless quantities:

$$v' = - \frac{s^2 + 3}{2s(s + 2\mu)} \quad (3.2.15)$$

$$vs' = - \frac{s^3 + 3\mu s^2 - 3s - 3\mu}{2s(s + 2\mu)} \quad (3.2.16)$$

subject to the initial conditions equations (3.2.11), (3.2.12) and (3.2.13) at $T = T^*$.

Since the equations of motion are valid only when the velocity of the mass is positive and the deformed region is non-decreasing it is necessary that

$$3s + 3\mu - s^3 - 3\mu s^2 \geq 0$$

This places an upper bound on s depending on μ ; it is found that

$$0 \leq s \leq \bar{s}$$

where $1 \leq \bar{s} \leq \sqrt{3}$ with $\bar{s} = 1$ corresponding to $\mu = \infty$ and $\bar{s} = \sqrt{3}$ corresponding to $\mu = 0$. Since it is clear from equation (3.2.16) that when

$$s^3 + 3\mu s^2 - 3s - 3\mu = 0 \quad (3.2.17)$$

i.e., $s = \bar{s}$, either $v = 0$, in which case the motion stops, or $s' = 0$, in which case the deformed region remains constant, that the limitation that $1 \leq \bar{s} \leq \sqrt{3}$ places close bounds on the final extent of the deformed

region. This allows a good estimate to be made of the final extent of the magnitude of the damage, regardless of the velocity or mass of the impacting object.

A general solution of equations (3.2.15) and (3.2.16) can be obtained by dividing them, giving:

$$\frac{v'}{v} = \frac{s^2 + 3}{s^3 + 3\mu s^2 - 3s - 3\mu} s' \quad (3.2.18)$$

writing $s^3 + 3\mu s^2 - 3s - 3\mu = (s - \alpha)(s + \beta)(s + \gamma)$

where:

$$\sqrt{3} \geq \alpha \geq 1$$

$$0 \leq \beta \leq 1$$

$$\sqrt{3} \leq \gamma \leq \infty$$

the left limit corresponding to $\mu = 0$ and the right to $\mu = \infty$, and integrating the above equations gives:

$$v/v^* = \left(\frac{s - \alpha}{s^* - \alpha}\right)^A \left(\frac{s + \beta}{s^* + \beta}\right)^B \left(\frac{s + \gamma}{s^* + \gamma}\right)^C \quad (3.2.19)$$

where:

$$A = (3 + \alpha^2)/(\alpha + \beta)(\alpha + \gamma)$$

$$B = (3 + \beta^2)/(\alpha + \beta)(\beta - \gamma)$$

$$C = (3 + \gamma^2)/(\gamma + \alpha)(\gamma - \beta)$$

Substitution of equation (3.2.18) into equation (3.2.16) gives:

$$-\frac{dT}{V^*} = \frac{2S(S + 2\mu)(S - \alpha)^A (S + \beta)^B (S + \gamma)^C dS}{(S^* - \alpha)^A (S^* + \beta)^B (S^* + \gamma)^C (S - \alpha)(S + \beta)(S + \gamma)}$$

which on integration provides the required relation between S and T in this phase in the form:

$$T = T^* + \frac{2V^*}{(\alpha - S^*)^A (S^* + \beta)^B (S^* + \gamma)^C} \int_{S^*}^S \frac{S(S + 2\mu)(S + \gamma)^{C-1} dS}{(\alpha - S)^{1-A} (S + \beta)^{1-B}} \quad (3.2.20)$$

The time T^{**} at which $S = \alpha$ when the motion ceases is given by:

$$T^{**} = T^* + \frac{2V^*}{(\alpha - S^*)^A (S^* + \beta)^B (S^* + \gamma)^C} \int_{S^*}^{\alpha} \frac{S(S + 2\mu)(S + \gamma)^{C-1} dS}{(\alpha - S)^{1-A} (S + \beta)^{1-B}}$$

and making use of the results that

$$0 \leq A \leq 1, \quad -1 \leq B \leq 0, \quad C \geq 1$$

and that $\alpha > S^*$ it is possible to establish an upper bound to the motion of the form:

$$T^{**} - T^* \leq \frac{2V^* \alpha (\alpha + 2\mu) (\alpha + \gamma)^{C-1}}{A(S^* + \beta)(S^* + \gamma)^C}$$

which is always finite for finite μ .

In the case where the impacting mass is rigid, for which $\phi = \infty$ and $T^* = 0$, $V^* = V_0$ and $S^* = 0$, a solution for small S can be obtained by neglecting powers of S higher than the first in equations (3.2.15) and (3.2.16) leading to:

$$S = \sqrt{3T/2V_0}$$

$$V/V_0 = e^{-\frac{1}{\mu} \sqrt{3T/2V_0}}$$

Valid for T/V_0 such that $S \ll 1$. An approximate solution valid over the entire range of S can be obtained for large values of μ , for example greater than 10. It is easy to show that as $\mu \rightarrow \infty$, $\alpha \rightarrow 1$, $\beta \rightarrow 1$, $\gamma \rightarrow 3\mu$ and $A \rightarrow 2/3\mu$, $B \rightarrow -2/3\mu$ and $C \rightarrow 1$ which when substituted into equation (3.2.20) leads after integration to:

$$T = \frac{2V_0}{3} \ln (1/1 - S^2)$$

and in equation (3.2.19) to:

$$V/V_0 = \left(\frac{1 - S}{1 + S} \right)^{2/3\mu}$$

from which by inversion is obtained:

$$S = \sqrt{1 - e^{-3T/2V_0}}$$

and

$$V/V_0 = \left(\frac{1 - \sqrt{1 - e^{-3T/2V_0}}}{1 + \sqrt{1 - e^{-3T/2V_0}}} \right)^{\frac{2}{3\mu}}$$

In these cases the deceleration of the mass at the instant of impact is infinite, and the assumption of a rigid mass clearly leads to results which are useless from the point of view assessing the decelerations experienced by the vehicle. In the following section certain more realistic examples will be presented.

Vehicle Damage

An estimate of the damage suffered by the impacting vehicle can be made

by noting that in the first phase of the motion the vehicle center of mass moves through a distance (in dimensionless variables) $V_0 T^* - \frac{1}{2} \frac{\phi}{\mu} T^{*2}$ while the point of contact on the beam moves a distance $\frac{1}{2} V_0 T^{*2}$. The difference between these gives the change in the distance between the center of mass and the point of contact during the impact. Denoting this by D , we find:

$$D = V_0 T^* \left(1 - \frac{1}{2} \frac{\phi}{\mu} \frac{T^*}{V_0} - \frac{1}{2} \frac{\phi - S_0}{S_0} \frac{T^*}{V_0} \right)$$

which for T^* as given by equation (3.2.14) reduces to

$$D = \frac{1}{2} V_0 T^*$$

Hence:

$$\frac{D}{V_0^2} = \frac{\mu[(\phi^2 + 3) - \phi]}{[\phi(\phi^2 + 3)^{1/2}] - \phi^2 + \mu[2\phi - (\phi^2 + 3)^{1/2}]}$$

Curves of D/V_0^2 against μ for various force ratios ϕ are given in figure 3.2.4. We note that the damage is bounded above by

$$\begin{aligned} D/V_0^2 &\leq \frac{(\phi^2 + 3) - \phi}{2\phi - (\phi^2 + 3)^{1/2}} \\ &\leq \frac{\sqrt{3}}{\phi - \sqrt{3}} \end{aligned}$$

(ii) Numerical Examples

In obtaining numerical values of the solution from equations (3.2.18) and (3.2.19) it is necessary first to specify ϕ and then compute T^* , S^* , V^* , and dimensionless deflection W^* . Newton's method may conveniently be used to compute α from equation (3.2.16) for the specified

value of μ since it is known to lie within the close limits 1 and $\sqrt{3}$. The other constants β , γ , A, B, and C are then computed in order.

It is then possible to compute V as a function of S from (3.2.19) and T as a function of S from (3.2.20) by quadrature.

It is worth noting that V and T for fixed values of S are proportional to V_0 and that W where

$$W = W^* + \int_{T^*}^T V(T') dT'$$

is proportional to V_0^2 .

In computing the time from equation (3.2.20) and the velocity from equation (3.2.19) it was found convenient to use a changing step width in variable S. The initial value S_0 is known, as is the final value $S = \alpha$, and the difference $\alpha - S_0$ was divided into steps which varied from $(\alpha - S_0)/10$ at the initial stage of the computation to $(\alpha - S_0)/1000$ at the final stage, this being necessary since the integrand becomes increasingly singular as $S \rightarrow \alpha$. The value for the time of the motion, denoted by T^{**}/V_0 , was computed by quadrature up to the step immediately before $S = \alpha$, to which was added the term I, where

$$I = \frac{V^*}{(\alpha - S_0)^A (S_0 + \beta)^B (S_0 + \gamma)^C} \int_{\alpha - \epsilon}^{\alpha} \frac{2S(S + 2\mu) dS}{(\alpha - S)^{1-A} (S + \beta)^{1-B} (S + \gamma)^{1-C}}$$

where $\epsilon = \frac{\alpha - S_0}{1000}$. The integral is evaluated by expanding the terms in $(\alpha - S)$ and retaining up to the second order. Integrating the result gives:

$$I = \frac{V^*}{(\alpha - s_0)^A (s_0 + \beta)^B (s_0 + \gamma)^C} \frac{2\alpha(2\mu + \alpha)}{(\alpha + \beta)^{1-B} (\alpha + \gamma)^{1-C}}$$

$$\left\{ \frac{\epsilon^A}{A} + \frac{1-B}{\alpha + \beta} + \frac{1-C}{\alpha + \gamma} - \frac{1}{\alpha} - \frac{1}{2\mu + \alpha} \frac{\epsilon^{1+A}}{1+A} \right\}$$

It is clear from this result that the computation in the final step is extremely sensitive if μ is large (when $A \rightarrow 0$), and including the second term allows us to obtain good accuracy while retaining a reasonable step length.

The results given in figure 3.2.2 show the motion of the hinges for different mass ratios. It is significant that the approach to $S = \alpha$ is very slow in the case of the large values of μ . The velocity and displacement increases with increasing mass ratio. It is significant that altering the force ratio has little effect on the motion.

The solution for a particular case involving a typical vehicle mass and velocity is given in terms of real variables in figure 3.2.3. These solutions given above can be used, if necessary, to give approximate results for the motion of the system and to provide estimates of the damage to the barrier system and to the vehicle, these estimates being in a particularly simple form. Of the physical parameters appearing in the solutions, the only one which cannot be readily determined is the value of P_0 for the vehicle. However, tests have recently been performed in which vehicles have been statically crushed or dropped onto a rigid surface. Such tests could provide the necessary data.

The results obtained are limited in range of validity by the neglect of axial forces produced by large displacements. This is probably not a

serious neglect in the case of the beam which has a continuous support. Another limitation is the neglect of strain rate effects implicit in the assumption of rate independent values for the yield parameters M_0 , q_0 , P_0 . Mild steel is known to be very strain rate sensitive. It is possible to estimate values of M_0 , q_0 , P_0 which are somewhat higher than the static values to take this effect into partial account. This is somewhat unsatisfactory since a correct theory including rate effects precludes the existence of hinges as assumed here. A study of the inclusion of this effect is given later in the report.

Although the solution obtained here is for an infinite beam it is applicable without modification to a finite beam with clamped ends providing the dimensionless length of the beam exceeds 2α . If the length is less than 2α the solution is the same up to the time when the hinge reaches the end of the beam; thereafter the rigid portion rotates about the end until the motion stops. When this happens the force between the mass and the beam is constant and consequently the mass experiences a constant deceleration.

(iii) Notation for Section 3.2

a, a_v	acceleration of barrier and vehicle
A, B, C	constants of integration
m	mass per unit length of barrier
M	mass of vehicle
M_0	yield moment of barrier
P	force between barrier and vehicle
P_0	yield force of vehicle
q_0	yield force per unit length of support
S	dimensionless hinge distance
S^*	dimensionless hinge distance at start of deceleration phase
t, T	time and dimensionless time
t^*, T^*	time and dimensionless time at start of deceleration phase
T^{**}	dimensionless time when motion stops
$v(x, t)$	velocity of points of barrier
$v_0(t)$	velocity of barrier at point of impact
V, V_0, V^*	dimensionless velocities corresponding to $v_0, v_0(0), v_0^*$
x, X	real and dimensionless coordinate along barrier axis
α, β, γ	constants
ϵ	small parameter
ϕ	force ratio
μ	mass ratio
ω	angular velocity
ξ	hinge distance

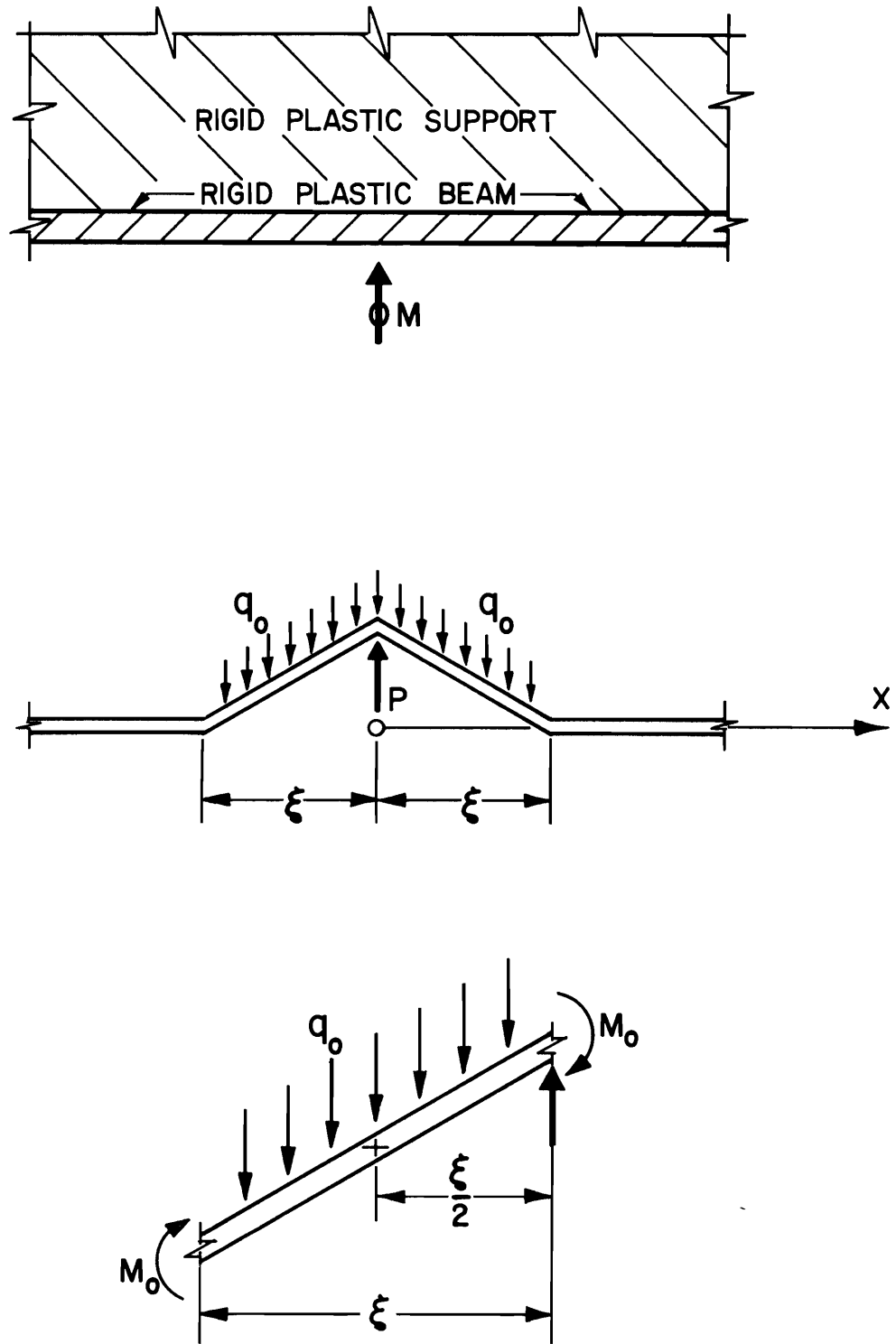


Figure 3.2.1 Coordinate System and Physical Quantities

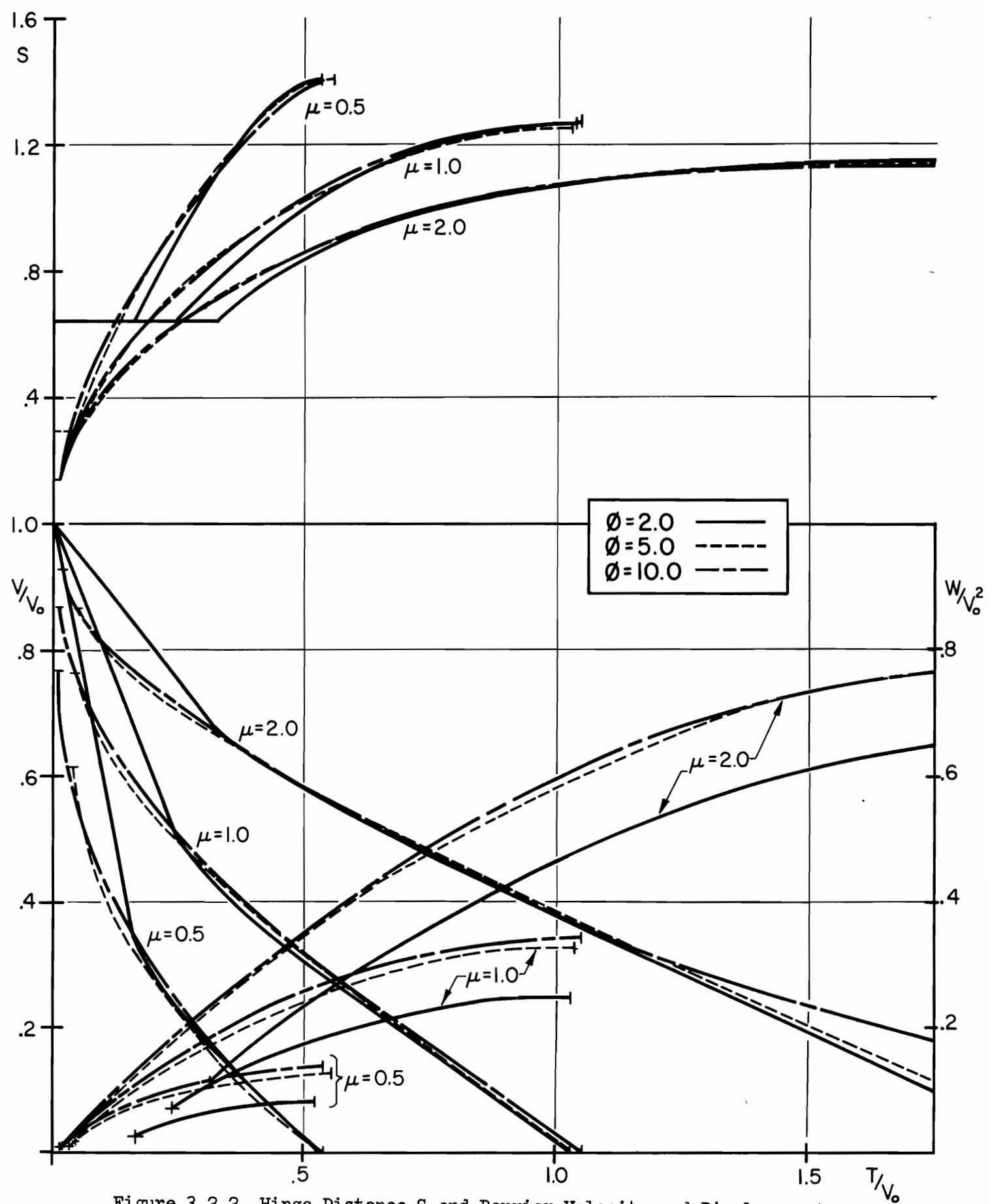


Figure 3.2.2 Hinge Distance S and Barrier Velocity and Displacement
Against T/V_0

BARRIER MASS = 14 lb/ft
 VEHICLE MASS = 2 Kips
 VEHICLE VELOCITY = 30 MPH
 YIELD MOMENT = 200K-in
 STIFFNESS = 0.105 K/in
 INITIAL FORCE = 40 K

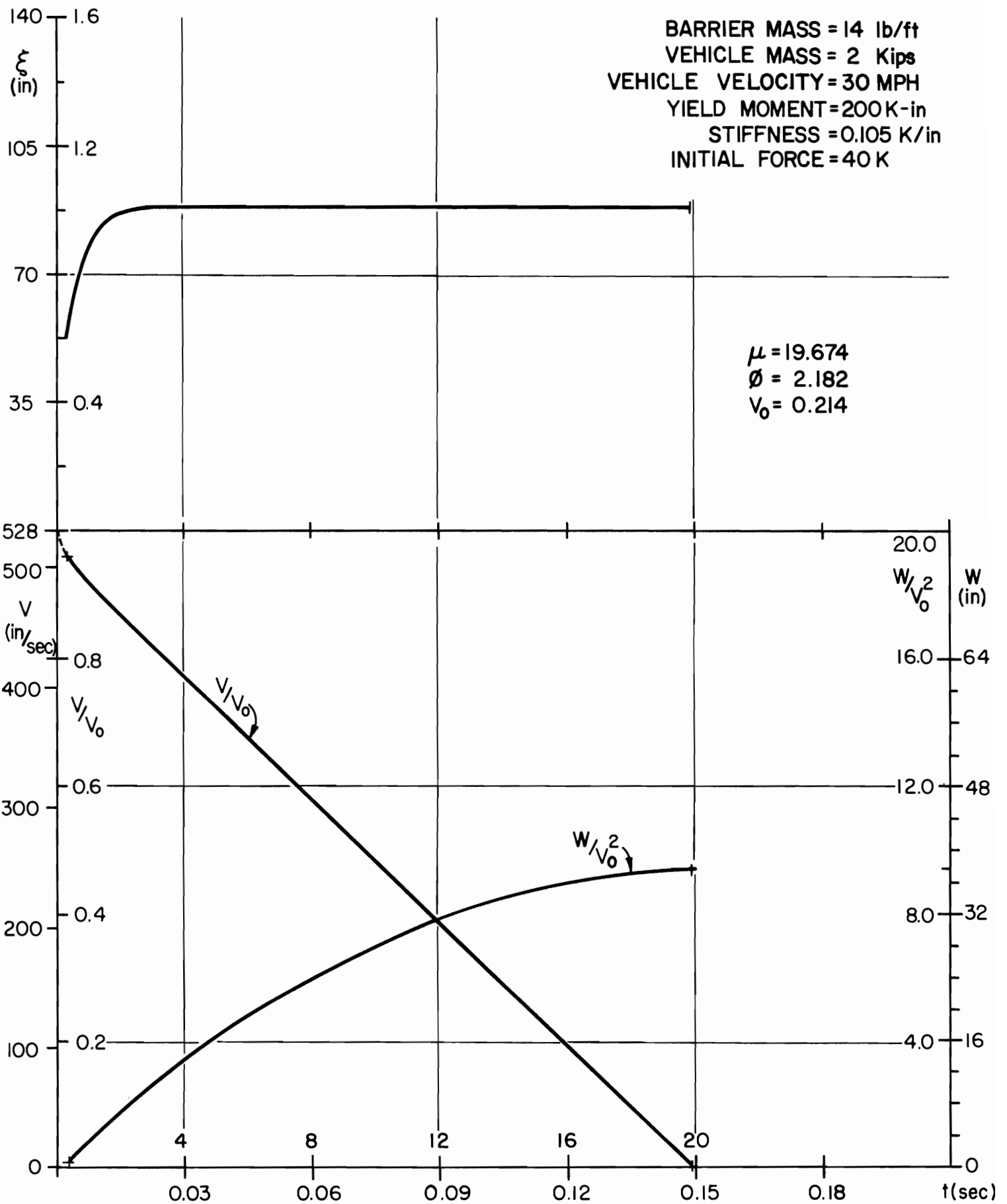


Figure 3.2.3 Solution for a Typical Impact in Terms of Real Variables

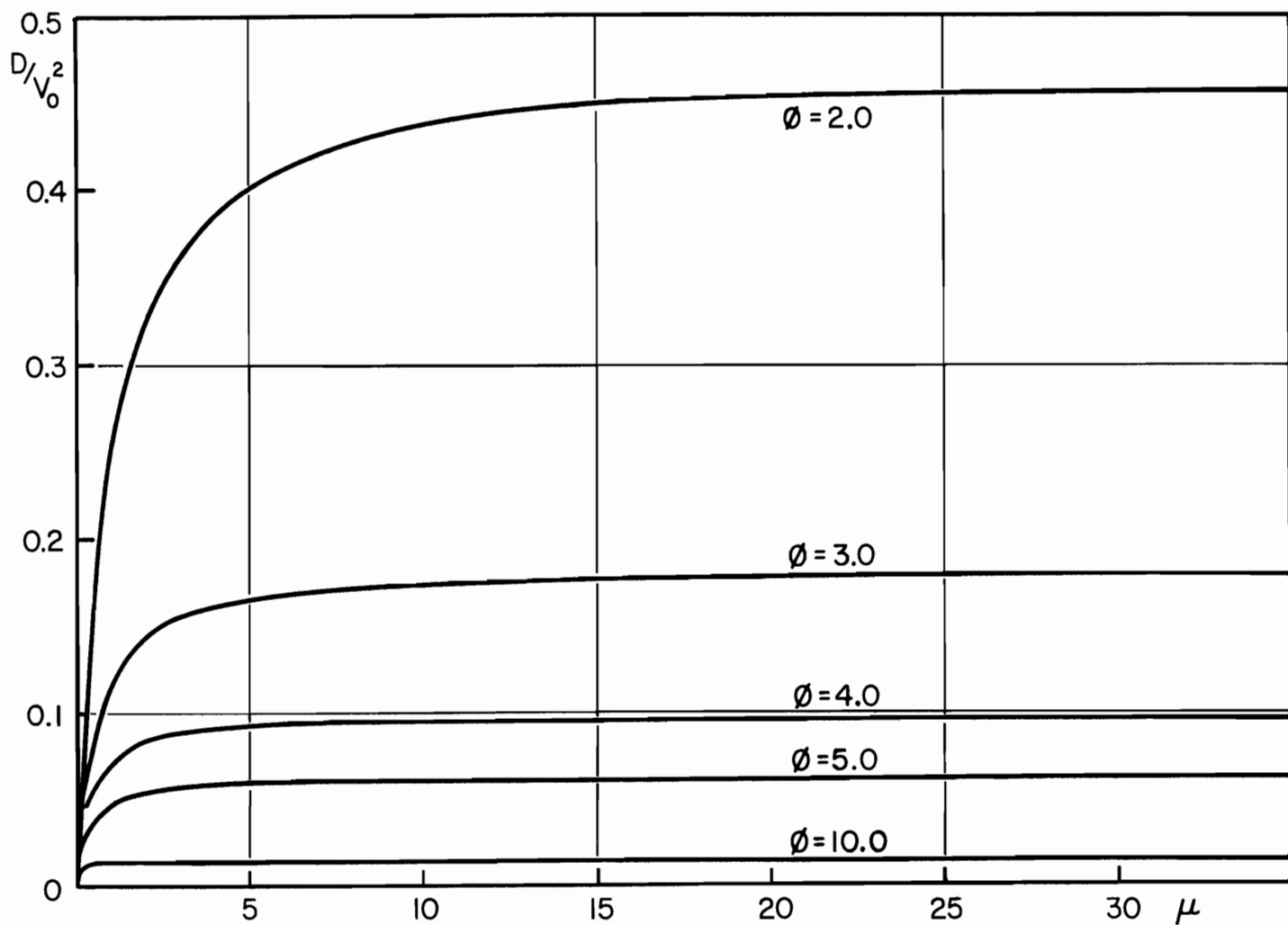


Figure 3.2.4 Vehicle Damage as a Function of Mass Ratio for Various Force Ratios

3.3 Oblique Impact of a Moving Mass on Rigid-Plastic System

In the previous section the problem of normal impact was treated and a rather simple closed form solution was obtained. In this section the more relevant oblique impact problem is considered and here it is no longer possible to obtain analytic solutions due to the increased number of unknown quantities which, in the absence of symmetry about the contact point, have to be treated. Also included in oblique impact but not in normal impact are terms which arise from convection of quantities by the moving load system.

Thus the approach used here is characterized by the same assumption as in section 3.2.

(i) Analytical Approach

Kinematic Relationships

In setting up the equations of motion it is assumed that there exists a system of three hinges, one at the point of contact, and the other two on either side of it. Since the bending moment is at the yield limit and negative at the central hinge and at the yield limit, and positive at the lateral hinges, it follows that the beam is rigid, but not necessarily straight between the central hinge and a lateral hinge.

The question of the continuity of various quantities across a hinge can be treated by the general kinematic compatibility relation for moving discontinuities, given for example by Thomas [3.13], which with $[f]$ denoting the jump in a quantity f across a moving section takes the form

$$\frac{d}{dt} [f] = \left[\frac{\partial f}{\partial t} \right] + c \left[\frac{\partial f}{\partial x} \right] \quad (3.3.1)$$

where C is the velocity of the moving section, x is the Lagrangian position of a point on the beam middle surface and t the time. If a hinge is moving, then it is easy to show that the lateral velocity and the slope of the beam are continuous, while the acceleration and curvature can be discontinuous. If the hinge is stationary the acceleration is continuous. In addition, the bending moment at a moving hinge is continuous as are the spatial and temporal derivatives of the bending moment. Since at a hinge the moment must be a maximum according to the yield condition it follows that the shear force must vanish if no concentrated loads act there. We consider a beam of unlimited extent $-\infty < x < \infty$, of mass m per unit length acted on by a force $P(t)$ at the point $x = f(t)$ where the origin $x = 0$ is taken to be the point of initial contact.

In the following, the lateral displacement of the centroidal axis of the beam will be denoted by $w(x, t)$ and the velocity $\partial w / \partial t$ by $v(x, t)$. It is assumed that the magnitude of the force is sufficient to produce plastic deformation of the beam and the velocity field of the beam $v(x, t)$ is taken (figure 3.3.1) to be:

$$\begin{aligned} v(x, t) &= 0 & , & \quad -\infty < x \leq f(t) - \xi_2(t) \\ &= v_0(t) \left\{ 1 + \frac{x - f(t)}{\xi_2(t)} \right\} & , & \quad f(t) - \xi_2(t) \leq x \leq f(t) \\ &= v_0(t) \left\{ 1 - \frac{x - f(t)}{\xi_1(t)} \right\} & , & \quad f(t) \leq x \leq f(t) + \xi_1(t) \\ &= 0 & , & \quad f(t) + \xi_1(t) \leq x < \infty \end{aligned} \quad (3.3.2)$$

Here $v_0(t)$ is the lateral velocity of the point of the beam in contact with the force $P(t)$, i.e., $v_0(t) = \left[\frac{\partial}{\partial t} w(x, t) \right]_{x=f(t)}$, $\xi_1(t)$, $\xi_2(t)$ are the variable distances from the point of contact to the lateral hinges.

If the force $P(t)$ is produced by a mass sliding along the beam, then it is necessary to relate the lateral component of the mass velocity v_n and acceleration \dot{v}_n^* to the above quantities. Assuming contact between mass and beam we have:

$$v_n = \frac{d}{dt} \left[w(x, t) \Big|_{x=f(t)} \right] = v_0(t) + \frac{\partial w}{\partial x} \Big|_{x=f(t)} v_H \quad (3.3.3)$$

where $v_H = \dot{f}$ is the longitudinal component of the vehicle velocity. We note that v_H may be either a specified function of time or may be computed on the basis of an idealized frictional behavior between mass and barrier. Further, the accelerations are related by

$$\dot{v}_n = \dot{v}_0 + \dot{v}_H \frac{\partial w}{\partial x} \Big|_{x=f(t)} + \frac{d}{dt} \left(\frac{\partial w}{\partial x} \Big|_{x=f(t)} \right)$$

Providing the point of contact is moving, i.e., $v_H \neq 0$, the slope of the beam is continuous and the third term may be interpreted as follows. The displacement $w(x, t)$ is obtained by integration from the velocity field and from this

$$\frac{\partial w}{\partial x} = \int_0^t \frac{\partial v(x, t)}{\partial t} dt$$

Substituting from equation (3.3.2) we have for any point x ,

*

$$(\dot{\quad}) \equiv \frac{d}{dt} (\quad); (\quad)_{,t} \equiv \frac{\partial}{\partial t} (\quad) .$$

$$\frac{\partial w}{\partial x} = 0 \quad , \quad 0 < t \leq t_1$$

$$= \int_{t_1}^t \frac{\partial v}{\partial x} (x, \tau) d\tau, \quad t_1 < t$$

In particular where $x = f(t)$ we have

$$\left. \frac{\partial w}{\partial x} \right|_{x=f(t)} = - \int_{t_1}^t \frac{v_0(\tau)}{\xi_1(\tau)} d\tau \quad (3.3.4)$$

where t_1 is the solution of

$$f(t) = f(t_1) + \xi_1(t_1) \quad (3.3.5)$$

i.e., t_1 is the time at which the right hinge passed the point $x = f(t)$ or is zero if t_1 from the above turns out to be negative. Using this we obtain:

$$\dot{v}_n = \dot{v}_0 - \frac{v_H v_0}{\xi_1} + v_H \frac{v_0(t_1)}{\xi_1(t_1)} \frac{dt_1}{dt} + \dot{v}_H \left\{ - \int_{t_1}^t \frac{v_0(\tau)}{\xi_1(\tau)} d\tau \right\} \quad (3.3.6)$$

The two terms following \dot{v}_0 are convective terms which arise from the rate of change in the slope of the beam at the point of contact and the last term from the variation in v_H . An approximate theory corresponding to a "linear" theory for elastic systems would be obtained by neglecting these terms. However, since the equations of motion neglecting them are highly nonlinear by virtue of the material response characteristics no useful simplification actually results by identifying \dot{v}_n and \dot{v}_0 and for this reason they have been retained in the subsequent analysis.

Equations of Motion

The forces and stress resultants acting on a typical element of the beam when it is deforming are shown in figure 3.3.2. The equations

of dynamic equilibrium are simply:

$$\frac{\partial Q}{\partial x} = p - q_0 - m \frac{\partial v}{\partial t} \quad (3.3.7)$$

$$\frac{\partial M}{\partial x} = Q \quad (3.3.8)$$

In these equations the beam moment is denoted by M and the shear force by Q ; p is zero except at the point of contact where it is a Dirac delta function of intensity $P(t)$ and q_0 is constant. Suitable equations of motion, which are the counterpart of conservation of momentum and moment of momentum for the two rigid elements of the deforming region, can be obtained by inserting $\frac{\partial v}{\partial t}$ from equation (3.3.2) in equation (3.3.7) above and integrating. From equation (3.3.2) $v_{,t}$ takes the form:

$$\begin{aligned} v_{,t} &= 0 && , -\infty < x < f(t) - \xi_2(t) \\ &= \dot{v}_0 \left\{ 1 + \frac{x - f(t)}{\xi_2(t)} \right\} - \frac{v_0 x}{\xi_2^2} \dot{\xi}_2 - \frac{v_0 v_H}{\xi_2} && , f(t) - \xi_2(t) < x < f(t) \\ &= \dot{v}_0 \left\{ 1 + \frac{x - f(t)}{\xi_1(t)} \right\} + \frac{v_0 x}{\xi_1^2} \dot{\xi}_1 + \frac{v_0 v_H}{\xi_1} && , f(t) < x < f(t) + \xi_1(t) \\ &= 0 && , f(t) + \xi_1(t) < x < \infty \end{aligned} \quad (3.3.9)$$

Using this and integrating equation (3.3.7) from $x = f(t) - \xi_2(t)$ to $x = f(t) + \xi_1(t)$, taking into account the fact that $Q = 0$ is zero at both limits, leads to:

$$P = q_0(\xi_1 + \xi_2) + \frac{1}{2} m \dot{v}_0(\xi_1 + \xi_2) + \frac{1}{2} m v_0(\dot{\xi}_1 + \dot{\xi}_2)$$

Insertion of the integrated form of Q from equation (3.3.7) in equation (3.3.8) and use the fact that $M = M_0$ at $x = f(t) - \xi_2(t)$, and $M = -M_0$ at $x = f(t)$, leads on integration to:

$$2M_0 = m \left\{ \frac{\dot{v}_0 \xi_2^2}{6} - \frac{1}{2} v_0 v_H \xi_2 + \frac{1}{3} v_0 \dot{\xi}_2 \xi_2 \right\} + \frac{1}{2} q_0 \xi_2^2$$

for the rigid portion on the left, and

$$2M_0 = m \left\{ \frac{\dot{v}_0 \xi_1^2}{6} + \frac{1}{2} v_0 v_H \xi_1 + \frac{1}{3} v_0 \dot{\xi}_1 \xi_1 \right\} + \frac{1}{2} q_0 \xi_1^2$$

for the rigid portion on the right.

By suitable manipulations the above equations can be put into the more convenient form:

$$\begin{aligned} \dot{v}_0 &= \frac{-12M_0}{m\xi_1\xi_2} + \frac{4P}{m(\xi_1 + \xi_2)} - \frac{q_0}{m} \\ v_0 \dot{\xi}_1 &= \frac{6M_0(\xi_1 + \xi_2)}{m\xi_1\xi_2} - \frac{2P\xi_1}{m(\xi_1 + \xi_2)} - \frac{q_0\xi_1}{m} - \frac{3}{2} v_0 v_H \\ v_0 \dot{\xi}_2 &= \frac{6M_0(\xi_1 + \xi_2)}{m\xi_1\xi_2} - \frac{2P\xi_1}{m(\xi_1 + \xi_2)} - \frac{q_0\xi_2}{m} + \frac{3}{2} v_0 v_H \end{aligned} \quad (3.3.10)$$

If the contact force is less than the yield threshold for the mass the contact force is given by:

$$P(t) = -M_v \dot{v}_n \quad (3.3.11)$$

where M_v is the mass of the vehicle and \dot{v}_n is given by equation (3.3.6). On the other hand if the mass is behaving plastically $P(t)$ is then prescribed and \dot{v}_n is to be determined. It is clear that at the instant of impact either or both the mass and barrier must yield. If the mass only yields the solution is trivial and need not be considered. If, on the

other hand, the yield force for the barrier is less than that of the vehicle the motion has two parts. In the first stage the contact force is given by the yield condition of the vehicle and the barrier accelerates from rest, after a certain time the contact force drops below the yield force of the vehicle at which time the mass becomes rigid. In the following stage, the motion of the barrier is decelerative.

It is convenient to carry out the subsequent analysis in dimensionless quantities and to this end we introduce a certain characteristic force and characteristic length. These are obtained from the static problem. It is easy to show that the static load carrying capacity of the system is given by a force:

$$P_b = 4(M_0 q_0)^{1/2} \quad (3.3.12)$$

and the mechanism of deformation corresponding to this collapse load is of the form of equation (3.3.2) with:

$$f(t) = 0, \quad \xi_1 = \xi_2 = L_c = 2(M_0/q_0)^{1/2} \quad (3.3.13)$$

Using P_b and L_c as above, the following are defined:

$$T, T_1 = \frac{t, t_1}{\frac{m^{1/2} M_0^{1/4}}{q_0^{3/4}}}; \quad X = \frac{x}{2(M_0/q_0)^{1/2}} \quad (3.3.14)$$

$$s_{1,2} = \frac{\xi_{1,2}}{2(M_0/q_0)^{1/2}}; \quad s'_{1,2} = \frac{ds}{dT} = \frac{\dot{\xi}_{1,2}}{\frac{2M_0^{1/4} q_0^{1/4}}{m^{1/2}}}$$

$$V_N, V_O, V_H = \frac{v_n, v_o, v_H}{\frac{2M_o^{1/4} q_o^{1/4}}{m^{1/2}}} ; \quad V_O = \frac{dV_O}{dT} = \frac{\dot{v}_O}{2q_o/m} \quad \text{etc.} \quad (3.3.14)$$

$$W = \frac{w}{2(M_o/q_o)^{1/2}} ; \quad F(T) = \frac{f(t)}{2(M_o/q_o)^{1/2}} \quad \text{(cont.)}$$

The mass ratio μ and the force ratio γ are defined by:

$$\mu = \frac{M_v}{2m(M_o/q_o)^{1/2}} ; \quad \gamma = \frac{P_o}{4(M_o q_o)^{1/2}} \quad (3.3.15)$$

It is advantageous to consider the two phases of motion separately.

Accelerative Phase

During the accelerative phase the contact force is given by the yield force of the vehicle and thus $P(t)$ in equations (3.3.10) is constant P_o . In dimensionless form equations (3.3.2) become:

$$v'_O = -\frac{3}{2} \frac{1}{s_1 s_2} - \frac{1}{2} + \frac{4\gamma}{s_1 + s_2}$$

$$v_O \left(s'_1 + \frac{3}{2} v_H \right) = \frac{3}{4} \frac{s_1 + s_2}{s_1 s_2} - \frac{1}{2} s_1 - \frac{2\gamma s_1}{s_1 + s_2} \quad (3.3.16)$$

$$v_O \left(s'_2 - \frac{3}{2} v_H \right) = \frac{3}{4} \frac{s_1 + s_2}{s_1 s_2} - \frac{1}{2} s_2 - \frac{2\gamma s_2}{s_1 + s_2}$$

At the instant of impact $T = 0$, the response of the system is identical to that of the normal impact problem since the effect of axial forces is neglected. Thus the initial conditions are (see [3.10]):

$$\begin{aligned}
s_1(0) = s_2(0) &= (\gamma^2 + 3)^{1/2} - \gamma \\
v_0(0) &= 0
\end{aligned}
\tag{3.3.17}$$

The equations are nonlinear and we have not been able to obtain a closed form solution. The numerical technique used to obtain a solution is given in detail in section 3.3 (ii).

However, if the constant load is moving with constant velocity along the beam it is clear that a steady condition will eventually be reached. Setting V'_0 , S'_1 and S'_2 zero in equations (3.3.16) and subtracting the second from third gives with the first:

$$s_1 s_2 = 1, \quad s_1 + s_2 = 2\gamma \tag{3.3.18}$$

Substitution of these results into the second and the third gives:

$$s_1 = \gamma - v_0 v_H$$

$$s_2 = \gamma + v_0 v_H$$

but from equation (3.3.18) we have:

$$\begin{aligned}
s_1 &= \gamma - (\gamma^2 - 1)^{1/2} \\
s_2 &= \gamma + (\gamma^2 - 1)^{1/2}
\end{aligned}
\tag{3.3.19}$$

giving:

$$v_0 = (\gamma^2 - 1)^{1/2} / v_H$$

This steady state solution can be used as a check on the accuracy of the numerical method. We might note that steady solution which bears a marked resemblance to the above was given by Eason and Shield [3.14] in

studying the steady state motion of a rigid perfectly plastic cylindrical shell subject to a moving ring of force. The mechanical behavior of the two systems at the level of approximation employed is very similar. Transient solutions for moving problems were not considered in [3.14].

A typical example of the transition from the initial hinge configuration of $S_1 = S_2$ to that given by equations (3.3.19) is shown in figure 3.3.3. In this γ was taken as 2 with V_H and V_N as 1 (which in physical terms for a typical system would represent a fairly high impact velocity). The rapid separation of the hinges is evident although the steady state value of S_1 is achieved much more rapidly than S_2 , and also it is interesting to note that V_0 goes above the asymptotic value and approaches it from above.

The steady state is not of practical importance since it is not achieved in the problem under study. During the transient phase the mass is decelerating and the beam accelerating. At a certain time the requirement of contact between barrier and vehicle will require that the contact force decrease below the value P_0 after which time the mass becomes rigid and the force $P(t)$ is then unknown, and must be determined from the equation

$$P(t) = - M_v \dot{v}_n$$

where \dot{v}_n is given by equation (3.3.6). The values of S_1 , S_2 and V_0 at which the accelerative phase ends become the initial conditions for the decelerative phase.

Decelerative Phase

In the second phase of the motion the contact force is given by equation (3.3.11) with \dot{v}_n related to \dot{v}_0 by equation (3.3.6). Taken together and normalized using equations (3.3.14), (3.3.15), these equations indicate that the term γ in equations (3.3.16) must be replaced by the expression

$$\gamma = -\mu \left\{ v_0' - \frac{v_H v_0}{s_1} \right\} - \mu R \quad (3.3.20)$$

where

$$R = v_H \frac{v_0(T_1)}{s_1(T_1)} \frac{dT_1}{dT} + v_H' \left[- \int_{T_1}^T \frac{v_0(\tau)}{s_1(\tau)} d\tau \right] \quad (3.3.21)$$

with γ so replaced the first of equations (3.3.16) can be put into the form:

$$v_0' = \frac{4\mu v_H v_0}{s_1(s_1 + s_2 + 4\mu)} - \frac{(s_1 s_2 + 3)(s_1 + s_2)}{2s_1 s_2 (s_1 + s_2 + 4\mu)} - \frac{4\mu R}{s_1 + s_2 + 4\mu}$$

When γ is replaced as above in the second and third of equations (3.3.16) and v_0' is eliminated using equation (3.3.22) above we obtain the following equations for s_1' , s_2' :

$$v_0 s_1' = \frac{3}{4} \frac{s_1 + s_2}{s_1 s_2} - \frac{s_1}{2} - \frac{\mu s_1 (s_1 s_2 + 3)}{s_1 s_2 (s_1 + s_2 + 4\mu)} \quad (3.3.23)$$

$$- \frac{3}{2} v_0 v_H - \frac{2\mu s_1}{s_1 + s_2 + 4\mu} \left(\frac{v_0 v_H}{s_1} - R \right)$$

$$\begin{aligned}
V_0 s_2' = & \frac{3}{4} \frac{s_1 + s_2}{s_1 s_2} - \frac{s_2}{2} - \frac{\mu s_2 (s_1 s_2 + 3)}{s_1 s_2 (s_1 + s_2 + 4\mu)} \\
& + \frac{3}{2} V_0 V_H - \frac{2\mu s_2}{s_1 + s_2 + 4\mu} \left(\frac{V_0 V_H}{s_1} - R \right)
\end{aligned}
\tag{3.3.24}$$

We note that when V_H is zero these equations simplify considerably and reduce to essentially one equation for which a closed form solution can be obtained. Including V_H makes it necessary to solve the problem numerically and the details of the approach are given in the following section.

(ii) Numerical Examples

Numerical Approach

Both sets of equations (3.3.16) and (3.3.21) (3.3.22), (3.3.23) can be put into the form:

$$\begin{aligned}
v_0' &= g(s_1, s_2, v_0) \\
v_0 \left(s_1' - \frac{3}{4} v_0 v_H \right) &= g_1(s_1, s_2, v_0) \\
v_0 \left(s_2 + \frac{3}{2} v_0 v_H \right) &= g_2(s_1, s_2, v_0)
\end{aligned}
\tag{3.3.25}$$

In the first phase, g , g_1 , g_2 are independent of v_0 and also $g_2(s_1, s_2) = g_1(s_2, s_1)$. The equations are linearized in each time step and the values of the functions g , g_1 , g_2 are estimated at the center of the step. For example, for the first of equations (3.3.25) we use:

$$v_0'(T_n) = g[s_1(T_n), s_2(T_n), v_0(T_n)] + \frac{1}{2} \frac{\partial g}{\partial s_1} [s_1(T_n), s_2(T_n), v_0(T_n)] s_1' \Delta T$$

$$+ \frac{\Delta T}{2} \frac{\partial g}{\partial g_2} [s_1(T_n), s_2(T_n), v_0(T_n)] s_2' + \frac{1}{2} \frac{\partial g}{\partial v_0} [s_1(T_n), s_2(T_n), v_0(T_n)] v_0' \Delta T$$

and similarly for the second and third of equations (3.3.25). These reduce to a system of the form $\sum_{j=1}^3 a_{ij} Y_j' = c_i$, $i = 1, 2, 3$ applicable in each time step where Y_1', Y_2', Y_3' denotes $v_0'(T_n), s_1'(T_n), s_2'(T_n)$ respectively in the time step in particular and the a_{ij}, c_i are computed from equations (3.3.25). These are solved for Y_j' and we obtain:

$$Y_j(T_{n+1}) = Y_j(T_n) + Y_j'(T_n) \Delta T, \quad j = 1, 2, 3$$

The initial conditions for the first phase are given by equations (3.3.17) and the initial conditions of the second phase are obtained as the final state of the first phase. It is necessary in the computation process to retain $V(X, T)$ for all X of interest and determine $W(X, T)$ by integration. Also it is necessary to retain the function $H(T) = F(T) + S_1(T)$ in order to solve for T_1 to be used in computing R in each time step.

Examples and Discussion

Numerical examples showing the hinge configuration and the velocity of the beam at the point of contact during the beam motion in both phases were carried out using the above numerical technique. In all cases, the mass and force parameters were taken to be $\mu = 5.0$, $\gamma = 2.0$, and V_H was taken to be constant. Figure 3.3.4 shows some results of computation for impact with vehicle arriving velocity $V_v = 0.6$ and impact angles $\alpha = 15^\circ, 30^\circ, 45^\circ$ with respect to the beam. Because of the

inclusion of the convective terms in the computation, the curves for V_0 in decelerative phase are concave downward in contrast to those in the normal impact case 3.10, which were fairly straight. It is also worth noting that when the beam motion comes to rest the final hinge distance S_1 is equal to S_2 . This is due to the fact that the beam motion is non-decreasing and if $V_0 = 0$ equations (3.3.23), (3.3.25), become identical. Using these equations, it is easy to show that the final hinge distance is given by the positive root of the cubic equation.

$$S^3 + (3 - 2R)\mu S^2 - 3S - 3\mu = 0$$

where R is given by equation (3.3.21).

A typical beam deflection pattern and vehicle impact trajectory during the motion is shown in figure 3.3.6. In this example, computations were performed for $V_H = 0.23$, $V_n = 0.4$ which correspond to $V_v = 0.46$ and $\alpha = 60$. The corresponding results for S_1 , S_2 , V_0 are shown in figure 3.3.5.

The results obtained in this section are limited in validity by the idealized assumptions stated in introduction. The neglect of the effect of the axial forces in the beam enables us to justify ignoring the effect of frictional forces on the beam itself while taking them into account in determining the horizontal component of the mass velocity as a prescribed function. This may be unsatisfactory in actual cases. Nevertheless, it is believed that the results presented herein are useful for gaining a qualitative picture of the characteristics of the problem.

One important feature of the present solution is the derivation of the relationships between $v_0(t)$ and $v_n(t)$, $\dot{v}_0(t)$ and $\dot{v}_n(t)$. The

convective terms included in these relations allow us to determine the impact mass trajectory. It is clear by equation (3.3.3) that at the end of the beam motion when $t = t_f$, $v_0(t_f) = 0$, therefore $v_n(t_f) = \left[\frac{\partial w}{\partial x} \Big|_{x=f(t_f)} \right] v_H(t_f)$ which, in fact, is negative. Thus the impacting mass leaves the system with velocity components $v_n(t_f)$ and $v_H(t_f)$. If however, these terms were neglected, the trajectory would be a non-decreasing function leading to an absurd conclusion in real cases.

The results are further limited in that strain rate effects are ignored by the assumption of fixed values of the yield parameters M_0 , q_0 , P_0 .

(iii) Notation for Section 3.3

C	velocity of a moving section in barrier
$f(t), F(t)$	Lagrangian position of point of contact of vehicle and barrier, and its dimensionless quantity
g, g_1, g_2	notations for function
$M(x,t), M_0$	moment and yield moment of barrier
M_v	mass of vehicle
m	mass per unit length of barrier
$P(t)$	force between impacting mass and barrier
P_b	static load carrying capacity of the barrier system
P_0	yield force of vehicle
$p(x,t)$	distributed load on per unit length of barrier
Q	shear force of barrier
q_0	yield force per unit length of support
S_1, S_2	dimensionless right and left lateral hinge distances with respect to the central hinge
t, T	time and dimensionless time
t_1, T_1	time and dimensionless time when the rightmost hinge passes a specific section of barrier
$v(x,t)$	velocity field of barrier
$v_0(t), V_0(T)$	velocity of barrier at point of contact with vehicle and its dimensionless quantity
$v_n(t), V_n(T)$	normal (to the barrier) component of the velocity of the vehicle and its dimensionless quantity
$v_H(t), V_H(T)$	horizontal (parallel to the barrier) component of the velocity of the vehicle and its dimensionless quantity

$w(x,t), W(X,T)$	displacement field of barrier and its dimensionless quantity
t_f	final time when the beam motion ends
x,X	real and dimensionless Lagrangian coordinate along barrier axis
Y_j	dimensionless variable
α	angle of impact with respect to barrier
μ	mass ratio
γ	force ratio
τ	dummy time variable
ξ_1, ξ_2	real distances of the right and left hinges with respect to the central hinge

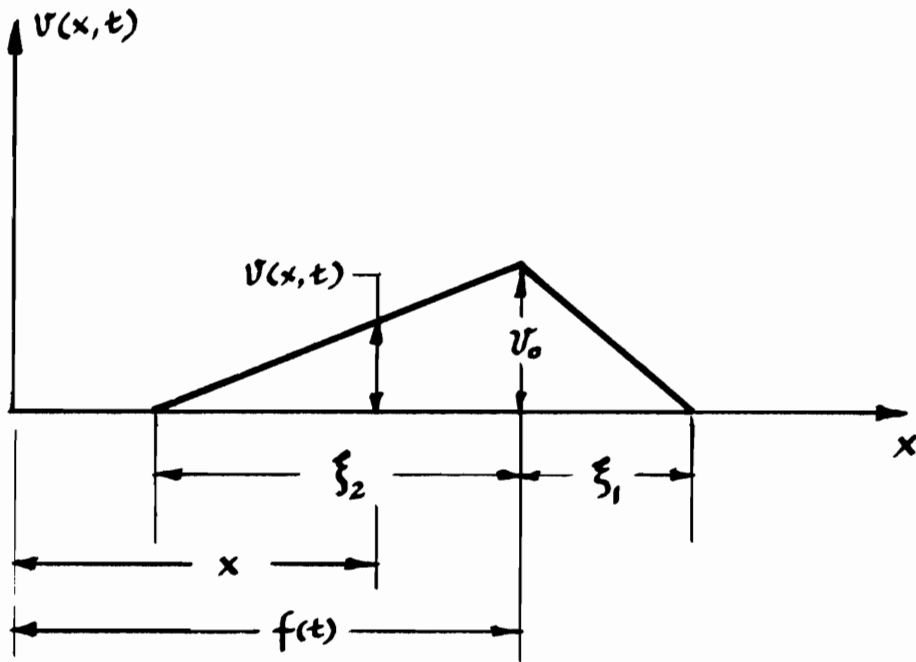


Figure 3.3.1. Velocity Field and Coordinate System

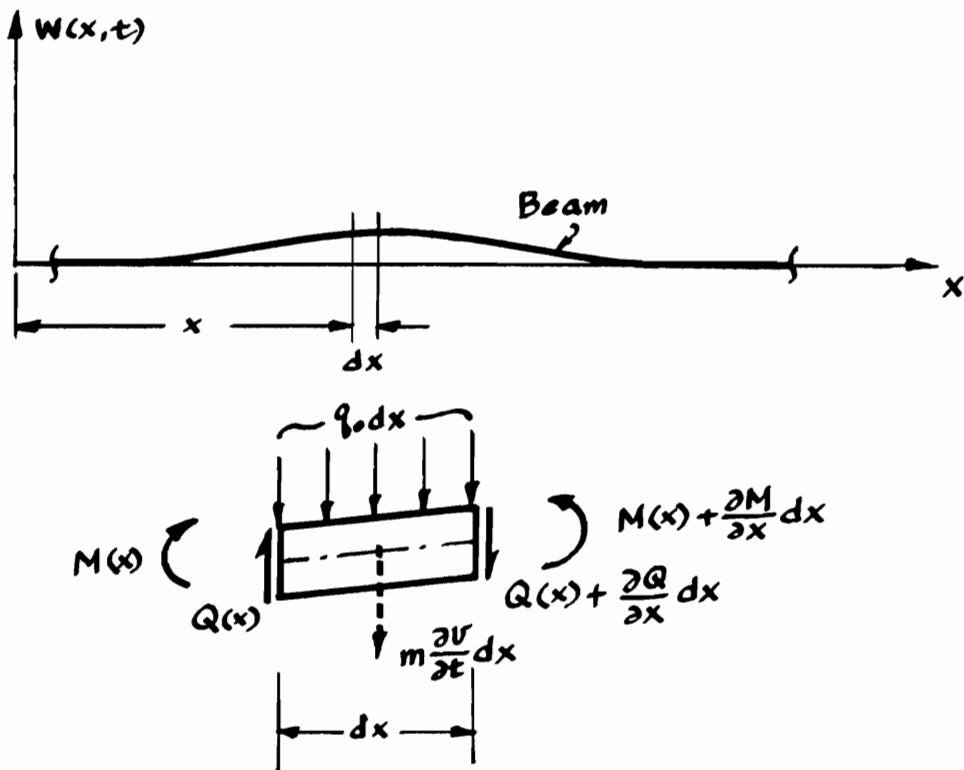


Figure 3.3.2. Displacement Field and Beam Element

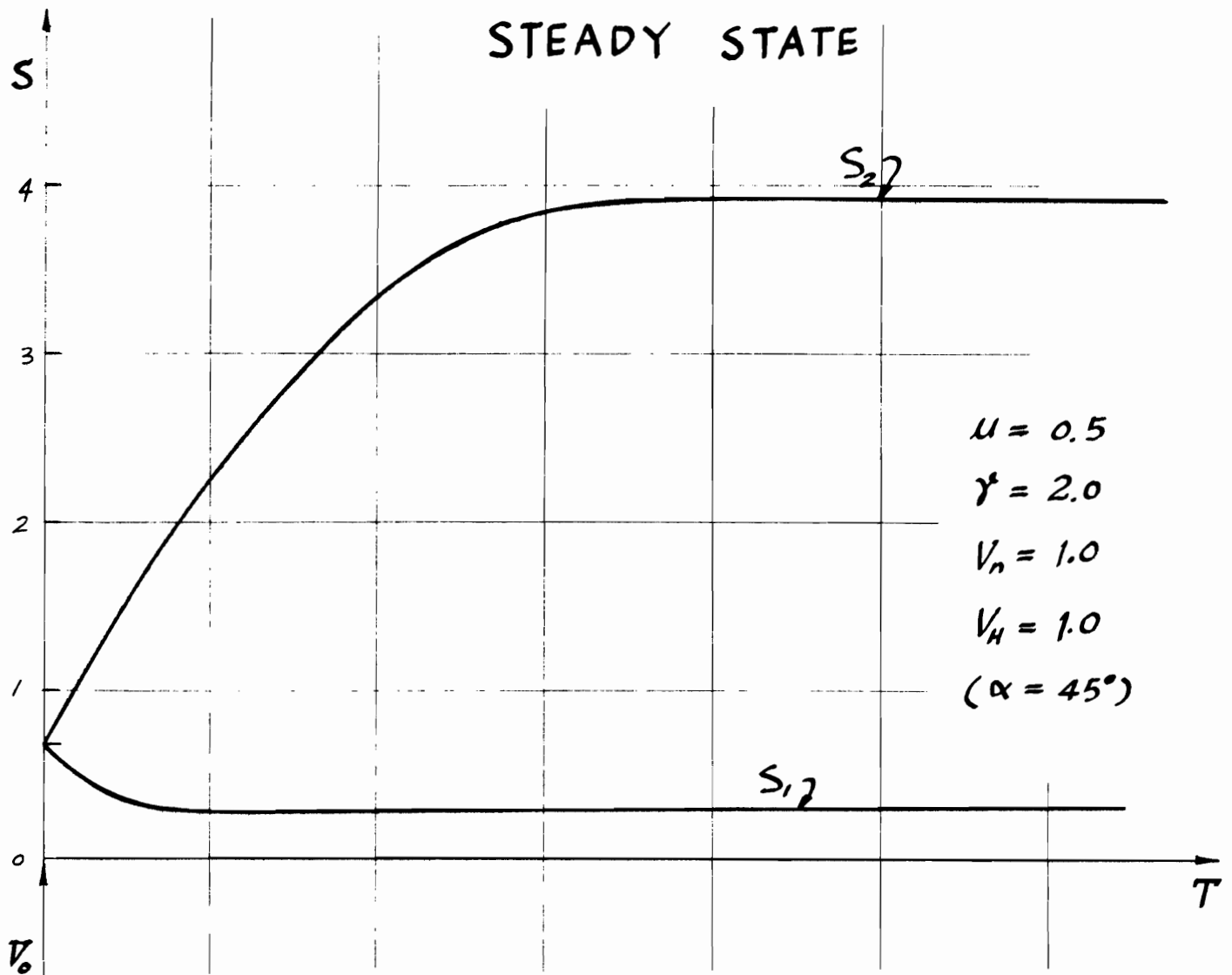
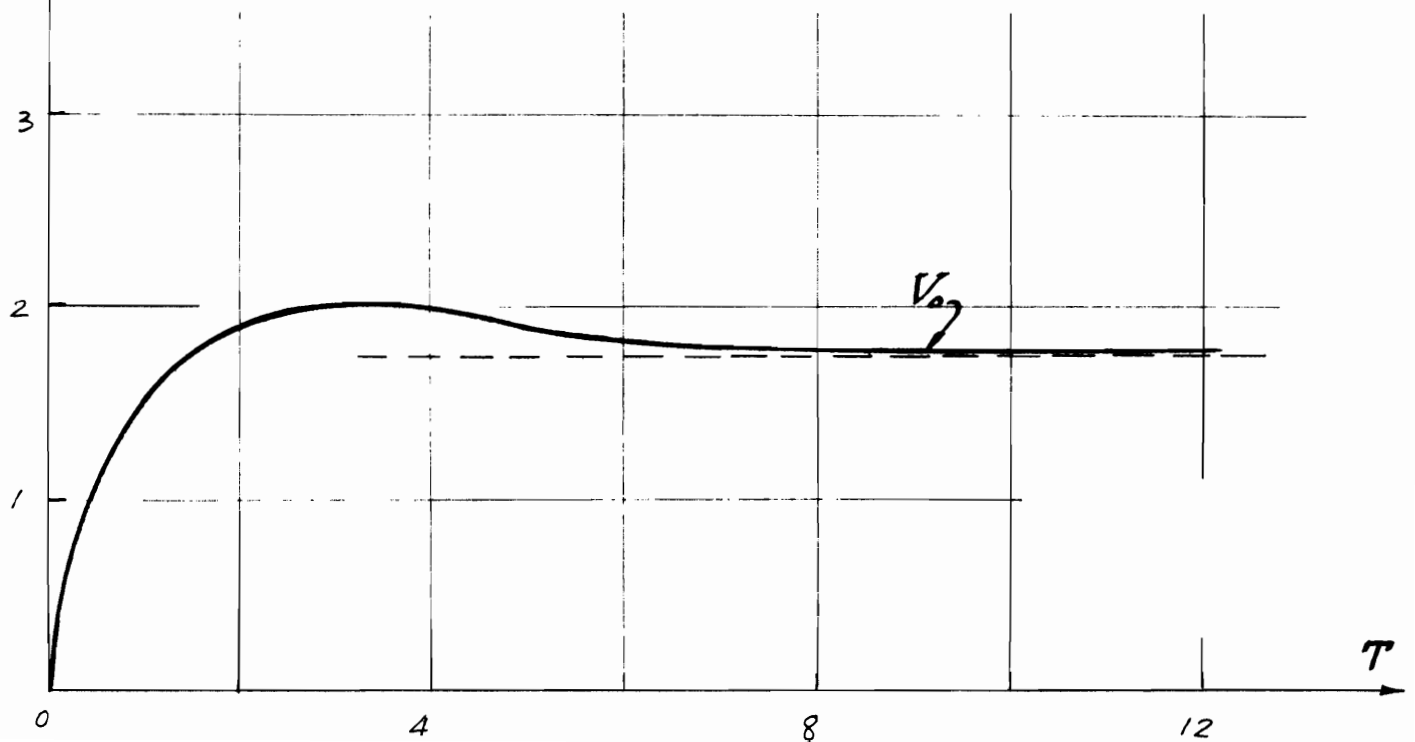


Figure 3.3.3. Steady-state Barrier Velocity at Point of Contact and Hinge Distances



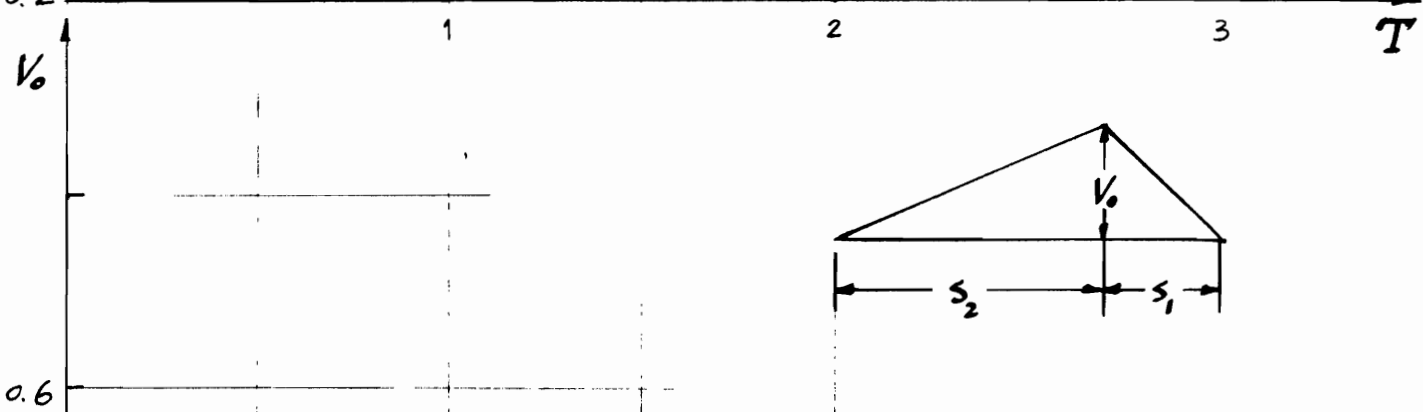
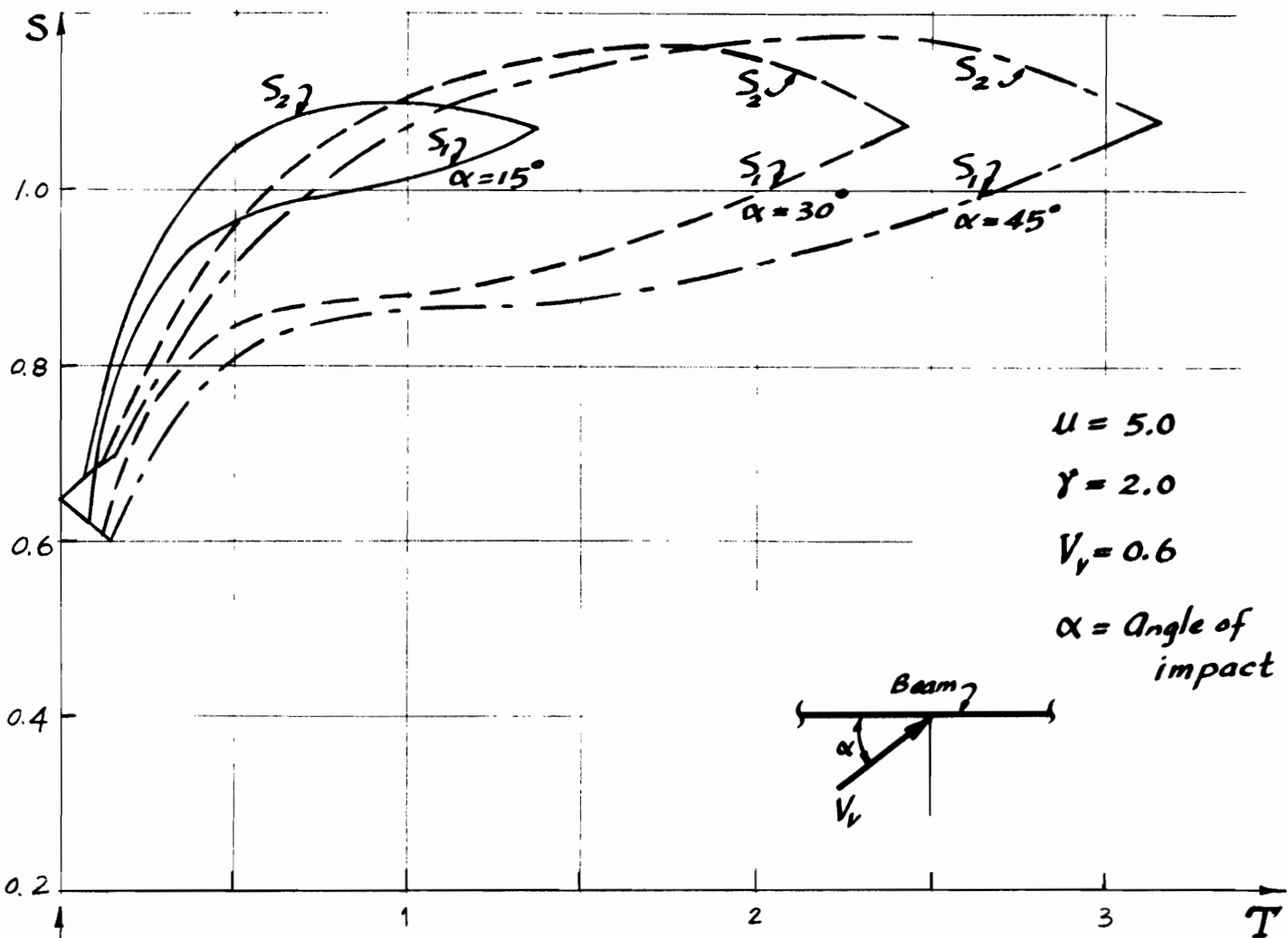
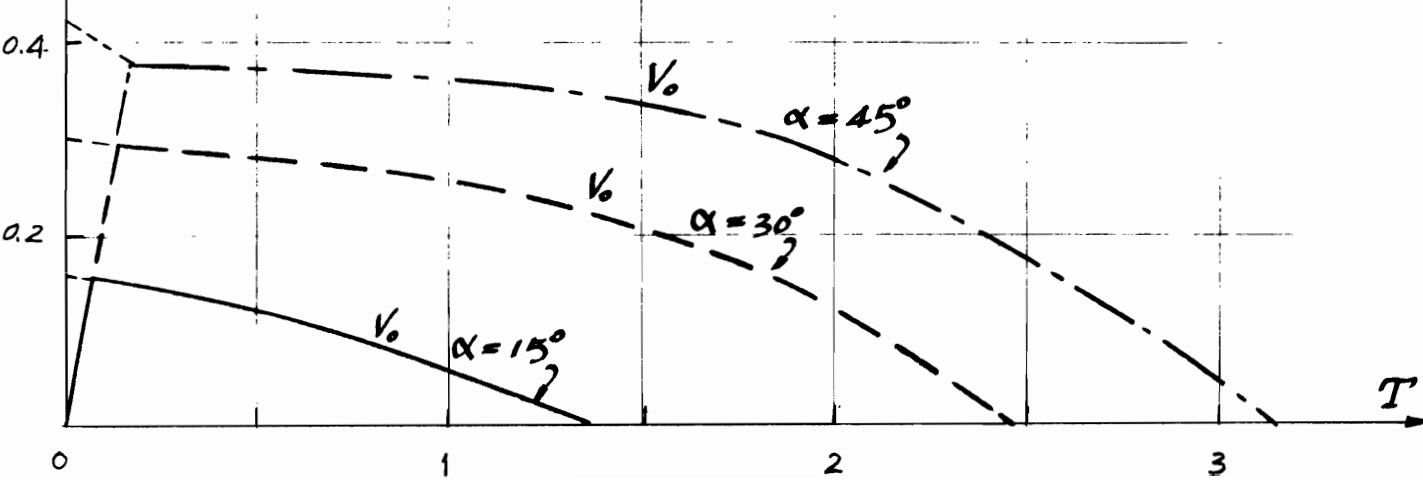


Figure 3.3.4. Barrier Velocity at Point of Contact and Hinge Distances as Angle of Impact Varying



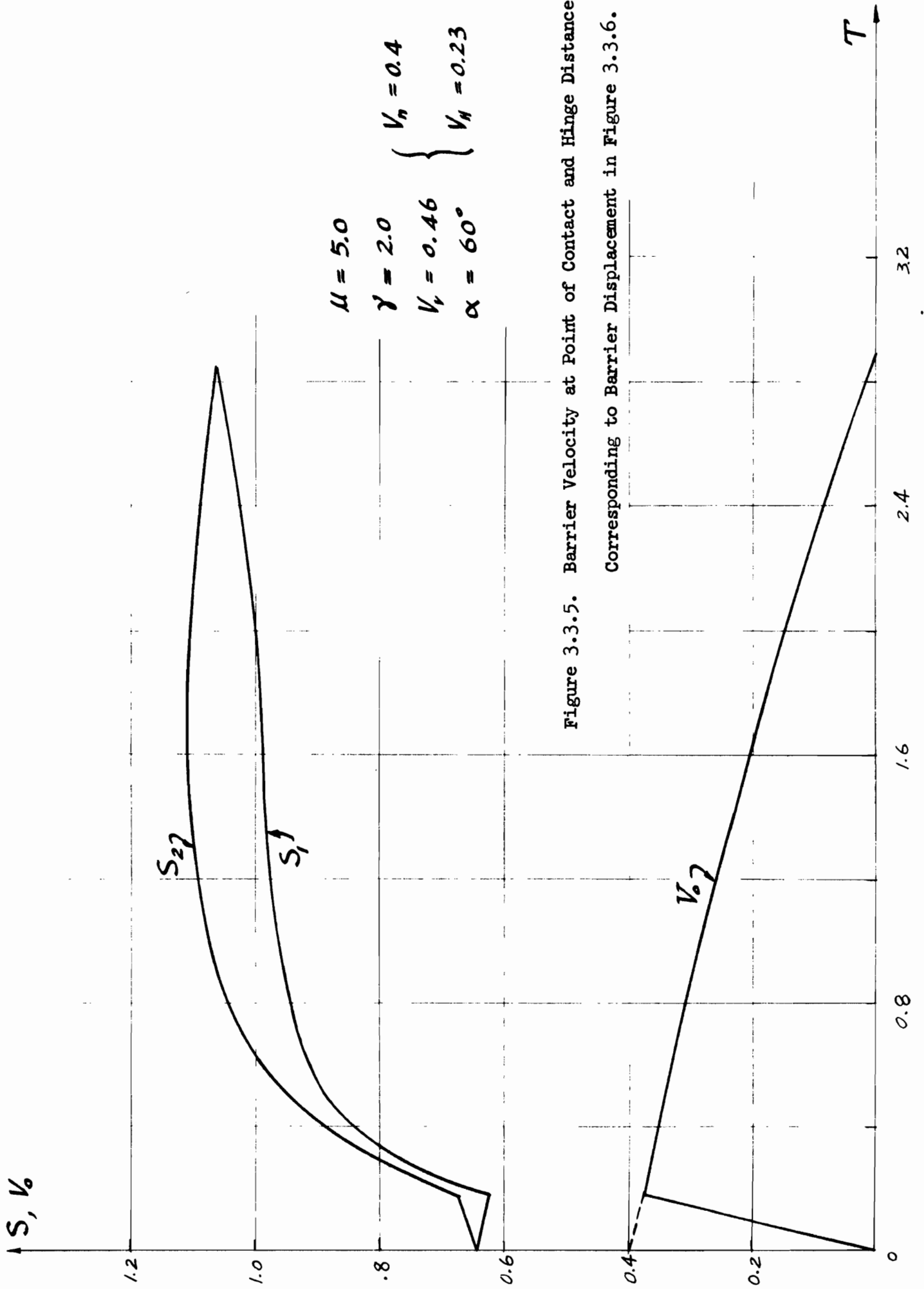


Figure 3.3.5. Barrier Velocity at Point of Contact and Hinge Distances Corresponding to Barrier Displacement in Figure 3.3.6.

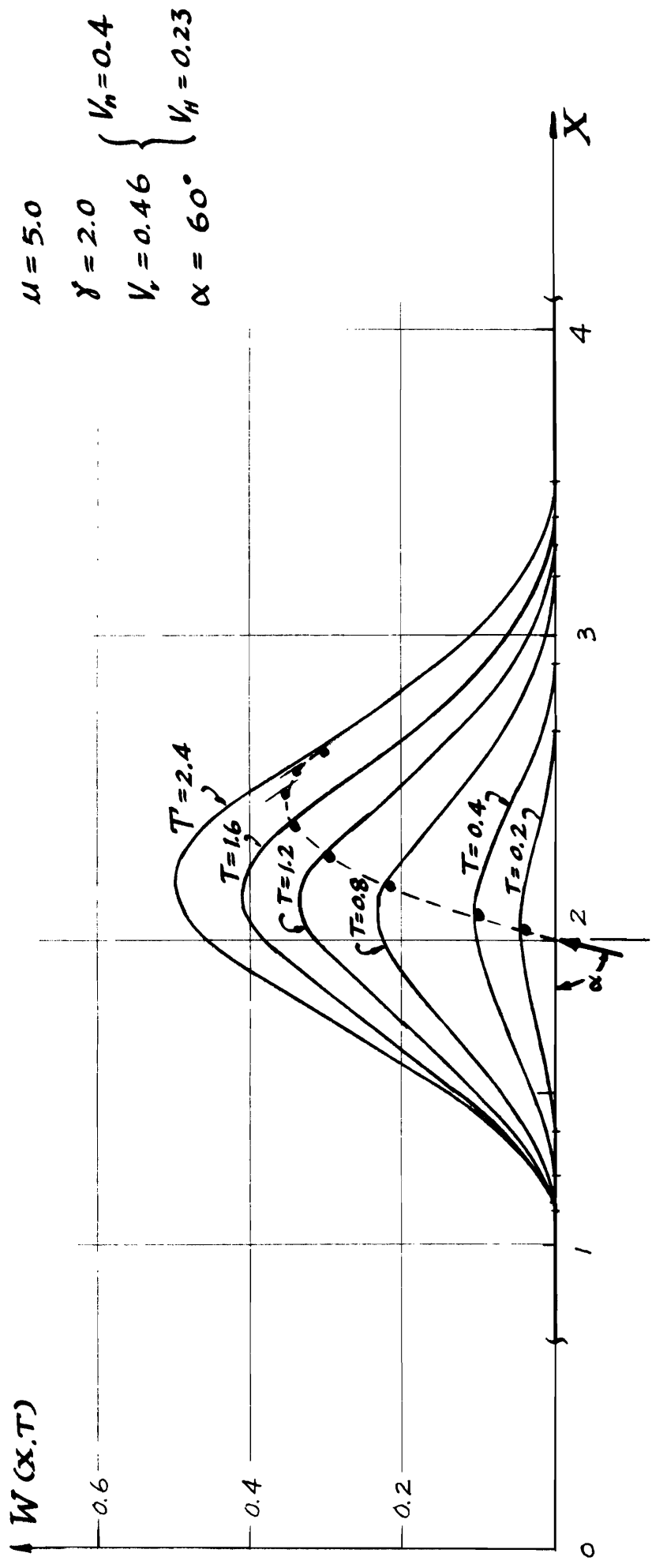


Figure 3.3.6. Barrier Displacement Pattern

3.4 Combined Loading in Rigid Perfectly Plastic Beams

(i) Interaction Effects due to Shear and Axial Forces

In a general one-dimensional structure such as a beam subject to general arbitrary static or dynamic loading, three stress resultants can exist in two principal planes of the beam, namely torsional moment, bending moment and shear force, and also an axial force may exist along the axis of the beam. For the present discussion, we assume that the beam has a plane of symmetry and the load is applied in this plane so that the torsional effect disappears and only the other three forces remain. Bending moment and shear forces are always present when the beam is under transverse load, while the axial force may arise due to the presence of initial tension (or compression) or may develop due to the existence of axial constraints and the geometric changes in the beam axis. The static analysis of a rigid plastic beam shows that the influences due to shear are small and can be neglected. However, this is not true in the case when the beam is subjected to large localized dynamic loading transverse to the beam axis like impact of a mass on the beam. Also in an indeterminate system, axial constraints are always present, and the axial force arises immediately when the transverse deflection of the beam axis is finite. The catenary effect of this axial force becomes very significant when the deflection is large. In an analysis of a fixed-fixed beam of rectangular section subjected to transverse dynamic loading, Symonds and Mentel [3.15] have shown that when the central deflection of the beam axis reaches a magnitude roughly equal to the beam depth, the axial force becomes equal to the yield limit of the beam in tension and the bending resistance vanishes. The beam thus behaves like a plastic string carrying the load purely by means

of the axial force without moment. Therefore, in a dynamic analysis of a rigid plastic beam with axial constraints, the effect of shear and axial force must be taken into account and a discussion of the interaction problem becomes necessary.

On the assumption of rigid perfectly plastic behavior of the beam material and according to the general theory of limit analysis [3.16], there exists some function of the stress resultants, the yield function, which along with the corresponding flow rule characterizes the material behavior in the plastic range. It is assumed that if, in a beam element, the yield function takes a certain critical value, the yield limit is reached and the beam element deforms plastically according to the flow rule. If we denote the bending moment, shear and axial forces by M , Q and N respectively, and the corresponding individual yield limits by M_0 , Q_0 , and N_0 , that is M_0 , Q_0 , and N_0 are the yield limits of the beam element in pure bending, pure shear and pure extension, then in a three dimensional Cartesian stress space with M/M_0 , Q/Q_0 , and N/N_0 as coordinate axes, the yield condition can be represented in the form:

$$f \equiv f \left(\frac{M}{M_0}, \frac{Q}{Q_0}, \frac{N}{N_0} \right) = 0 \quad (3.4.1)$$

Assuming that the plastic strain rate sensitivity is ignored in the present treatment, the yield function in equation (3.4.1) represents a fixed closed surface called yield surface in the stress space for both static or dynamic loading. The stress state in a beam element is identified by a stress point in this space with coordinates $(M/M_0, Q/Q_0, N/N_0)$. When inside the yield surface, no plastic deformation takes place. A stress point outside the yield surface is not acceptable. Plastic strains (generalized strains) can only occur when the point lies

on the yield surface. In such case, the associated flow rule requires that the strain rate vector with components $(M_0 \dot{\kappa}, Q_0 \dot{\gamma}, N_0 \dot{\epsilon})$ is in the direction of the outward normal to the yield surface, wherever the surface is smooth and must lie in the region bounded by the normals to the adjacent yield surface when the stress point corresponds to a point on a corner of the yield surface. Mathematically, we can represent the flow rule as

$$M_0 \dot{\kappa} : Q_0 \dot{\gamma} : N_0 \dot{\epsilon} = \frac{\partial f}{\partial \left(\frac{M}{M_0} \right)} : \frac{\partial f}{\partial \left(\frac{Q}{Q_0} \right)} : \frac{\partial f}{\partial \left(\frac{N}{N_0} \right)} \quad (3.4.2)$$

where $\dot{\kappa}$ is the curvature rate of the beam axis, $\dot{\gamma}$ the shearing strain rate and $\dot{\epsilon}$ the extensional strain rate. In spite of the fact that shear cannot be considered properly as a purely local yielding condition [3.17], approximate forms of the yield function for combined action of M , Q , and N have been proposed and used by various authors (see Symonds [3.18]) for the analysis of a particular beam cross section and a specific type of structure. For example, Symonds and Nonaka [3.19] have suggested a yield function for a rectangular beam in the form:

$$f \equiv \left\{ \left| \frac{M}{M_0} \right| + \left(\frac{N}{N_0} \right)^2 - 1 \right\} \left\{ \left| \frac{Q}{Q_0} \right| - 1 \right\} \quad (3.4.3)$$

while Neal [3.20] has used the different form

$$f \equiv \left| \frac{M}{M_0} \right| + \left(\frac{N}{N_0} \right)^2 + \frac{\left(\frac{Q}{Q_0} \right)^4}{1 - \left(\frac{N}{N_0} \right)^2} - 1 \quad (3.4.4)$$

for analysis of a cantilever beam under tip loading.

The fact that the interaction of shear with bending moment and axial force in a yield function is approximate and uncertain and also that comparison between theoretical and experimental results for a fixed-fixed beam under dynamic loading [3.21] has shown that dynamic rigid plastic analysis neglecting strain rate sensitivity over-estimates the final deflection and the inclusion of shear effects would worsen rather than improve the correspondence, suggests that it is reasonable for the present analysis to ignore the shear interaction in the yield function. Thus in the subsequence analysis, we will use the yield function in the form:

$$f \equiv f \left(\frac{M}{M_0}, \frac{N}{N_0} \right) = 0 \quad (3.4.5)$$

and the associated flow rule:

$$\frac{N_0 \dot{\epsilon}}{M_0 \dot{k}} = \frac{\partial f / \partial \left(\frac{N}{N_0} \right)}{\partial f / \partial \left(\frac{M}{M_0} \right)} \quad (3.4.6)$$

For a rectangular beam section, Eqs. (3.4.5) and (3.4.6) are:

$$f \equiv \left| \frac{M}{M_0} \right| + \left(\frac{N}{N_0} \right)^2 - 1 = 0 \quad (3.4.7)$$

and

$$\frac{N_0 \dot{\epsilon}}{M_0 \dot{k}} = 2 \frac{N}{N_0} \quad (3.4.8)$$

To obtain a qualitative picture of the influence of axial force on dynamic beam behavior in plastic deformation, it is worthwhile to examine

first its influence on static cases. Consider here a pin-pin supported uniform beam of rectangular section with length L subjected to a static concentrated load P at mid-span. The pin supports at both ends constraint the beam against axial motion. Suppose the load P is sufficiently large to cause collapse of the beam, a central plastic hinge forms under the load P and the beam deforms plastically as shown in Figure 3.4.1.

Denoting the central deflection of the beam axis by δ , the rotation at central plastic hinge by θ , and the corresponding rates by $\dot{\delta}$ and $\dot{\theta}$, and choosing the origin of the coordinate of beam axis at mid-span, the curvature rate becomes $\dot{\kappa} = \dot{\theta}\delta(x)^*$. The flow rule (3.4.8) requires that

$$\dot{\epsilon} = 2 \frac{M_0}{N_0} \frac{N}{N_0} \dot{\kappa} \quad (3.4.9)$$

hence

$$\dot{u} = \int_{-l/2}^{l/2} \dot{\epsilon} dx = 2 \frac{M_0}{N_0} \frac{N}{N_0} \dot{\theta} = 2 \frac{M_0}{N_0} \frac{N}{N_0} \frac{4\dot{\delta}}{l} \quad (3.4.10)$$

where \dot{u} is the extensional rate of the beam and $N(x)$ is assumed uniform along the beam axis.

From the geometry of the deformation we have:

$$u = 2 \left[\left(\frac{l}{2} \right)^2 + \delta^2 \right]^{1/2} - l \approx \frac{2\delta^2}{l}$$

thus:

$$\dot{u} = \frac{4\delta\dot{\delta}}{l} \quad (3.4.11)$$

Comparing (3.4.10) and (3.4.11) we get:

* $\delta(x)$ is the Dirac Delta Function.

$$\frac{N}{N_0} = \frac{N_0}{M_0} \frac{\delta}{2} \quad (3.4.12)$$

It is therefore clear that when the beam is at incipient collapse, $\delta = 0$, thus $N = 0$ and no axial force develops. However, when δ becomes finite then N develops according to (3.4.12). Since for a rectangular beam $N_0/M_0 = 4/h$, hence when $\delta = h/2$, $N/N_0 = 1$, that is when the central deflection of the beam increases to half of the beam depth at which time the beam reaches the yield limit in tension, the bending resistance of the beam vanishes and the beam then behaves like a "plastic string."

If we picture the stress states of the beam element at mid-span (yield hinge) by points on the yield curve figure 3.4.2, it can be seen that when the beam is at incipient collapse the stress state corresponds to the point A on the yield curve. As δ increases from zero to a finite value, N grows and the point A shifts along the yield curve to an intermediate point B, where the components of plastic strain rate vector has the ratio

$$\frac{N_0 \dot{\epsilon}}{M_0 \dot{\kappa}} = 2 \frac{N}{N_0} \quad .$$

When $\delta = h/2$ and $N = N_0$, the point B reaches the corner C of the yield curve and this beam element deforms according to $-2 \leq N_0 \dot{\epsilon}/M_0 \dot{\kappa} \leq 2$.

An interesting result is that if the beam was originally subjected to an initial tension N_1 , this initial tension releases instantaneously when the beam is at incipient collapse, provided that the end supports are constrained to move axially. The reason is that if the beam carries an initial tension N_1 , at incipient collapse the stress state at yield hinge corresponds to the point, say B on the yield curve, thus according

to (3.4.9), we have:

$$\dot{\epsilon} = 2 \frac{M_0}{N_0} \frac{N_1}{N_0} \dot{\kappa}$$

Since $N_1 \neq 0$, $\dot{\kappa} \neq 0$ at incipient collapse, hence $\dot{\epsilon} \neq 0$, and the beam extends instantaneously and releases the initial tension N_1 due to the rigid axial constraints. Thus the point B shifts instantaneously to the point A on the yield curve.

By equilibrium consideration of the system, we are led to

$$Q = \frac{2M}{l}$$

$$2Q + N\theta = P$$

after incipient collapse. Combining two equations, we get:

$$\frac{4M}{l} + N\theta = P \quad (3.4.13)$$

Eliminating N from (3.4.13) and the yield condition (3.4.7) and use of (3.4.12) gives

$$\frac{4M_0}{l} + \frac{N_0^2}{M_0} \frac{\delta^2}{l} = P$$

or

$$\frac{Pl}{4M_0} = 1 + \left(\frac{N_0 l}{M_0}\right)^2 \left(\frac{\delta}{2l}\right)^2 \quad (3.4.14)$$

Since for a rectangular beam $M_0/N_0 = h/4$, thus equation (3.4.14) becomes:

$$\frac{Pl}{4M_0} = 1 + \left(\frac{\delta}{h/2}\right)^2, \quad \delta \leq \frac{h}{2} \quad (3.4.15)$$

For $\delta > h/2$ we have

$$P = \frac{4N_0}{\ell} \delta$$

or

$$\frac{P\ell}{4M_0} = \frac{N_0}{M_0} \delta = \frac{4}{h} \delta \quad (3.4.16)$$

The $P - \delta$ relationship is shown in figure 3.4.3.

If, instead of a rectangular beam, we consider the general case where the yield condition can be represented as

$$f \equiv \left| \frac{M}{M_0} \right| + \left(\frac{N}{N_0} \right)^\alpha - 1 = 0 \quad (3.4.17)$$

we note that as $\alpha = 1$, it represents the yield condition for an ideal I Section; $\alpha = 2$ for rectangular beam. The family of yield curves for (3.4.17) are plotted for one quadrant as shown in figure 3.4.4. The limiting case when $\alpha \rightarrow \infty$ represents a yield curve formed by two straight lines $M/M_0 = 1$ and $N/N_0 = 1$ in the first quadrant.

With the yield condition (3.4.17), the $P - \delta$ relationship for this beam system can be obtained easily, following the same derivation, in the form

$$\frac{P\ell}{4M_0} = 1 + \left(\frac{N_0\ell}{M_0} \right)^{\frac{\alpha}{\alpha-1}} \left(\frac{\delta}{\alpha\ell} \right)^{\frac{\alpha}{\alpha-1}} (\alpha - 1), \quad 1 \leq \alpha < \infty \quad (3.4.18)$$

for $N/N_0 < 1$ and where

$$\frac{N}{N_0} = \left(\frac{N_0\ell}{M_0} \right)^{\frac{1}{\alpha-1}} \left(\frac{\delta}{\alpha\ell} \right)^{\frac{1}{\alpha-1}} \quad (3.4.19)$$

when $N/N_0 = 1$ we obtain

$$\frac{Pl}{4M_0} = \frac{N_0}{M_0} \delta \quad (3.4.20)$$

A family of $P - \delta$ curves for values of α is shown in figure 3.4.5.

It is worthwhile to note that if the beam in previous discussion is clamped at both ends, the same argument follows except for some minor changes to account for the resisting moments at the two additional yield hinges at the clamped ends. For example, if the beam is of rectangular section, we can easily find that

$$\frac{N}{N_0} = \frac{N_0}{M_0} \cdot \frac{\delta}{l} \quad (3.4.21)$$

and

$$\frac{Pl}{8M_0} = 1 + \left(\frac{N_0 l}{M_0}\right)^2 \left(\frac{\delta}{2l}\right)^2, \quad \frac{N}{N_0} < 1 \quad (3.4.22)$$

(ii) Moving Mass Impact on a Rigid Perfectly Plastic Beam with Axial Force Interaction

Consider a beam of unlimited extent, $-\infty < x < \infty$ of mass m per unit length subjected to a concentrated impact force $P(t)$ normal to the beam axis at $x = 0$. The beam is supported laterally by a rigid perfectly plastic backing material which provides a continuous normal reaction to the beam. The lateral beam displacement rate is zero if the normal reaction is below a yield value denoted by q_0 (force per unit length). The shear resistance of the backing material parallel to the beam axis is assumed to be zero, so that no distributed axial force acts along the beam during deformation and no combined stress problem is considered in the supporting material. Furthermore, it is assumed that the beam is held rigid at infinity so that the axial motion of the beam is constrained.

It is clear that at the instant of impact the beam remains straight and, as discussed in the preceding section, no axial force can be developed. However, finite axial force can arise as soon as the beam acquires a finite deflection, and the axial force will grow continuously as the beam deflection increases. The axial force may or may not reach the limiting value N_0 at some later time. The correlations between the axial force and the beam deflection will be discussed in the following section.

It is assumed that the change of the slope angle of the deformed beam is sufficiently small that the axial force N can practically be taken as uniform throughout the beam. Mathematically, this requires that the slope $\partial w / \partial x$ be so small that $(\partial w / \partial x)^2 \ll 1$, where $w = w(x, t)$ is the deflection of the beam. Due to the magnitude of the axial force,

the mechanical behavior of the beam-support system during motion should be separated into two cases, namely (i) when $N/N_0 < 1$ (ii) when $N/N_0 = 1$ and discussed separately.

At the instance of impact, the beam is subjected to a concentrated impact force $P(t)$ at $x = 0$. The beam will deform provided that the magnitude of the force is sufficiently large to produce plastic deformation of the beam and convert the beam into a mechanism. It is assumed that there exists a system of three yield hinges one at the point of contact and the other two on either side of it with distance $\pm \xi(t)$ from the central hinge. In the first stage of the beam motion, the axial force N is small and uniform throughout the beam, the bending moment takes the same maximum value at the yield hinges as in the case of no axial force interaction according to the yield condition. Since the bending moment at the central hinge is at negative maximum and are at the positive maximum at the lateral hinges, it follows that the beam is rigid between the central hinge and a lateral hinge, and that the shear force must vanish at the yield hinges if no concentrated load acts there. With this consideration, the velocity field of the beam $v(x, t)$ assumes the form

$$\begin{aligned}
 v(x, t) &= v_0(t) \left\{ 1 - \frac{x}{\xi(t)} \right\}, & 0 \leq x \leq \xi(t) \\
 &= 0, & \xi(t) \leq x
 \end{aligned}
 \tag{3.4.23}$$

where $v_0(t) = v(0, t)$ is the velocity of the central yield hinge (figure 3.4.6). The deflection $w(x, t)$ of the beam is then given by

$$w(x, t) = \int_0^t v(x, t') dt'$$

i.e.

$$w(x, t) = \int_0^t v_0(t') \left[1 - \frac{x}{\xi(t')} \right] dt', \quad 0 \leq x \leq \xi(t)$$

$$= 0, \quad \xi(t) \leq x \quad (3.4.24)$$

provided that $\xi(t)$ is a non-decreasing function.

Dynamic Equations of Motion

To include the effect of the axial force N in a consistent manner the dynamical equations of the motion of the beam are written in the deformed configuration. However the spatial variation of the axial force N is neglected thus ignoring the effects of inertia due to axial accelerations of the beam. The notation and sign conventions are indicated in figure 3.4.7.

By considering the dynamic equilibrium of a beam element as shown in figure 3.4.7, we obtain the differential equations of motion as

$$\frac{\partial Q}{\partial x} = -q_0 - m\ddot{w} + N \frac{\partial^2 w}{\partial x^2}$$

$$N(x, t) = N(t) \quad (3.4.25)$$

$$\frac{\partial M}{\partial x} = Q$$

where, as before, $Q = Q(x, t)$ denotes the shear force in the beam element $N = N(x, t)$ the axial force; $M = M(x, t)$ the bending moment.

Combining and integrating equations (3.4.25) from $x = 0$ to x and using the fact that

$$\ddot{w} = \dot{v}_0 \left(1 - \frac{x}{\xi}\right) + v_0 \frac{x\dot{\xi}}{\xi^2}$$

we obtain

$$\begin{aligned} Q(x, t) = Q(0, t) = q_0 x - mv_0 \left(x - \frac{x^2}{2\xi}\right) \\ - mv_0 \frac{x\dot{\xi}}{2\xi^2} + Nw'(x, t) - Nw'(0, t) \end{aligned} \quad (3.4.26)$$

And integrating the above equation from $x = 0$ to x leads to

$$\begin{aligned} M(x, t) = M(0, t) + \frac{Px}{2} - \frac{q_0 x^2}{2} - mv_0 \left(\frac{x^2}{2} - \frac{x^3}{6\xi}\right) \\ - mv_0 \frac{x^3 \dot{\xi}}{6\xi^2} + Nw(x, t) - Nw(0, t) \end{aligned} \quad (3.4.27)$$

When $x = \xi$ is inserted in the two equations above, and using the boundary conditions $x = 0, \xi$, that is

$$Q(0, t) = \frac{P}{2} + Nw'(0, t), \quad Q(\xi, t) = 0$$

and

$$M(0, t) = -\bar{M}, \quad M(\xi, t) = \bar{M}$$

where \bar{M} according to the yield condition

$$f \equiv \left| \frac{\bar{M}}{M_0} \right| + \left(\frac{N}{N_0} \right)^2 - 1 = 0$$

is the reduced yield moment of the beam due to interaction of axial force N , we then obtain the dynamical equations of motion

$$\frac{P}{2} = q_0 \xi + \frac{m}{2} (\dot{v}_0 \xi + v_0 \dot{\xi}) \quad (3.4.28)$$

and

$$2M + Nw_0 = \frac{P\xi}{2} - \frac{q_0 \xi^2}{2} - \frac{m}{6} (2\dot{v}_0 \xi^2 + v_0 \dot{\xi}^2)$$

Kinematic Constraints

To obtain the necessary kinematic conditions we consider the successive displacement pattern of a beam segment OA as shown in figure 3.4.8. in a small time interval Δt . In Δt , the beam segment OA between the central hinge and one lateral hinge, undergoes plastic deformation which consists of a rotation $\Delta\theta$ and an extension of amount $\epsilon\Delta\xi$ to a new configuration O'A'. It is clear that these plastic deformations occur at each yield hinge.

From the examination of the successive geometric change in the interval Δt it is clear that

$$BB' = A''B' \tan \theta$$

$$BB' = \epsilon\Delta\xi = \epsilon_0 \frac{\Delta\xi_0}{2} + \epsilon_A \Delta\xi_A$$

where the subscripts 0 and A denote the corresponding quantities at the hinge 0 and the lateral hinge A.

Assuming small deflection so that the projective length of the beam will not differ from its real length appreciably, we have

$$A''B' = \xi \cdot \Delta\theta$$

and

$$\tan \theta = \frac{w_0(t)}{\xi(t)}$$

Therefore

$$\epsilon\Delta\xi = \frac{1}{2} \epsilon_0 \Delta\xi_0 + \epsilon_A \Delta\xi_A = \xi \cdot \Delta\theta \cdot \frac{w_0}{\xi} = w_0 \cdot \Delta\theta$$

i.e.

$$\frac{1}{2} \varepsilon_0 \Delta \xi_0 + \varepsilon_A \Delta \xi_A = w_0 \cdot \Delta \theta \quad (3.4.29)$$

the curvature changes at central hinge 0 and lateral hinge A are respectively

$$\kappa_0 = \frac{-\Delta \theta}{\Delta \xi_0 / 2} ; \quad \kappa_A = \frac{+\Delta \theta}{\Delta \xi_A} \quad (3.4.30)$$

Combining (3.4.29) and (3.4.30) and considering the limiting values when Δt approaches to zero, we get

$$-\frac{\dot{\varepsilon}_0}{\dot{\kappa}_0} + \frac{\dot{\varepsilon}_A}{\dot{\kappa}_A} = w_0(t) \quad (3.4.31)$$

where $w_0(t)$, as defined before, is the displacement of the beam at central hinge $w(0, t)$.

Using the flow rule (3.4.6) we then have

$$\frac{N_0 \dot{\varepsilon}_0}{M_0 \dot{\kappa}_0} = \left[\frac{\partial f}{\partial \left(\frac{N}{N_0} \right)} / \frac{\partial f}{\partial \left(\frac{M}{M_0} \right)} \right]_0 \quad \text{and} \quad \frac{N_0 \dot{\varepsilon}_A}{M_0 \dot{\kappa}_A} = \left[\frac{\partial f}{\partial \left(\frac{N}{N_0} \right)} / \frac{\partial f}{\partial \left(\frac{M}{M_0} \right)} \right]_A$$

therefore

$$-\left[\frac{\partial f}{\partial \left(\frac{N}{N_0} \right)} / \frac{\partial f}{\partial \left(\frac{M}{M_0} \right)} \right]_0 + \left[\frac{\partial f}{\partial \left(\frac{N}{N_0} \right)} / \frac{\partial f}{\partial \left(\frac{M}{M_0} \right)} \right]_A = \frac{N_0}{M_0} w_0(t) \quad (3.4.32)$$

Equations (3.4.5), (3.4.28) and (3.4.32) in unknowns M, N, v_0, ξ thus completely describe the beam motion valid for $N/N_0 < 1$ if the impact force $P(t)$ is prescribed.

For a rectangular beam, the yield function and flow rule take the forms as in (3.4.7) and (3.4.8). Therefore we have

$$-\left(\frac{N_0 \dot{\xi}}{M_0 k}\right)_A = 2 \frac{N}{N_0} = \left(\frac{N_0 \dot{\xi}}{M_0 k}\right)_A$$

Since N is uniform throughout the beam. Equation (3.4.32) thus becomes

$$-\left(\frac{N_0 \dot{\xi}}{M_0 k}\right)_0 + \left(\frac{N_0 \dot{\xi}}{M_0 k}\right)_A = 4 \frac{N}{N_0} = \frac{N_0}{M_0} w_0(t) \quad (3.4.33)$$

Substituting (3.4.33) into the yield condition (3.4.7) gives

$$\frac{\bar{M}}{M_0} = 1 - \frac{1}{16} \frac{N_0^2}{M_0^2} w_0^2$$

Inserting the above two equations into (3.4.28) leads to

$$2M_0 = \frac{P\xi}{2} - \frac{q_0 \xi^2}{2} - \frac{m}{6} \left\{ 2\dot{v}_0 \xi^2 + v_0 \xi \dot{\xi} \right\} - \frac{1}{8} \frac{N_0^2}{M_0^2} w_0^2$$

which is substituted into (3.4.28) gives

$$\dot{v}_0 = \frac{1}{m\xi} \left\{ 2P - q_0 \xi - \frac{1}{\xi} \left(12M_0 + \frac{3}{4} \frac{N_0^2}{M_0^2} w_0^2 \right) \right\} \quad (3.4.34)$$

and

$$v_0 \dot{\xi} = \frac{1}{m\xi} \left\{ 12M_0 + \frac{3}{4} \frac{N_0^2}{M_0^2} w_0^2 - P\xi - q_0 \xi^2 \right\}$$

These two equations in unknowns v_0 and ξ are to be solved.

The same non-dimensionalization is followed here as in Section 3.3 with the addition of an axial force parameter

$$\eta_0, \eta = \frac{N_0, N}{4(M_0 q_0)^{1/2}}$$

In dimensionless variables defined in 3.3 and the above, equations (3.4.34) becomes

$$v'_0 = \frac{2\phi}{s} - \frac{1}{2} - \frac{1}{s^2} \left(\frac{3}{2} + 6\eta_0^2 w_0^2 \right) \quad (3.4.35)$$

$$v_0 s' = \frac{1}{s} \left(\frac{3}{2} + 6\eta_0^2 w_0^2 \right) - \frac{s}{2} - \phi$$

Accelerative Phase

In this phase, the impact force $P(t)$ is given by the yield force, or limiting load P_0 of the impact mass, i.e. $P(t) = P_0 = \text{constant}$ in this phase. Equations of motion are obtained from (3.4.34) by replacing P by P_0 , i.e.

$$\dot{v}_0 = \frac{1}{m\xi} \left\{ 2P_0 - q_0\xi - \frac{1}{\xi} \left(12M_0 + \frac{3}{4} \frac{N_0^2}{M_0} w_0^2 \right) \right\}$$

$$v_0 \dot{\xi} = \frac{1}{m\xi} \left\{ 12M_0 + \frac{3}{4} \frac{N_0^2}{M_0} w_0^2 - P_0\xi - q_0\xi^2 \right\}$$

In dimensionless parameters and using the force ratio ϕ_0 defined before, these become

$$v'_0 = \frac{2\phi_0}{s} - \frac{1}{2} - \frac{1}{s^2} \left(\frac{3}{2} + 6\eta_0^2 w_0^2 \right) \quad (3.4.36)$$

$$v_0 s' = \frac{1}{s} \left(\frac{3}{2} + 6\eta_0^2 w_0^2 \right) - \frac{s}{2} - \phi_0$$

Thus V_0 and S can be solved using these two equations with the initial conditions

$$v_0(0) = 0, \quad w_0(0) = 0$$

and

$$s(0) = -\phi_0 + \sqrt{\phi_0^2 + 3} \quad (3.4.37)$$

as previously discussed.

During the accelerative phase, the impact mass M_v decelerates with deceleration a_v

$$a_v = \frac{-P_0}{M_v} = \text{const.}$$

and the velocity of the impact mass is

$$v_v(t) = v_v(0) - \frac{P_0}{M_v} t$$

At a certain time t^* , the central velocity of the beam $v_0(t^*)$ is equal to the velocity of the impact mass $v_v(t^*)$. Whence the accelerative phase ends. The time t^* is given by

$$v_0(t^*) = v_v(0) - \frac{P_0}{M_v} t^*$$

or in dimensionless form

$$V_0(T^*) = V_v(0) - \frac{\phi_0}{\mu} T^* \quad (3.4.38)$$

When the accelerative phase ends, the corresponding quantities $V_0(T^*)$, $S(T^*)$, $W_0(T^*)$ then become the initial conditions for the subsequent beam motion.

Decelerative Phase

In this phase the contact force $P(t)$ drops down below the yield force of the impact mass P_0 , thus the impact mass becomes rigid. Assuming that there is always contact between the impact mass and the beam then the deceleration of the mass a_v is equal to the central beam acceleration \dot{v}_0 , and the contact force is given by

$$P(t) = -M_v a_v = -M_v \dot{v}_0$$

or in dimensionless variables

$$\phi = -\mu V'_0 \quad (3.4.38)$$

Substituting this into the equation (3.4.35) for ϕ gives

$$V'_0 = \frac{-1}{S+2\mu} \left\{ \frac{S}{2} + \frac{1}{S} \left(\frac{3}{2} + 6\eta_0^2 W_0^2 \right) \right\} \quad (3.4.39)$$

$$V_0 S' = \frac{S+\mu}{S(S+2\mu)} \left(\frac{3}{2} + 6\eta_0^2 W_0^2 \right) - \frac{S(S+3\mu)}{2(S+2\mu)}$$

which are the equations governing the beam motion in this phase with the initial conditions $V_0(T^*)$, $S(T^*)$, $W_0(T^*)$ given in (3.4.37). It is clear that V'_0 in equation (3.4.39) is strictly negative and thus the beam motion decelerates in this phase.

At some later time T_f , when the beam motion decelerates till $V_0(T_f) = 0$, the beam comes to rest. Denoting the corresponding final central displacement of the beam $W_0(T_f)$ by δ_f and setting $V_0 = 0$ in equation (3.4.39), we get

$$2(S+\mu) \left(\frac{3}{2} + 6\eta_0^2 \delta_f^2 \right) - S^2(S+3\mu) = 0$$

then we obtain, by $\eta_0^2 \delta_f^2 = \lambda_f^2$,

$$3(S+\mu)(1+4\lambda_f^2) - S^2(S+3\mu) = 0$$

i.e.

$$S^3 + 3\mu S^2 - 3(1+4\lambda_f^2)S - 3\mu(1+4\lambda_f^2) = 0 \quad (3.4.40)$$

It is seen that if $\lambda_f^2 = 0$, this reduces to the previous case where the axial force interaction of the beam was neglected. Denoting the three roots of equation (3.4.40) by α , β , γ and by equating the coefficients

we obtain the system of equations as

$$\begin{aligned}\alpha + \beta + \gamma &= -3 \leq 0, & \mu &\geq 0 \\ \alpha\beta + \beta\gamma + \gamma\alpha &= -3(1 + 4\lambda_f^2) < 0, & \lambda_f^2 &\geq 0 \\ \alpha\beta\gamma &= 3(1 + 4\lambda_f^2) \geq 0, & \mu &\geq 0\end{aligned}$$

The mass ratio μ can take the value in the range $0 \leq \mu < \infty$ and by above equations, the corresponding bounds for the three roots α, β, γ are

$$\begin{aligned}0 &\leq \mu < \infty, \\ \sqrt{3(1 + 4\lambda_f^2)} &\geq \alpha > 1, \\ 0 &\geq \beta > -1, \\ -\sqrt{3(1 + 4\lambda_f^2)} &\geq \gamma > -\infty.\end{aligned}$$

Since the equations of motion are valid only when S is non-decreasing i.e., $S' \geq 0$, therefore the final hinge distance is bounded by

$$\sqrt{3(1 + 4\lambda_f^2)} \geq \alpha > 1$$

which corresponds to the range $0 \leq \mu < \infty$.

If the analysis were to neglect the effects of the axial constraints, then $\lambda_f^2 = 0$, and the final hinge distance is simply bounded by

$$\sqrt{3} \geq \alpha > 1$$

This confirms the result obtained in the previous analysis as in section 3.2.

Numerical Solution

Since the differential equations in (3.4.36) for the beam motion in the accelerative phase and (3.4.39) for the motion in the decelerative phase are highly non-linear and also involve the integral of an unknown function, the closed form solution has not been able to obtain. It is thus necessary to adapt the same numerical technique as discussed in section 3.3, in which both sets of the equations in (3.4.36) are put into the form

$$\begin{aligned}V_0' &= f(S, V_0) \\V_0 S' &= g(S, V_0)\end{aligned}\tag{3.4.41}$$

and the unknown functions V_0 and S are obtained by integrating equations (3.4.41) step by step. The set of equations in (3.4.41) are linearized using Taylor Series expansion in each time step and we are lead to solve the system of linear equations in the form

$$\begin{aligned}a_{11}^{(n)} \Delta V_0^{(n)} + a_{12}^{(n)} \Delta S^{(n)} &= a_{13}^{(n)} \\a_{21}^{(n)} \Delta V_0^{(n)} + a_{22}^{(n)} \Delta S^{(n)} &= a_{23}^{(n)}\end{aligned}\tag{3.4.42}$$

at a certain time instant T_n , $n = 1, 2, 3, \dots$

where

$$\begin{aligned}a_{11}^{(n)} &= 1 - \frac{\Delta T}{2} \left(\frac{\partial f}{\partial V_0} \right)_{(n)} \\a_{12}^{(n)} &= - \frac{\Delta T}{2} \left(\frac{\partial f}{\partial S} \right)_{(n)} \\a_{13}^{(n)} &= f_{(n)} \cdot \Delta T\end{aligned}$$

and

$$a_{21}^{(n)} = -\frac{\Delta T}{2} \left(\frac{\partial g}{\partial V_0} \right)_{(n)}$$

$$a_{22}^{(n)} = v^{(n)} + \frac{\Delta V_0^{(n-1)}}{2} - \frac{\Delta T}{2} \left(\frac{\partial g}{\partial S} \right)_{(n)}$$

$$a_{23}^{(n)} = g_{(n)} \cdot \Delta T$$

Knowing $\Delta V^{(n)}$ and $\Delta S^{(n)}$ at T_n then we can compute V_0 and S at T_{n+1} by

$$V_0^{(n+1)} = V_0^{(n)} + \Delta V_0^{(n)}$$

$$S^{(n+1)} = S^{(n)} + \Delta S^{(n)}$$

and

$$\begin{aligned} W_0^{(n+1)} &= W_0^{(n)} + \int_{T_n}^{T_{n+1}} V_0(T') dT' \\ &= W_0^{(n)} + V_0^{(n)} \Delta T + \frac{\Delta V_0^{(n)}}{2} \Delta T \end{aligned}$$

The procedure can be repeated for every time interval ΔT , until the end of the beam motion when $V_0(T_f) = 0$.

In accelerative phase, we have by equations (3.4.36)

$$V_0' = f(S, V_0) = \frac{2\phi_0}{S} - \frac{1}{2} - \frac{1}{2} \left(\frac{3}{2} + 6\eta_0^2 W_0^2 \right)$$

$$V_0 S' = g(S, V_0) = \frac{1}{S} \left(\frac{3}{2} + 6\eta_0^2 W_0^2 \right) - \frac{S}{2} = \phi_0$$

and

$$\frac{\partial f}{\partial s} = -\frac{2\phi_0}{s^2} + \frac{3}{s^3} (1 + 4\eta_0^2 W_0^2)$$

$$\frac{\partial f}{\partial v_0} = -\frac{1}{s^2} \left(12\eta_0^2 W_0 \frac{\partial W_0}{\partial v_0} \right)$$

$$\frac{\partial g}{\partial s} = -\frac{1}{s^2} \left(\frac{3}{2} + 6\eta_0^2 W_0^2 \right) - \frac{1}{2}$$

$$\frac{\partial g}{\partial v_0} = \frac{1}{s} \left(12\eta_0^2 W_0 \frac{\partial W_0}{\partial v_0} \right)$$

where

$$\frac{\partial W_0}{\partial v_0} = \frac{\partial W_0(T)}{\partial T} / \frac{\partial v_0}{\partial T} = \frac{v_0}{v_0'} = \frac{v_0}{f(s, v_0)}$$

Starting at time $T_1 = 0$ with the initial conditions

$$v_0^{(1)} = 0$$

$$W_0^{(1)} = 0$$

$$s^{(1)} = -\phi_0 + \sqrt{\phi_0^2 + 3}$$

we can successively compute $v_0^{(n)}$, $W_0^{(n)}$, $s^{(n)}$, $n = 2, 3, \dots$ till $T = T^*$ when $v_0(T^*) = v_v$ then accelerative phase ends.

The beam motion in decelerative phase follows after $T = T^*$, where T^* is determined by equation (3.4.37). In this phase, we have by
(3.4.39)

$$v_0' = f(s, v_0) = \frac{-1}{s+2\mu} \left\{ \frac{s}{2} + \frac{1}{s} \left(\frac{3}{2} + 6\eta_0^2 w_0^2 \right) \right\}$$

$$v_0 s' = g(s, v_0) = \frac{s+\mu}{s(s+2\mu)} \left(\frac{3}{2} + 6\eta_0^2 w_0^2 \right) - \frac{s(s+3\mu)}{2(s+2\mu)}$$

and

$$\frac{\partial f}{\partial s} = -\frac{(s+2\mu-1)}{2(s+2\mu)^2} + \frac{3(s+\mu)}{s^2(s+2\mu)^2} (1+4\eta_0^2 w_0^2)$$

$$\frac{\partial f}{\partial v_0} = \frac{-1}{s(s+2\mu)} \left(12\eta_0^2 w_0 \frac{\partial w_0}{\partial v_0} \right)$$

$$\begin{aligned} \frac{\partial g}{\partial s} = & \left\{ \frac{1}{s(s+2\mu)} - \frac{2(s+\mu)^2}{s^2(s+2\mu)^2} \right\} \left(\frac{3}{2} + 6\eta_0^2 w_0^2 \right) \\ & - \frac{2s+3\mu}{2(s+2\mu)} + \frac{s(s+3\mu)}{2(s+2\mu)^2} \end{aligned}$$

$$\frac{\partial g}{\partial s} = \frac{s+\mu}{s(s+2\mu)} \left(12\eta_0^2 w_0 \frac{\partial w_0}{\partial v_0} \right)$$

and similarly $\frac{\partial w_0}{\partial v_0} = \frac{v_0}{v_0'} = \frac{\partial v_0}{f(s, v_0)}$

The complete beam motion ends at time T_f when $v_0(T_f) = 0$.

By previous discussion, the final hinge distance $s(T_f) = \alpha$ is given by the only positive real root of the equation

$$s^3 + 3\mu s^2 - 3(1+4\lambda_f^2)s - 3\mu(1+4\lambda_f^2) = 0$$

for a specified μ , and α is bounded by

$$1 < \alpha \leq \sqrt{3(1 + 4\lambda_f^2)}$$

This result can be used to check the accuracy of the numerical output.

A numerical example was computed and the results were plotted for S , V_0 and W_0 as shown in Figure 3.4.9.

In this example, we have used the values $\mu = 0.5$, $\phi = 2.0$, $V_v = 1.0$ and $\eta_0 = 2.5$ and the results are compared to the case where the axial force interaction is ignored ($\eta_0 = 0$). It is noted that the inclusion of the axial force effect in the analysis reduces the final central displacement of the beam by 2.5% for $\eta_0 = 2$, 12.5% for $\eta_0 = 5$ in this example and also reduces the time duration for the beam motion to end.

Plastic String Behavior

The foregoing treatment of the dynamic motion of a rectangular beam in both accelerative and decelerative phases is valid only for the case when $N/N_0 < 1$ during the entire history of motion. This restriction on the mechanical behavior of the beam also imposes a necessary bound on the maximum central displacement of the beam. By equation (3.4.33) we have

$$\frac{N}{N_0} = \frac{1}{4} \frac{N_0}{M_0} w_0(t) < 1$$

or

$$N_0 w_0 < 4M_0$$

in dimensionless parameters, this is

$$\eta_0 W_0 < \frac{1}{2} \tag{3.4.43}$$

Hence, for the previous analysis to hold, the condition must be satisfied i.e. $\eta_0 W_0(T^*) < 1/2$ in accelerative phase and $\eta_0 W_0(T_f) < 1/2$ in decelerative phase. Since $\eta_0 W_0(T_f) = \eta_0 \delta_f = \lambda_f$ and since $\lambda_f \geq 0$ thus the condition (3.4.43) becomes

$$0 \leq \lambda_f^2 < 1/4 \quad (3.4.44)$$

The final hinge distance $\alpha = s(T_f)$ is therefore bounded by

$$\sqrt{6} > \sqrt{3(1 + 4\lambda_f^2)} \geq \alpha > 1$$

for

$$1 \leq \mu < \infty$$

If, however, at a certain time $t = t_p$, the condition (3.4.43) is violated and $N/N_0 = 1$ i.e. $N_0 W_0(t_p) = 4M_0$ or $\eta_0 W_0(T_p) = 1/2$, the axial force in the beam reaches its yield limit N_0 and the whole beam behaves as a "Plastic String."

For $t \geq t_p$, the differential equation governing the beam motion in this phase can be obtained by combining equations in (3.4.35) and setting $M = 0$. Hence we get

$$\frac{\partial^2 w}{\partial x^2} = \frac{q_0}{N_0} + \frac{m}{N_0} \frac{\partial^2 w}{\partial t^2} \quad (3.4.45)$$

The necessary initial conditions for the above equation can be obtained by considering the quantities $v(x, t_p)$ and $w(x, t_p)$. By equations (3.4.23) and (3.4.34), we have

$$\begin{aligned} v(x, t_p) &= v_0(t_p) \left[1 - \frac{x}{\xi(t_p)} \right], & 0 \leq x \leq \xi(t_p) \\ &= 0, & \xi(t_p) \leq x \end{aligned} \quad (3.4.46)$$

and

$$w(x, t_p) = \int_0^{t_p} v(x, t') dt'$$

Since $v_0(t_p)$ and $\xi(t_p)$ can be determined from the previous analysis, the initial conditions $v(x, t_p)$ and $w(x, t_p)$ are prescribed at $t = t_p$.

To obtain the proper boundary conditions for equation (3.4.45), we consider the mechanical behavior of the system for $t = t_p$. By equation (3.4.46) the velocity field $v(x, t_p)$ is non-vanishing only in the range $-\xi(t_p) \leq x \leq \xi(t_p)$, and is zero elsewhere. It follows from the assumption that the supporting material is rigid if the beam displacement rate is zero, hence the supporting material provides a rigid base for the string $|x| \geq \xi(t_p)$, and the subsequent beam motion takes place only in the range $|x| \leq \xi(t_p)$.

Since $\xi(t)$ is a non-decreasing function of, hence

$$w(x, t) \Big|_{x=\xi(t_p)} = 0, \quad t \geq t_p \quad (3.4.47)$$

the other boundary condition may be obtained by considering the local equilibrium at $x = 0$, for $t \geq t_p$. It is clear that

$$P(t) = 2N_0 \frac{\partial w}{\partial x}(0^+, t), \quad t \geq t_p \quad (3.4.48)$$

If $t_p < t^*$, the transition from the plastic beam behavior to the plastic string behavior occurs in the accelerative phase, then $P(t) = P_0 =$ constant, and hence condition (3.4.48) is prescribed. However, if $t_p > t^*$, since $P(t) = -M_V \ddot{w}(0, t)$ in this phase, thus the condition (3.4.48) becomes

$$2 N_0 \frac{\partial w}{\partial x}(0, t) + M_v \frac{\partial^2 w}{\partial t^2}(0, t) = 0, \quad t \geq t_p$$

which is not a prescribed condition but is the equation which has to be satisfied along with equation (3.4.45).

Due to the complicated behavior in this phase, further details concerning the solution of the wave equation (3.4.45) subjected to the initial conditions (3.4.46) and boundary conditions (3.4.47) and (3.4.48) has not been attempted. Nevertheless, some general results concerning the mechanical behavior of the beam can be drawn by considering the mechanical equations [3.15].

When the beam motion becomes a plastic string motion governed by (3.4.45), the entire beam is strictly in tension, and so all strains in the beam must also be extensional. This places a limitation on the ratio of the rate of curvature change $\dot{\kappa}$ and the beam centerline extensional strain rate $\dot{\epsilon}$.

By flow rule (3.4.6) for $N/N_0 = 1$, we have

$$\frac{N_0 \dot{\epsilon}}{M_0 \dot{\kappa}} = \left[\frac{\partial f}{\partial \left(\frac{N}{N_0} \right)} / \frac{\partial f}{\partial \left(\frac{M}{M_0} \right)} \right] \frac{N}{N_0} = 1$$

i.e. the flow rule requires that the condition

$$-2 \leq \frac{N_0 \dot{\epsilon}}{M_0 \dot{\kappa}} \leq 2$$

should be satisfied for the entire plastic string. Since for a rectangular beam $N_0/M_0 = 4/h$, thus

$$-\frac{h}{2} \leq \frac{\dot{\varepsilon}}{\kappa} \leq \frac{h}{2} \quad (3.4.49)$$

Since

$$\dot{\varepsilon} = \left[\frac{1}{2} \left(\frac{\partial w}{\partial x} \right)^2 \right]_{,t}$$

and

$$\dot{\kappa} = \left[\frac{\partial^2 w}{\partial x^2} \right]_{,t}$$

therefore inequality (3.4.49) is equivalent to

$$-\frac{h}{2} \leq \frac{\left[\frac{1}{2} \left(\frac{\partial w}{\partial x} \right)^2 \right]_{,t}}{\left[\frac{\partial^2 w}{\partial x^2} \right]_{,t}} \leq \frac{h}{2}$$

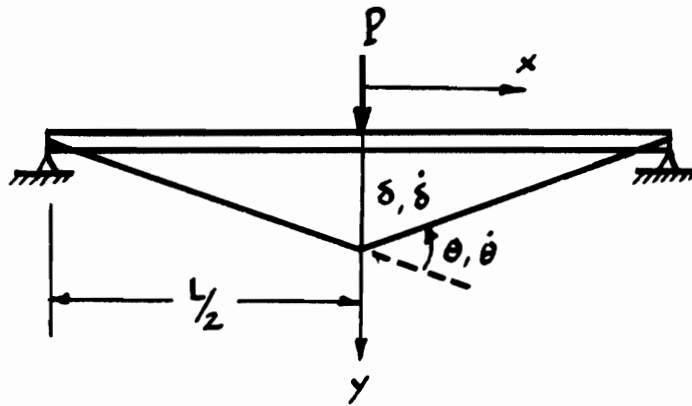


Figure 3.4.1. Pin-Pin Rigid Perfectly Plastic Beam under Concentrated Load at Mid-span.

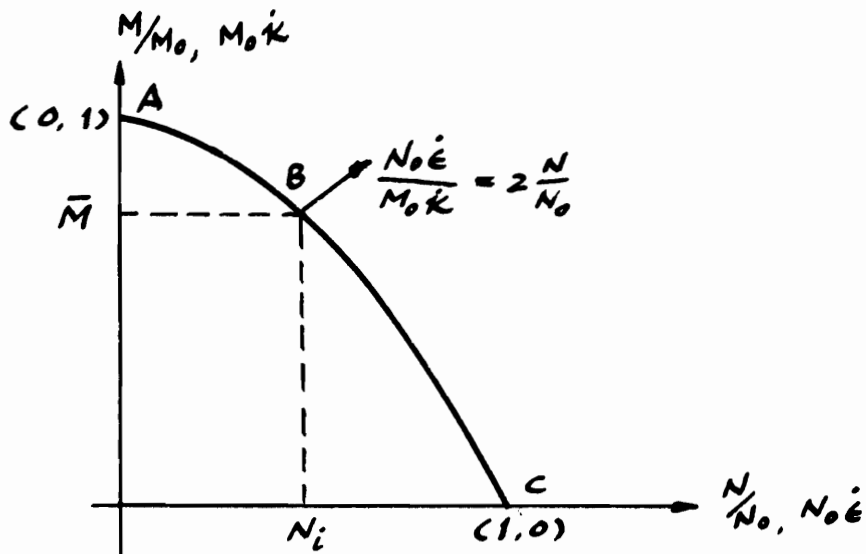


Figure 3.4.2. $M/M_0 - N/N_0$ Interaction Curve for a Rectangular Beam.

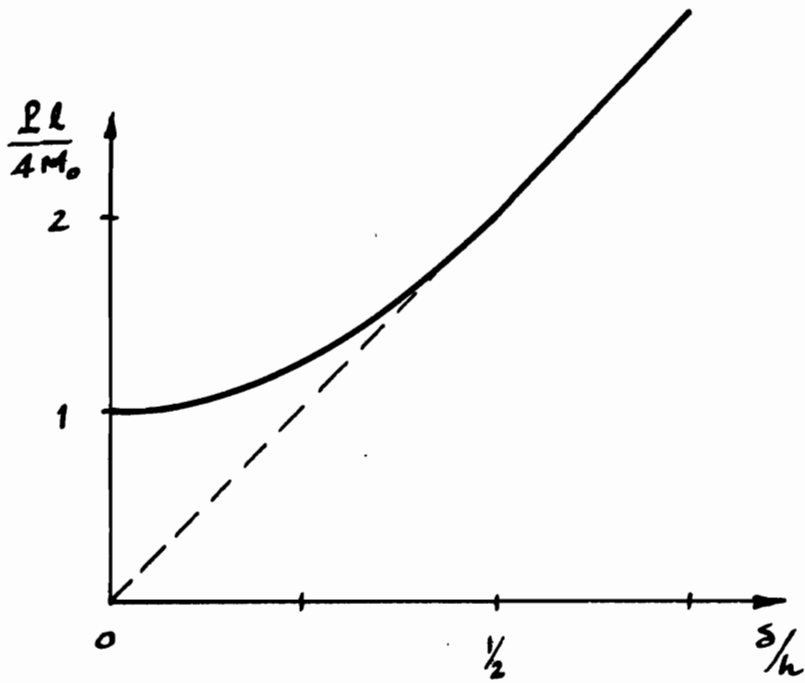


Figure 3.4.3. $P - \delta$ Curve for a Pin-Pin Beam in Figure 3.4.1.

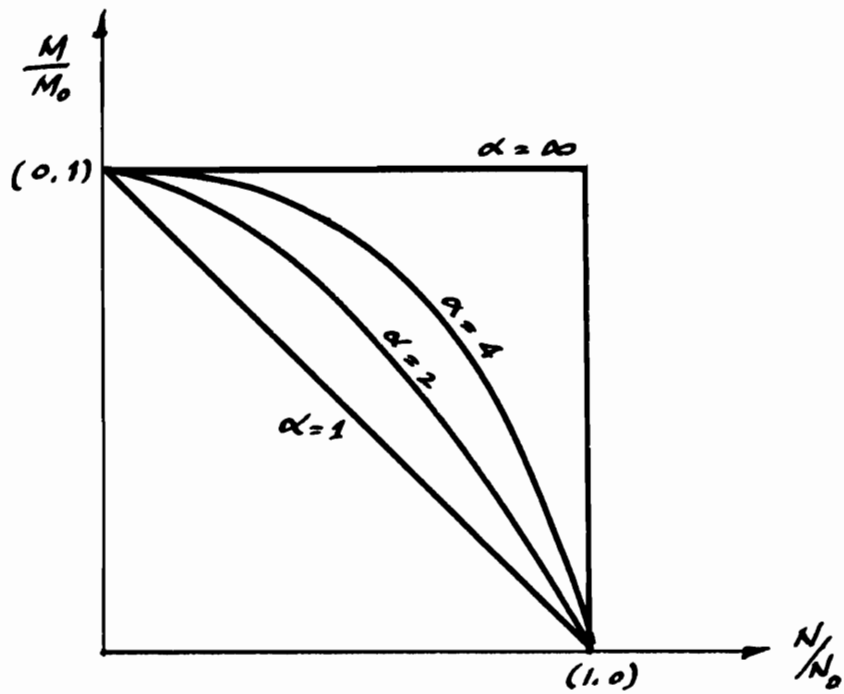


Figure 3.4.4. Yielding Curves for General Sections.

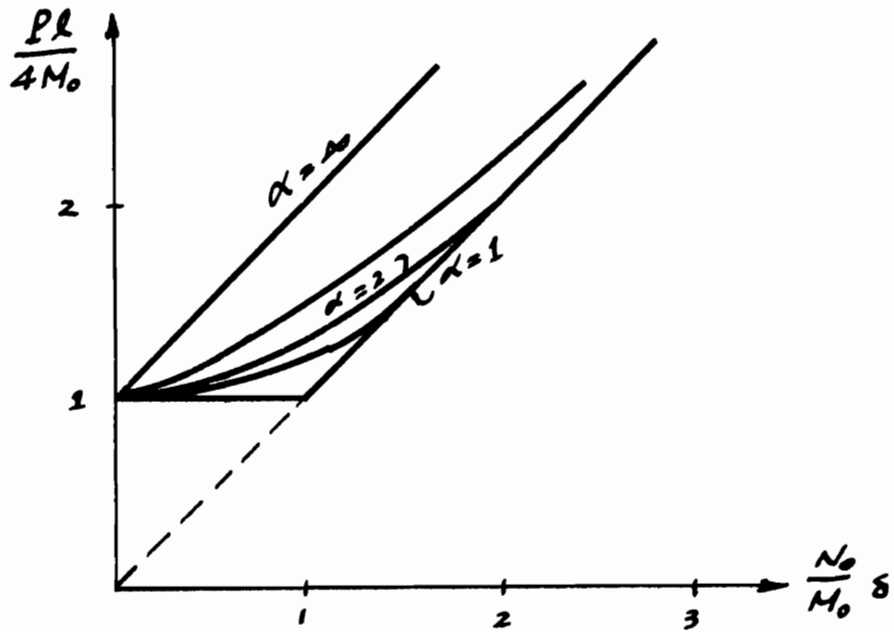


Figure 3.4.5. P - δ Curves for the Pin-Pin Beam in Figure 3.4.1 using the Yielding Conditions in Figure 3.4.4.

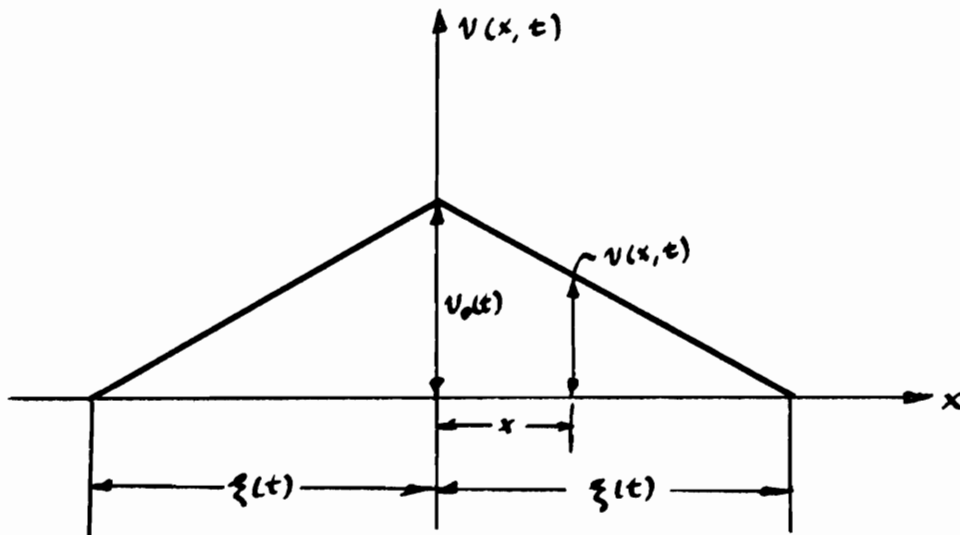


Figure 3.4.6. Velocity Field $v(x, t)$.

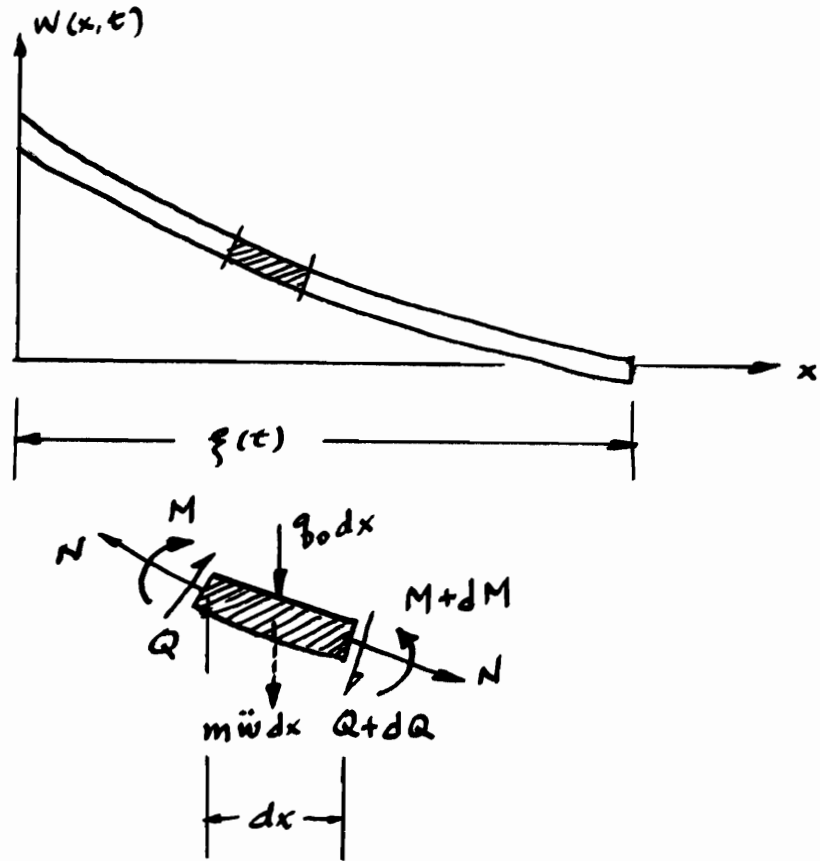


Figure 3.4.7. Notations and Signs of the Forces in a Beam Element.

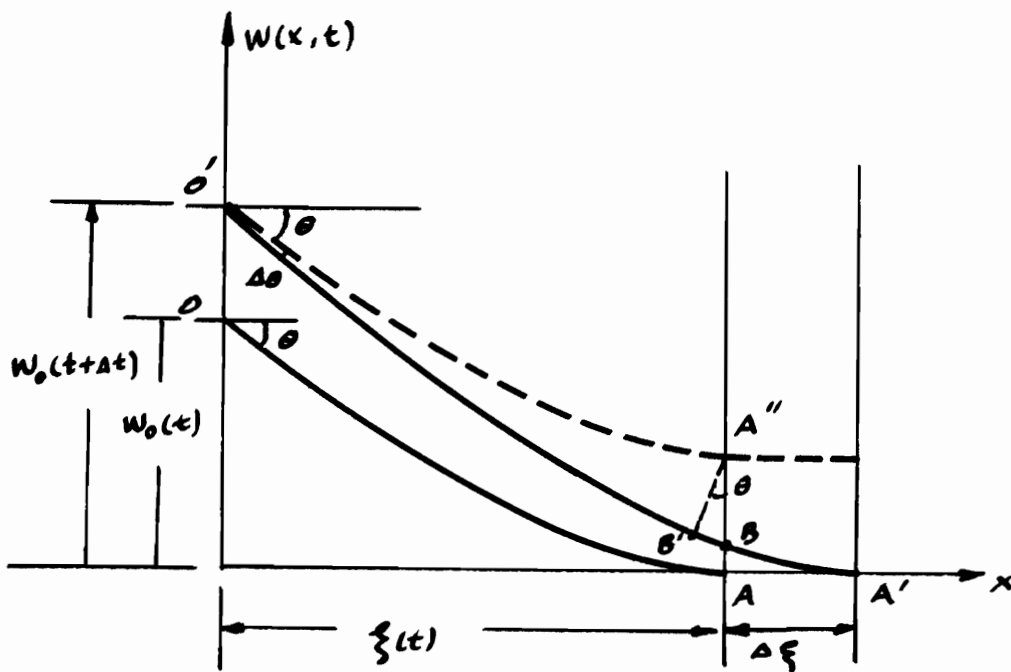


Figure 3.4.8. Beam Displacement Patterns in Time Interval Δt .

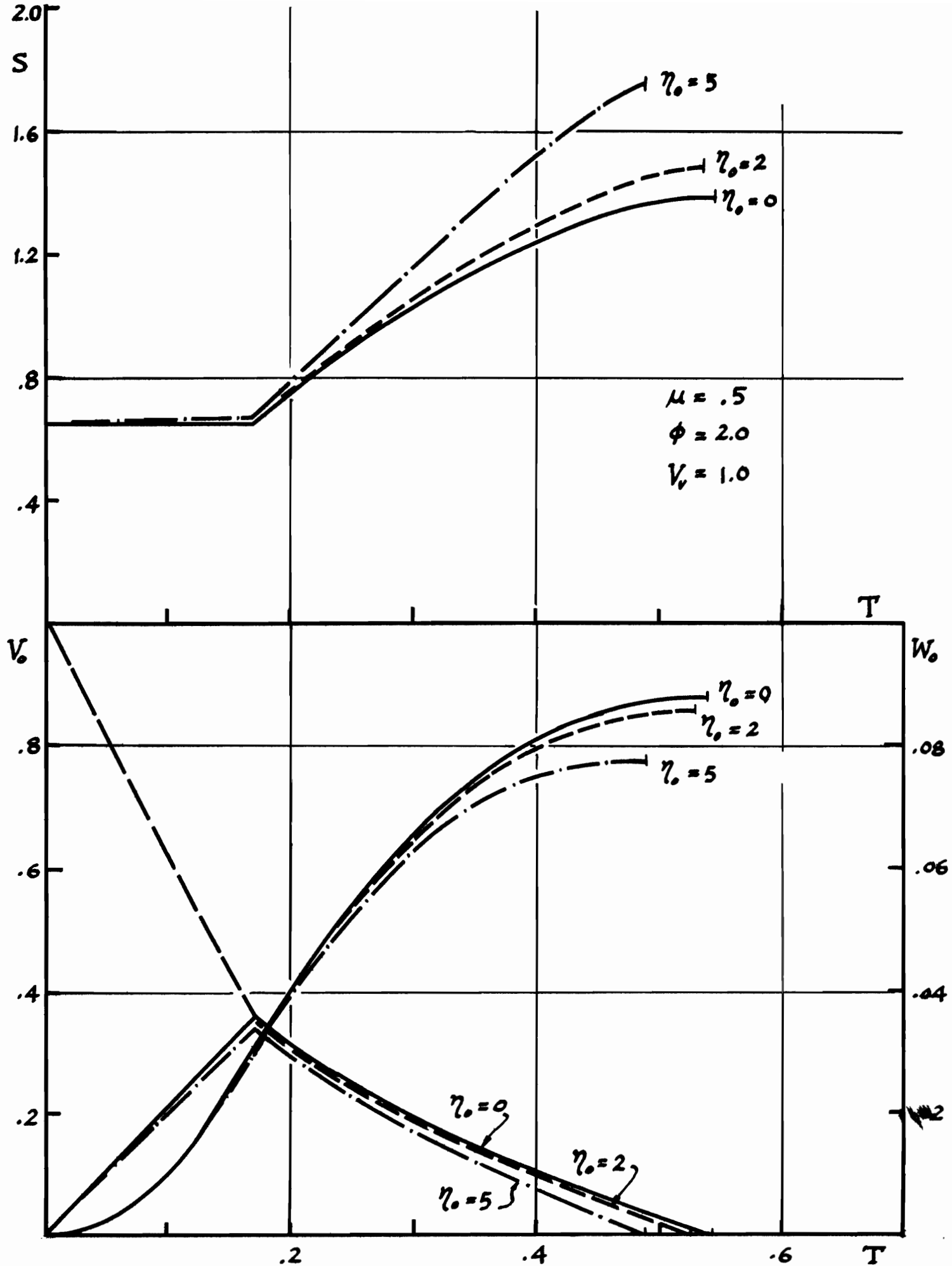


Figure 3.4.9. Resulting Curves of the Example in Section 3.4 (ii).

3.5 Influence of Delay Time on Mass Impact on Beams

The discussion of yield delay time given in section 2.3 allows a useful extension to the bending of beams. In obtaining a moment-curvature relation the usual assumptions of beam theory will be made, namely, that plane-sections normal to the middle surface remain plane and normal and that the behavior of the material in tension is identical to that in compression.

Since the strain rate varies linearly through the cross section, the fiber furthest from the neutral axis will have the smallest delay time. Thus the cross section will behave elastically up to a yield moment M^* given by the σ^* of the outermost fiber. For times greater than the delay time of the outermost fiber a yield zone will spread into the beam, the stress in fibers lying outside this yield zone will be relaxing from the σ^* corresponding to the strain rate at the fiber in question. The material lying inside the yield zone will have an elastically increasing fiber stress.

Consider first a rectangular cross section ($b \times 2c$) subject to a constant rate of curvature. The strain at a point in the cross section distant y from the neutral axis is

$$\epsilon = \epsilon_{\max} y/c$$

The maximum elastic moment carried by the section is

$$M^* = \frac{2}{3} bc^2 \sigma^*$$

where

$$\sigma^* = \left(\frac{E(1 + \beta) A \sigma_0^\beta \dot{\epsilon}_{\max}}{d^3} \right)^{1/1+\beta} \quad (3.5.1)$$

At any time greater than the delay time of the material at $y = \pm c$ the material in the region $|y| < \bar{y}$ is relaxing viscoplastically. The plastic region is determined by the fact that $\bar{\sigma}(\bar{y})$ is on the point of yielding. Thus,

$$\begin{aligned}\sigma^*(\bar{y}) &= \left(\frac{E(1 + \beta)A\sigma_0^\beta \dot{\epsilon}_{\max}}{d^3} \right)^{1/1+\beta} \left(\frac{\bar{y}}{c} \right)^{1/1+\beta} \\ &= E \epsilon_{\max} \bar{y}/c\end{aligned}$$

Thus

$$\bar{y}/c = \left(\frac{E(1 + \beta)A\sigma_0^\beta \dot{\epsilon}_{\max}}{d^3} \right)^{1/\beta} (E \epsilon_{\max})^{-(1+\beta)/\beta}$$

For $|y| > \bar{y}$ the stress is given by (2.2.8a) with $\alpha = \dot{\epsilon}_{\max} y/c$ and in this region the integration with respect to y , needed for the computation of the moment induced in the cross section, must be carried out numerically. For ϵ_{\max} greater 0.5 percent the approximation to (2.2.8b) becomes sufficiently accurate to be used in the computation and the result for the moment can be given in simple terms.

Transverse Impact of a Mass on a Beam

It has been shown in section 3.1 that the bending moment at the point of impact in an infinite elastic beam of cross sectional area A , moment of inertia I , density ρ and modulus of elasticity E that is struck transversely by a mass M moving before the instant of impact with velocity V_0 and which remains in contact with the beam after impact, is given by

$$M(0, t) = 2EI k^2 V_0 e^{\alpha^2 t} \operatorname{erfc}(\alpha \sqrt{t}) \quad (3.5.2)$$

where $K = (\rho A / 4EI)^{1/4}$ and $\alpha = \delta EI k^2 / M$. The above equation implies that the bending moment at the instant of impact jumps to the value $2EI k^2 V_0$, which is independent of M and decays from this value more or less rapidly depending on α and thus on M . If the upper yield point is ignored then the velocity to produce plastic behavior is given by

$$V_0 / c_1 = (r/y) \epsilon_y$$

where $r = (I/A)^{1/2}$ is the radius of gyration of the section, ϵ_y , is the yield strain and c_1 the velocity of longitudinal waves in the beam material. However, if the upper yield point is considered the possibility exists that for finite values of the mass the stresses induced by the impact might decay rapidly enough that they fall to values below the yield stress in a time which is less than the delay time at the most highly stressed fiber.

The delay time t_d for the extreme fiber is given by (. .) with (3.5.2) in the form

$$\frac{d^3}{A} \left(\frac{2EI k^2 V_0 y}{\sigma_0 I} \right)^\beta \int_0^{t_d} e^{\beta \alpha^2 t} \left\{ \operatorname{erfc}[\alpha \sqrt{t}] \right\}^\beta dt = 1$$

Due to the high value of the exponent β the contribution to the integral when the stress is below the lower yield point is negligible and thus to obtain a bound on V_0 for finite M it is enough to set $t_d \rightarrow \infty$. Using the substitution $s = \alpha^2 t$ and suitable manipulations the above equation can be transformed into an inequality for the range of velocity leading to elastic impacts. Using the notation

$$\lambda(\beta) = \int_0^{\infty} e^{\beta s} (\operatorname{erfc} \sqrt{s})^{\beta} ds$$

the result becomes

$$\frac{V_0}{c_1} \cong \frac{r\sigma_0}{yE} \left(\frac{A}{d^3}\right)^{1/\beta} \left(\frac{M}{8EI k^3}\right)^{-2/\beta} \lambda(\beta)$$

The integral for $\lambda(\beta)$ is easily computed numerically and on substituting the same values of the parameters as used in section 2.3 the limiting velocities for the two grain sizes are given by

$$\frac{V_0}{c_1} \cong \frac{r}{y} 1.75 \times 10^{-3} \left(\frac{M}{8EI k^3}\right)^{-2/} \quad \text{for 2030 grains/mm}^2$$

and

$$\frac{V_0}{c_1} \cong \frac{r}{y} 1.295 \times 10^{-3} \left(\frac{M}{8EI k^3}\right)^{-2/} \quad \text{for 346 grains/mm}^2$$

It is clear from these results that for values of $M/8EI k^3$ greater than 1 the increased in V_0 predicted by this theory over that predicted by the simple theory is not important. However, for smaller values of $M/8EI k^3$ the increase in V_0 can be very substantial.

4. IMPULSIVE LOADING ON RATE DEPENDENT STRUCTURAL SYSTEMS

4.1 Combined Loading on Viscoplastic Beams

4.1 (i) The Generalized Constitutive Equation for the Pure Bending of Viscoplastic Beams

In this part of the study, the constitutive equation of a viscoplastic material will be generalized in terms of moments, curvature and their rates, to obtain a moment curvature relation for a typical beam element with a vertical axis of symmetry.

The assumption that plane sections remain plane leads to a linear strain rate distribution over the cross section given by

$$\dot{\epsilon} = \dot{\kappa}z \quad (4.1.1)$$

where z is the distance from the center section.

The form of the constitutive equation to be used in the analysis is the following

$$E\dot{\epsilon} = \dot{\sigma} + \frac{\sigma_0}{\tau^*} \left\langle \frac{\sigma}{\sigma_0} - 1 \right\rangle \quad (4.1.2)$$

Substituting (4.1.1) in the constitutive equation (4.1.2) gives

$$E\dot{\kappa}z = \dot{\sigma} + \frac{\sigma_0}{\tau^*} \left\langle \frac{\sigma}{\sigma_0} - 1 \right\rangle \quad (4.1.3)$$

It is convenient to express this equation in terms of the following dimensionless quantities

$$\begin{aligned}
\bar{z} &= \frac{z}{h} \\
\bar{\sigma} &= \frac{\sigma}{\sigma_0} \\
\dot{\bar{\sigma}} &= \frac{\dot{\sigma} \tau^*}{\sigma_0} \\
\bar{t} &= \frac{t}{\tau^*} \\
\dot{\bar{\kappa}} &= \frac{E \dot{\kappa} \tau^* h}{\sigma_0}
\end{aligned} \tag{4.1.4}$$

in terms of which equation (4.1.3) becomes

$$\dot{\bar{\kappa}} \bar{z} = \dot{\bar{\sigma}} + (\bar{\sigma} - 1) \tag{4.1.5}$$

Before we can generalize equation (4.1.5), the boundary line between the elastic and viscoplastic zones in the cross section has to be established. The boundary line is a moving one, and its position is a function of the time \bar{t} . This line is established by integrating equation (4.1.5) between the limits

when

$$\bar{t} = 0 \quad \bar{\sigma} = 0$$

and when

$$\bar{t} = \bar{t} \quad \bar{\sigma} = 1.0$$

Therefore, for time \bar{t} the position of the boundary line is given by,

$$\bar{z}_0 = \frac{1}{\dot{\bar{\kappa}} \bar{t}} \tag{4.1.6}$$

It is clear that with increase in time the elastic zone shrinks and when $\bar{t} \rightarrow \infty$, $\bar{z}_0 \rightarrow 0$, when the section is fully plastic, and the stresses have relaxed to the steady state level. Figure 4.1.1 shows the stress

distribution over the cross section.

Now, multiplying equation (4.1.5) by z and integrating over the cross section gives

$$2 \int_0^{1.0} \frac{\dot{\kappa} z^2}{\kappa} d\bar{z} = 2 \int_0^{1.0} \frac{\dot{\sigma} z}{\sigma} d\bar{z} + 2 \int_0^{1.0} (\bar{\sigma} - 1) \bar{z} d\bar{z}$$

The second integral on the right hand side of the above equation will be different from zero in the viscoplastic zone of the cross section. Therefore, two conditions are recognized, either the cross section is still elastic, and this corresponds to a time $\bar{t} \leq \frac{\dot{\kappa}^{-1}}{\kappa}$ or the cross section is partially elastic, partially viscoplastic, and this corresponds to a time $\bar{t} \geq \frac{\dot{\kappa}^{-1}}{\kappa}$. Therefore, for $\bar{t} \leq \frac{\dot{\kappa}^{-1}}{\kappa}$

$$\frac{2}{3} \frac{\dot{\kappa}}{\kappa} = \dot{\bar{M}} \quad (4.1.7)$$

and for

$$\bar{t} \geq \frac{\dot{\kappa}^{-1}}{\kappa}$$

$$\frac{2}{3} \frac{\dot{\kappa}}{\kappa} = \dot{\bar{M}} + \bar{M} - 1.0 + \frac{1}{3} \frac{1}{(\kappa \bar{t})^2} \quad (4.1.8)$$

where \bar{M} : is the bending moment in the cross section, $\dot{\bar{M}}$: is the bending moment rate of change.

Equations (4.1.7) and (4.1.8) are the generalized constitutive equations for pure bending of a rectangular cross section. Equation (4.1.7) applies only when the cross section is still elastic. Equation (4.1.8) applies when the cross section is partially elastic and partially viscoplastic.

For the moment curvature relationship we integrate equations (4.1.7) and (4.1.8) with appropriate initial conditions.

The solution of equation (4.1.7) with $\dot{\kappa}$ constant and the initial condition $\bar{M} = 0$ when $\bar{t} = 0$ is

$$\bar{M} = \frac{2}{3} \frac{\dot{\kappa} \bar{t}}{\kappa}, \quad \bar{t} \leq \frac{\dot{\kappa}^{-1}}{\kappa} \quad (4.1.9)$$

and the solution of differential equation (4.1.8) with the initial condition $\bar{M} = \frac{2}{3}$ when $\bar{t} = \frac{\dot{\kappa}^{-1}}{\kappa}$ is

$$\begin{aligned} \bar{M} = 1.0 + \frac{2}{3} \frac{\dot{\kappa}}{\kappa} + \frac{1}{3\kappa^2} \frac{1}{\bar{t}} \\ - \frac{e^{-\bar{t}}}{3\kappa^2} \int_{1/\kappa}^{\bar{t}} \frac{e^x}{x} dx \quad \bar{t} \geq \frac{\dot{\kappa}}{\kappa} \quad (4.1.10) \\ - \left(\frac{1}{3\kappa} + \frac{1}{3} + \frac{2}{3} \frac{\dot{\kappa}}{\kappa} \right) e^{1/\kappa} e^{-\bar{t}} \end{aligned}$$

To transform equations (4.1.9) and (4.1.10) into a moment curvature relationship, substitute the following

$$\bar{\kappa} = \frac{\dot{\kappa}}{\kappa \bar{t}}$$

where κ is the curvature, in equations (4.1.9) and (4.1.10).

$$\bar{M} = \frac{2}{3} \bar{\kappa}, \quad \bar{\kappa} \leq 1.0 \quad (4.1.11)$$

$$\bar{M} = 1.0 + \frac{2}{3} \dot{\bar{\kappa}} + \frac{1}{3\dot{\bar{\kappa}}} \frac{1}{\bar{\kappa}} - e^{1/\dot{\bar{\kappa}}} \left(\frac{1}{3} + \frac{2}{3} \dot{\bar{\kappa}} + \frac{1}{3\dot{\bar{\kappa}}} \right) e^{-\bar{\kappa}/\dot{\bar{\kappa}}} - \frac{1}{3\dot{\bar{\kappa}}^2} e^{-\bar{\kappa}/\dot{\bar{\kappa}}} \int_{1/\dot{\bar{\kappa}}}^{\bar{\kappa}/\dot{\bar{\kappa}}} \frac{e^x}{x} dx \quad \bar{\kappa} \geq 1.0 \quad (4.1.12)$$

Equation (4.1.12) gives the moment curvature relationship for a rectangular cross section subject to constant curvature rate. A plot of equation (4.1.12) for different curvature rates is shown in figure 4.1.2.

Figure 4.1.2 shows that with the increase in curvature rate the dynamic moment curvature curve is raised above the static one. It is clear that the rate effect has an influence only after the elastic moment capacity of the cross section is reached.

In order to find the maximum value of the dynamic moment capacity of a cross section, we let $\bar{t} \rightarrow \infty$ in equation (4.1.10), therefore,

$$\bar{M} = 1.0 + \frac{2}{3} \dot{\bar{\kappa}} \quad (4.1.13)$$

Equation (4.1.13) shows that the increase in moment capacity of a cross section above the static fully plastic capacity ($\bar{M} = 1.0$) is proportional to the curvature rate.

It is important to emphasize that the above development was based on the constitutive equation (4.1.2). If another constitutive equation is used, it will give a different moment curvature relationship. However, it is clear that similar conclusions will be reached.

Based on the above development of moment curvature relations for viscoplastic material, approximate but simplified relations could be obtained, in the following way

$$1) \quad \bar{M} = 1.0 + \frac{2}{3} \dot{\bar{K}} \quad \text{if } \bar{K} > 0 \quad (4.1.14)$$

In this model the cross section will remain undeformed until the dynamic moment capacity of the cross section is reached; after that the curvature increases indefinitely, as in figure 4.1.3

$$2) \quad \bar{M} = \frac{2}{3} \bar{K} \quad \text{if } \bar{K} \leq 1.5 + \dot{\bar{K}} \quad (4.1.15)$$

$$\bar{M} = 1.0 + \frac{2}{3} \dot{\bar{K}} \quad \text{if } \bar{K} \geq 1.5 + \dot{\bar{K}}$$

In this model the cross section is assumed to be elastic until the dynamic moment capacity of the cross section is reached. Then the curvature will increase indefinitely, as in figure 4.1.3.

$$3) \quad \bar{M} = \frac{2}{3} \bar{K} \quad \text{if } \bar{K} \leq 1.0$$

$$\bar{M} = \frac{2}{3} \bar{K} e^{-(\bar{K}-1)} + \left(1.0 + \frac{2}{3} \dot{\bar{K}}\right) (1.0 - e^{-(\bar{K}-1)}) \quad (4.1.16)$$

$$\text{if } \bar{K} \geq 1.0$$

This model is close to the viscoplastic one. It assumes elastic behavior until the elastic moment capacity of the cross section is reached and then assumes an exponential behavior in the viscoplastic zone, as in figure 4.1.3.

This model could be improved by introducing in the exponential term a constant α , which depends on $\dot{\bar{K}}$.

$$\bar{M} = \frac{2}{3} \bar{k} e^{-\alpha(\bar{k}-1)} + \left(1.0 + \frac{2}{3} \frac{\dot{\bar{k}}}{\bar{k}}\right) (1.0 - e^{-\alpha(\bar{k}-1)}) \quad (4.1.17)$$

if $\bar{k} \geq 1.0$

α has to be chosen in such a way so as to have (4.1.17) represent the exact curve as closely as possible.

Equations (4.1.12) to (4.1.17) are possible approximate forms of dynamic moment curvature relations.

4.1 (ii) The Generalized Constitutive Equation for Combined Bending and Extension

To study the effect of combined bending and axial rates on a rectangular cross section of a beam, a curvature rate $\dot{\kappa}$ and an extension rate $\dot{\lambda}$ will be applied to that cross section, as in figure 4.1.4. Two different cases can be recognized immediately

- a) $\frac{\dot{\lambda}}{\dot{\kappa}} \leq 1.0$
- b) $\frac{\dot{\lambda}}{\dot{\kappa}} \geq 1.0$

In case (a) the bending rate is dominant, while in case (b) the extension rate is dominant.

To account for the fact that the strain rate could be here negative as well as positive, the constitutive equation has to be modified in the following way. For positive viscoplastic strain rate we have the following

$$E\dot{\epsilon} = \dot{\sigma} + \frac{\sigma_0}{\tau^*} \phi\left(\frac{\sigma}{\sigma_0} - 1\right) \quad (4.1.18)$$

where

$$\phi\left(\frac{\sigma}{\sigma_0} - 1\right) = 0 \quad \text{if } \frac{\sigma}{\sigma_0} \leq 1.0$$

or

$$\phi\left(\frac{\sigma}{\sigma_0} - 1\right) = \phi\left(\frac{\sigma}{\sigma_0} - 1\right) \quad \text{if } \frac{\sigma}{\sigma_0} \geq 1.0$$

and for negative viscoplastic strain rate we have

$$E\dot{\epsilon} = \dot{\sigma} + \frac{\sigma_0}{\tau^*} \phi\left(\frac{\sigma}{\sigma_0} + 1\right) \quad (4.1.19)$$

where

$$\phi\left(\frac{\sigma}{\sigma_0} + 1\right) = 0 \quad \text{if } \frac{\sigma}{\sigma_0} > -1.0$$

or

$$\phi\left(\frac{\sigma}{\sigma_0} + 1\right) = \phi\left(\frac{\sigma}{\sigma_0} + 1\right) \quad \text{if } \frac{\sigma}{\sigma_0} < -1.0$$

Now taking the function ϕ to be a linear one, the constitutive equations (4.1.18) and (4.1.19) will be

$$E\dot{\epsilon} = \dot{\sigma} + \frac{\sigma_0}{\tau^*} \left\langle \frac{\sigma}{\sigma_0} - 1 \right\rangle \quad \text{if } \dot{\epsilon}^{VP} \geq 0$$

or

(4.1.20)

$$E\dot{\epsilon} = \dot{\sigma} + \frac{\sigma_0}{\tau^*} \left\langle \frac{\sigma}{\sigma_0} + 1 \right\rangle \quad \text{if } \dot{\epsilon}^{VP} \leq 0$$

From figure 4.1.4, assuming plane sections remain plane, the strain rate at any level z in the cross section will be

$$\dot{\epsilon} = \dot{\lambda} + \dot{\kappa}z \quad (4.1.21)$$

Substituting (4.1.21) into the constitutive equation (4.1.20) gives

$$E(\dot{\lambda} + \dot{\kappa}z) = \dot{\sigma} + \frac{\sigma_0}{\tau^*} \left\langle \frac{\sigma}{\sigma_0} - 1 \right\rangle \quad \text{if } \dot{\epsilon}^{VP} \geq 0$$

$$E(\dot{\lambda} + \dot{\kappa}z) = \dot{\sigma} + \frac{\sigma_0}{\tau^*} \left\langle \frac{\sigma}{\sigma_0} + 1 \right\rangle \quad \text{if } \dot{\epsilon}^{VP} \leq 0 \quad (4.1.22)$$

To be able to integrate equation (4.1.22) over the cross section, the boundary lines between the elastic and the viscoplastic zones have to be established, and these are different in case (a) and (b).

Case (a):

$$\frac{\dot{\lambda}}{\dot{\kappa}} \leq 1.0$$

There are two lines in this case which separate the elastic zone from the viscoplastic zones. One line is in the positive strain rate area, and the second one is in the negative strain rate area. These boundaries are obtained easily from equation (4.1.22), by integrating with respect to time and finding the z corresponding to positive and negative yield stress. The results are

$$\begin{aligned} z_0^+ &= \frac{\sigma_0}{E\dot{\kappa}t} - \frac{\dot{\lambda}}{\dot{\kappa}} \quad \text{for } \dot{\epsilon}^{VP} \geq 0 \\ z_0^- &= -\frac{\sigma_0}{E\dot{\kappa}t} - \frac{\dot{\lambda}}{\dot{\kappa}} \quad \text{for } \dot{\epsilon}^{VP} \leq 0 \end{aligned} \tag{4.1.23}$$

The position of the boundary lines is changing with time, and as $t \rightarrow \infty$ the elastic zone shrinks to zero, as it is clear from (4.1.23). Three main conditions are recognized, namely

$$1) \quad 0 \leq t \leq \frac{\sigma_0}{E(\dot{\kappa}h + \dot{\lambda})}$$

during which the stresses at the cross section at every point are still below the static yield stress.

$$2) \quad \frac{\sigma_0}{E(\dot{\kappa}h + \dot{\lambda})} \leq t \leq \frac{\sigma_0}{E(\dot{\kappa}h - \dot{\lambda})}$$

In this condition some of the stresses have exceeded the static yield stress in the positive strain rate area

$$3) \quad t \geq \frac{\sigma_0}{E(\dot{\kappa}h - \dot{\lambda})}$$

Here some of the stresses have exceeded the static yield stress in both the negative as well as the positive strain rate areas. Figure 4.1.5 shows the stress distribution over the cross section.

For the first condition, the integration of the constitutive equation (4.1.22) over the cross section gives

$$\int_{-h}^h (\dot{\lambda} + \dot{\kappa}z) dz = \int_{-h}^h \dot{\sigma} dz$$

or (4.1.24)

$$EA\dot{\lambda} = \dot{N}$$

and multiplying the constitutive equation (4.1.22) by z and integrating it over the cross section leads to

$$\int_{-h}^h (\dot{\lambda} + \dot{\kappa}z)z dz = \int_{-h}^h \dot{\sigma}z dz$$

or (4.1.25)

$$EI\dot{\kappa} = \dot{M}$$

where A: is the area of the cross section

I: is the moment of inertia of the cross section

\dot{N} : is the rate of change of the axial force over the cross section

\dot{M} : is the rate of change of the moment over the cross section

For the second condition, the integration of the constitutive equation gives

$$EA\dot{\lambda} = \dot{N} + \frac{\sigma_0}{\tau^*} \int_{\frac{\sigma_0}{E\dot{\kappa}t} - \frac{\dot{\lambda}}{\dot{\kappa}}}^h \left(\frac{\sigma}{\sigma_0} - 1 \right) dz$$

and

$$EI\dot{\kappa} = \dot{M} + \frac{\sigma_0}{\tau^*} \int_{\sigma_0}^h \left(\frac{\sigma}{\sigma_0} - 1 \right) z dz - \frac{\dot{\lambda}}{E\dot{\kappa}t} - \frac{\dot{\lambda}}{\dot{\kappa}}$$

this leads to

$$EA\dot{\lambda} = \dot{N} + \frac{1}{\tau^*} \left[N - N_0 \left(\frac{1}{2} - \frac{1}{4} \frac{\sigma_0}{E\dot{\kappa}th} + \frac{3}{4} \frac{\dot{\lambda}}{\dot{\kappa}h} + \frac{1}{4} \frac{\dot{\lambda}}{\dot{\kappa}h} \frac{E\dot{\kappa}th}{\sigma_0} - \frac{1}{4} \frac{E\dot{\kappa}th}{\sigma_0} \right) \right] \quad (4.1.26)$$

and

$$EI\dot{\kappa} = \dot{M} + \frac{1}{\tau^*} \left\{ M - M_0 \left[\frac{1}{2} - \frac{1}{6} \left(\frac{\sigma_0}{E\dot{\kappa}th} \right)^2 - \frac{1}{2} \left(\frac{\sigma_0}{E\dot{\kappa}th} \right)^2 \left(\frac{E\dot{\lambda}\tau^*}{\sigma_0} \right) + \frac{1}{2} \frac{E\dot{\lambda}\tau^*}{\sigma_0} \left(\frac{\sigma_0}{E\dot{\kappa}\tau^*h} \right)^2 \frac{\tau^*}{t} + \frac{1}{3} \frac{E\dot{\kappa}th}{\sigma_0} - \frac{1}{2} \frac{E\dot{\lambda}t}{\sigma_0} + \frac{1}{6} \left(\frac{\sigma_0}{E\dot{\kappa}\tau^*h} \right)^2 \left(\frac{E\dot{\lambda}\tau^*}{\sigma_0} \right)^3 \frac{t}{\tau^*} \right] \right\} \quad (4.1.27)$$

where N : is the axial force in the cross section

N_0 : is the static, fully plastic axial capacity of the cross section

M : is the bending moment in the cross section

M_0 : is the static, fully plastic bending capacity of the cross section

For the third condition, we get

$$EA\dot{\lambda} = \dot{N} + \frac{1}{\tau^*} \left[N - N_0 \frac{\dot{\lambda}}{\dot{\kappa}h} \right] \quad (4.1.28)$$

and

$$EI\dot{\kappa} = \dot{M} + \frac{1}{\tau^*} \left\{ M - M_0 \left[1 - \left(\frac{\dot{\lambda}}{\dot{\kappa}h} \right)^2 - \frac{1}{3} \left(\frac{\sigma_0}{E\dot{\kappa}th} \right)^2 \right] \right\} \quad (4.1.29)$$

Case (b): $\frac{\dot{\lambda}}{\dot{\kappa}} \geq 1.0$

In this case there is only one boundary line between the elastic and viscoplastic zone. This boundary line is obtained in a similar way to what was done in (a). The main difference between (a) and (b) is that in (b), there will be no change in the sign of the strain rate over the cross section. Figure 4.1.6 shows the stress distribution in the cross section. Again three main cases are recognized here.

1)
$$0 \leq t \leq \frac{\sigma_0}{E(\dot{\lambda} + \dot{\kappa}h)}$$

For this the integration of the constitutive equation will give

$$EA\dot{\lambda} = \dot{N}$$

$$EI\dot{\kappa} = \dot{M}$$

which is similar to case (a).

2)
$$\frac{\sigma_0}{E(\dot{\lambda} + \dot{\kappa}h)} \leq t \leq \frac{\sigma_0}{E(\dot{\lambda} - \dot{\kappa}h)}$$

And the integration of the constitutive equation gives

$$EA\dot{\lambda} = \dot{N} + \frac{1}{\tau^*} \left\{ N - N_0 \left[\frac{1}{2} - \frac{1}{4} \frac{\sigma_0}{E\dot{\kappa}th} + \frac{3}{4} \frac{\dot{\lambda}}{\dot{\kappa}h} + \frac{1}{4} \frac{\dot{\lambda}}{\dot{\kappa}h} \frac{E\dot{\kappa}th}{\sigma_0} - \frac{1}{4} \frac{E\dot{\kappa}th}{\sigma_0} \right] \right\}$$

and

$$\begin{aligned}
EI\dot{\kappa} = \dot{M} + \frac{1}{\tau^*} \left\{ M - M_0 \left[\frac{1}{2} - \frac{1}{6} \left(\frac{\sigma_0}{E\dot{\kappa}th} \right)^2 - \frac{1}{2} \left(\frac{\sigma_0}{E\dot{\kappa}th} \right)^2 \left(\frac{E\dot{\lambda}\tau^*}{\sigma_0} \right) \right. \right. \\
+ \frac{1}{2} \left(\frac{E\dot{\lambda}\tau^*}{\sigma_0} \right) \left(\frac{\sigma_0}{E\dot{\kappa}th} \right)^2 \frac{\tau^*}{t} + \frac{1}{3} \left(\frac{E\dot{\kappa}th}{\sigma_0} \right) - \frac{1}{2} \frac{E\dot{\lambda}t}{\sigma_0} \\
\left. \left. + \frac{1}{6} \left(\frac{\sigma_0}{E\dot{\kappa}\tau^*h} \right)^2 \left(\frac{E\dot{\lambda}\tau^*}{\sigma_0} \right) \frac{t}{\tau^*} \right] \right\}
\end{aligned}$$

which is again the same as in (a)

$$3) \quad t > \frac{\sigma_0}{E(\dot{\lambda} - \dot{\kappa}h)}$$

and this gives

$$EA\dot{\lambda} = \dot{N} + \frac{1}{\tau^*} (N - N_0) \quad (4.1.30)$$

and

$$EI\dot{\kappa} = \dot{M} + \frac{M}{\tau^*} \quad (4.1.31)$$

It is only here where there is a difference between case (a) and case (b). This could be explained easily due to the fact that, only in this condition is there a change in sign of the strain rate in case (a), while there is no change in (b).

In order to have the generalized constitutive equations in dimensionless forms which would help in establishing the yield surface, the following generalized dimensionless quantities will be used

$$\bar{M} = \frac{M}{M_0}$$

$$\bar{N} = \frac{N}{N_0}$$

$$\dot{\bar{\kappa}} = \frac{E\dot{\kappa}h\tau^*}{\sigma_0} \quad (4.1.32)$$

$$\dot{\bar{\lambda}} = \frac{2E\dot{\lambda}\tau^*}{\sigma_0}$$

$$\bar{t} = \frac{t}{\tau^*}$$

We should mention here that the generalized rates are chosen in such a way as to have the product $\dot{\bar{\lambda}}\bar{N} + \dot{\bar{\kappa}}\bar{M}$ give the rate of work. Therefore, equations (4.1.24) to (4.1.31) in a dimensionless form will be as follows

Case (a): $\frac{\dot{\bar{\lambda}}}{\dot{\bar{\kappa}}} \leq 2.0$

for

1) $0 \leq \bar{t} \leq \frac{1}{\dot{\bar{\kappa}} + \frac{\dot{\bar{\lambda}}}{2}}$

we get

$$\frac{\dot{\bar{\lambda}}}{2} = \dot{\bar{N}} \quad (4.1.33)$$

$$\frac{2}{3} \dot{\bar{\kappa}} = \dot{\bar{M}}$$

for

$$2) \quad \frac{1}{\dot{\kappa} + \frac{\dot{\lambda}}{2}} \leq \bar{\tau} \leq \frac{1}{\dot{\kappa} - \frac{\dot{\lambda}}{2}}$$

we get

$$\frac{\dot{\lambda}}{2} = \dot{N} + \bar{N} - \frac{1}{2} + \frac{1}{4} \frac{1}{\dot{\kappa}} \bar{\tau} - \frac{3}{8} \frac{\dot{\lambda}}{\dot{\kappa}} - \frac{1}{8} \dot{\lambda} \bar{\tau} + \frac{1}{4} \dot{\kappa} \bar{\tau}$$

$$\frac{2}{3} \dot{\kappa} = \dot{M} + \bar{M} - \frac{1}{2} + \frac{1}{6} \frac{1}{(\dot{\kappa} \bar{\tau})^2} + \frac{1}{8} \left(\frac{\dot{\lambda}}{\dot{\kappa}} \right)^2 - \frac{1}{4} \frac{\dot{\lambda} \bar{\tau}}{(\dot{\kappa} \bar{\tau})^2} - \frac{1}{3} \dot{\kappa} \bar{\tau}$$

$$+ \frac{1}{4} \dot{\lambda} \bar{\tau} - \frac{1}{48} \frac{(\dot{\lambda} \bar{\tau})^3}{(\dot{\kappa} \bar{\tau})^2}$$

(4.1.34)

or

$$\frac{\dot{\lambda}}{2} = \dot{N} + \bar{N} - N_1(\dot{\lambda}, \dot{\kappa}, \bar{\tau})$$

and

(4.1.35)

$$\frac{2}{3} \dot{\kappa} = \dot{M} + \bar{M} - M_1(\dot{\lambda}, \dot{\kappa}, \bar{\tau})$$

where N_1 and M_1 are functions of $\dot{\lambda}$, $\dot{\kappa}$, $\bar{\tau}$.

For

$$3) \quad \bar{\tau} > \frac{1}{\dot{\kappa} - \frac{\dot{\lambda}}{2}}$$

we get

$$\frac{\dot{\lambda}}{2} = \dot{N} + \bar{N} - \frac{1}{2} \frac{\dot{\lambda}}{\dot{\kappa}}$$

(4.1.36)

$$\frac{2}{3} \dot{\kappa} = \dot{M} + \bar{M} - 1 + \frac{1}{4} \left(\frac{\dot{\lambda}}{\dot{\kappa}} \right)^2 + \frac{1}{3} \frac{1}{(\dot{\kappa} \bar{\tau})^2}$$

or

$$\frac{\dot{\lambda}}{2} = \dot{N} + \bar{N} - N_2(\dot{\lambda}, \dot{\kappa})$$

(4.1.37)

$$\frac{2}{3} \dot{\kappa} = \dot{M} + \bar{M} - M_2(\dot{\lambda}, \dot{\kappa}, \bar{\tau})$$

where N_2, M_2 are functions of $\dot{\lambda}, \dot{\kappa}, \bar{\tau}$.

Case (b):

$$\frac{\dot{\lambda}}{\dot{\kappa}} \geq 2.0$$

For

1)

$$0 \leq t \leq \frac{1}{\frac{\dot{\lambda}}{2} + \dot{\kappa}}$$

we get

$$\frac{\dot{\lambda}}{2} = \dot{N}$$

(4.1.38)

$$\frac{2}{3} \dot{\kappa} = \dot{M}$$

for

2)

$$\frac{1}{\frac{\dot{\lambda}}{2} + \dot{\kappa}} \leq \bar{\tau} \leq \frac{1}{\frac{\dot{\lambda}}{2} - \dot{\kappa}}$$

we get

$$\frac{\dot{\lambda}}{2} = \dot{N} + \bar{N} - \frac{1}{2} + \frac{1}{4} \frac{1}{\dot{\kappa} \bar{\tau}}$$

(4.1.39)

$$- \frac{3}{8} \frac{\dot{\lambda}}{\dot{\kappa}} - \frac{1}{8} \dot{\lambda} \bar{\tau} + \frac{1}{4} \dot{\kappa} \bar{\tau}$$

and

$$\begin{aligned} \frac{2}{3} \dot{\kappa} &= \dot{\bar{M}} + M - \frac{1}{2} + \frac{1}{6} \frac{1}{(\dot{\kappa} \bar{t})^2} \\ &+ \frac{1}{8} \left(\frac{\dot{\lambda}}{\dot{\kappa}} \right)^2 - \frac{1}{4} \frac{\dot{\lambda} \bar{t}}{(\dot{\kappa} \bar{t})^2} - \frac{1}{3} \dot{\kappa} \bar{t} \\ &+ \frac{1}{4} \dot{\lambda} \bar{t} - \frac{1}{48} \frac{(\dot{\lambda} \bar{t})^3}{(\dot{\kappa} \bar{t})^2} \end{aligned}$$

or

$$\frac{\dot{\lambda}}{2} = \dot{\bar{N}} + \bar{N} - N_1(\dot{\lambda}, \dot{\kappa}, \bar{t})$$

and

(4.1.40)

$$\frac{2}{3} \dot{\kappa} = \dot{\bar{M}} + \bar{M} - M_1(\dot{\lambda}, \dot{\kappa}, \bar{t})$$

for

$$3) \quad \bar{t} \geq \frac{1}{\frac{\dot{\lambda}}{2} - \dot{\kappa}}$$

we get

$$\frac{\dot{\lambda}}{2} = \dot{\bar{N}} + \bar{N} - 1$$

$$\frac{2}{3} \dot{\kappa} = \dot{\bar{M}} + \bar{M} \quad (4.1.41)$$

Equations (4.1.33) to (4.1.41) are the generalized constitutive equations for bending and extension of a rectangular cross section made of viscoplastic material. They are in terms of the axial force, bending moment and their rates, and curvature and extension and their rates also. They are an uncoupled system of linear first order differential equations, which could be solved in a way similar to that of the pure bending case, taking into account the different initial conditions.

4.1 (iii) The Dynamic Yield Surface for Combined Bending and Extension

In the previous section the constitutive equation of the elastic viscoplastic material was generalized in terms of moments, axial force, curvature rate and extension rate. In this section a yield surface which is a function of axial force N and bending moment M will be developed for different rate effects.

When $\bar{t} \rightarrow \infty$ in equations (4.1.36) and (4.1.41), the following will result

Case (a):

$$\bar{N} = \frac{1}{2} \frac{\dot{\lambda}}{\dot{\kappa}} + \frac{\dot{\lambda}}{2}$$

$$\bar{M} = 1.0 - \frac{1}{4} \left(\frac{\dot{\lambda}}{\dot{\kappa}} \right)^2 + \frac{2}{3} \frac{\dot{\lambda}}{\dot{\kappa}}$$

For $\frac{\dot{\lambda}}{\dot{\kappa}} \leq 2.0$ (4.1.42)

Case (b):

$$\bar{N} = 1 + \frac{\dot{\lambda}}{2}$$

$$\bar{M} = \frac{2}{3} \frac{\dot{\lambda}}{\dot{\kappa}}$$

For $\frac{\dot{\lambda}}{\dot{\kappa}} \geq 2.0$ (4.1.43)

Equations (4.1.42) and (4.1.43) are in terms of two parameters $\dot{\lambda}$ and $\dot{\kappa}$. However, for the purpose of establishing the dynamic yield surface, two new parameters will be used

$$\dot{D} = \sqrt{\dot{\lambda}^2 + \frac{4}{3} \dot{\kappa}^2}$$

$$R = \frac{\dot{\lambda}}{\dot{\kappa}}$$

(4.1.44)

\dot{D} : is a measure of a generalized rate effect which is a combination of the extension and bending rates.

R : is the ratio between the generalized extension and generalized curvature rates. It varies from 0, which is the pure bending case to ∞ which is the pure extension case.

Substituting (4.1.44) in (4.1.42) and (4.1.43) will give

Case (a): $R \leq 2.0$

$$\bar{N} = \frac{1}{2} R + \frac{1}{2} \frac{R\dot{D}}{\sqrt{R^2 + \frac{4}{3}}} \quad (4.1.45)$$

$$\bar{M} = 1.0 - \frac{1}{4} R^2 + \frac{2}{3} \frac{\dot{D}}{\sqrt{R^2 + \frac{4}{3}}}$$

Case (b): $R \geq 2.0$

$$\bar{N} = 1 + \frac{1}{2} \frac{\dot{D}R}{\sqrt{R^2 + \frac{4}{3}}} \quad (4.1.46)$$

$$\bar{M} = \frac{2}{3} \frac{\dot{D}}{\sqrt{R^2 + \frac{4}{3}}}$$

Now, given any value for \dot{D} , the generalized rate parameter, equations (4.1.45) and (4.1.46) will give the yield surface for that rate. In equation (4.1.45), there is no way of getting explicitly the equation of the yield surface, so we have to use the parametric representation. However, for equation (4.1.46), an explicit form of the yield

surface is possible. By eliminating R from equation (4.1.46) we get

$$4(\bar{N} - 1)^2 + 3\bar{M}^2 = \dot{D}^2 \quad (4.1.47)$$

Equation (4.1.47) is applicable for all $R \geq 2.0$. Differentiating equation (4.1.47) with respect to \bar{N} will give

$$8(\bar{N} - 1) + 6\bar{M} \frac{\partial \bar{M}}{\partial \bar{N}} = 0$$

or (4.1.48)

$$\frac{\partial \bar{M}}{\partial \bar{N}} = -R$$

Equation (4.1.48) indicates that the rate vector which has two components $\dot{\bar{\lambda}}$ and $\dot{\bar{\kappa}}$ is normal to the yield surface. This is an appropriate flow law for that surface. Figure 4.1.7 shows the yield surface for different rates.

It is of interest to look at some extreme cases of the yield surface

$$1) \quad \dot{D} = 0 \quad \text{and} \quad \dot{\bar{\lambda}} = \dot{\bar{\kappa}} = 0$$

This will give the static yield surface

$$\bar{M} + \bar{N}^2 = 1.0, \quad 0 \leq R \leq \infty$$

$$2) \quad \dot{D} \gg 1.0$$

In this case, equations (4.1.45) and (4.1.46) will give the same results

$$4\bar{N}^2 + 3\bar{M}^2 = \dot{D}^2, \quad 0 \leq R \leq \infty$$

Therefore the dynamic yield surface for high rates is approximately an elliptical one. It is an expanding surface. It has the property that the flow vector is normal to the yield surface.

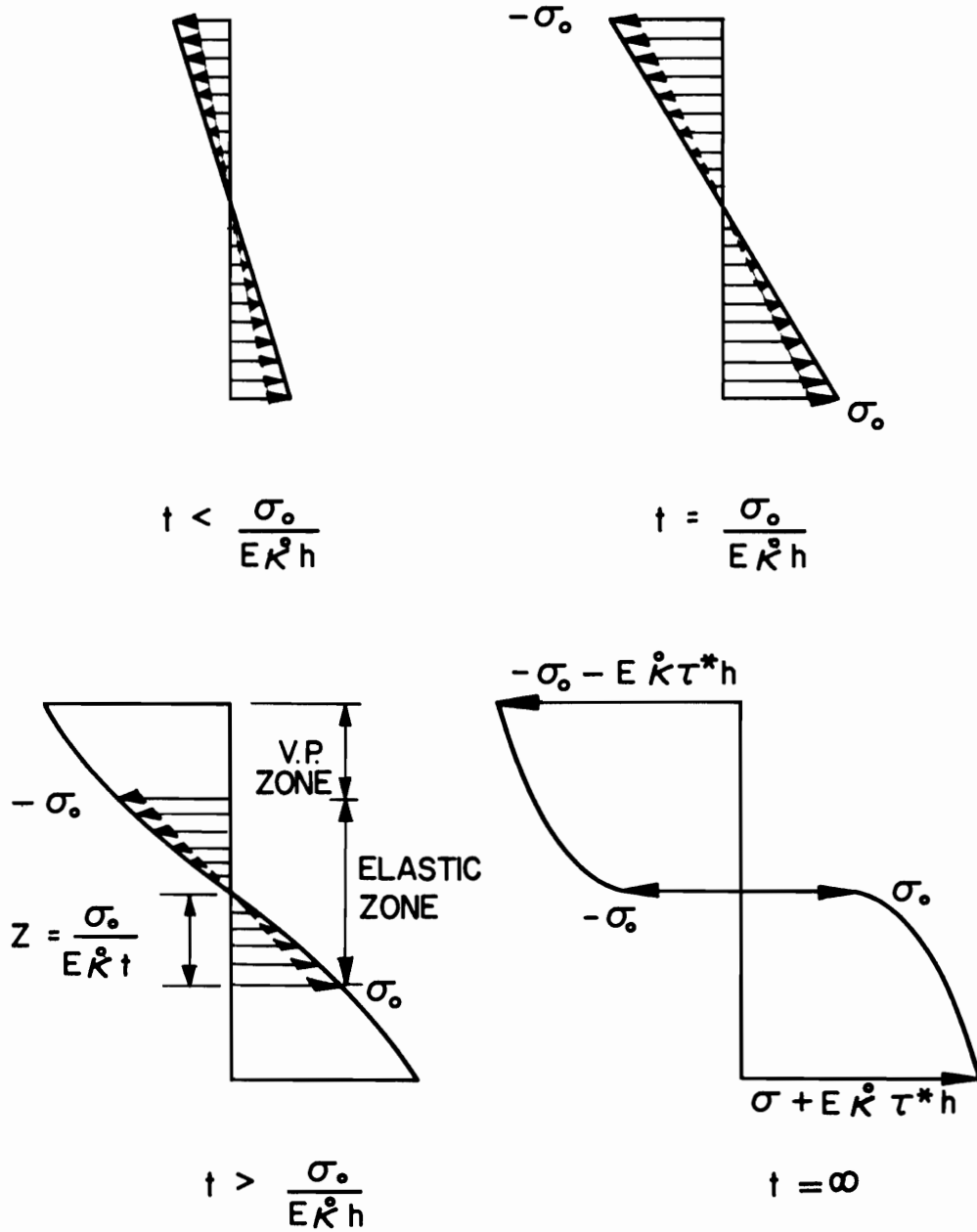


FIG. 4·1·1 STRESS DISTRIBUTION OVER THE CROSS SECTION

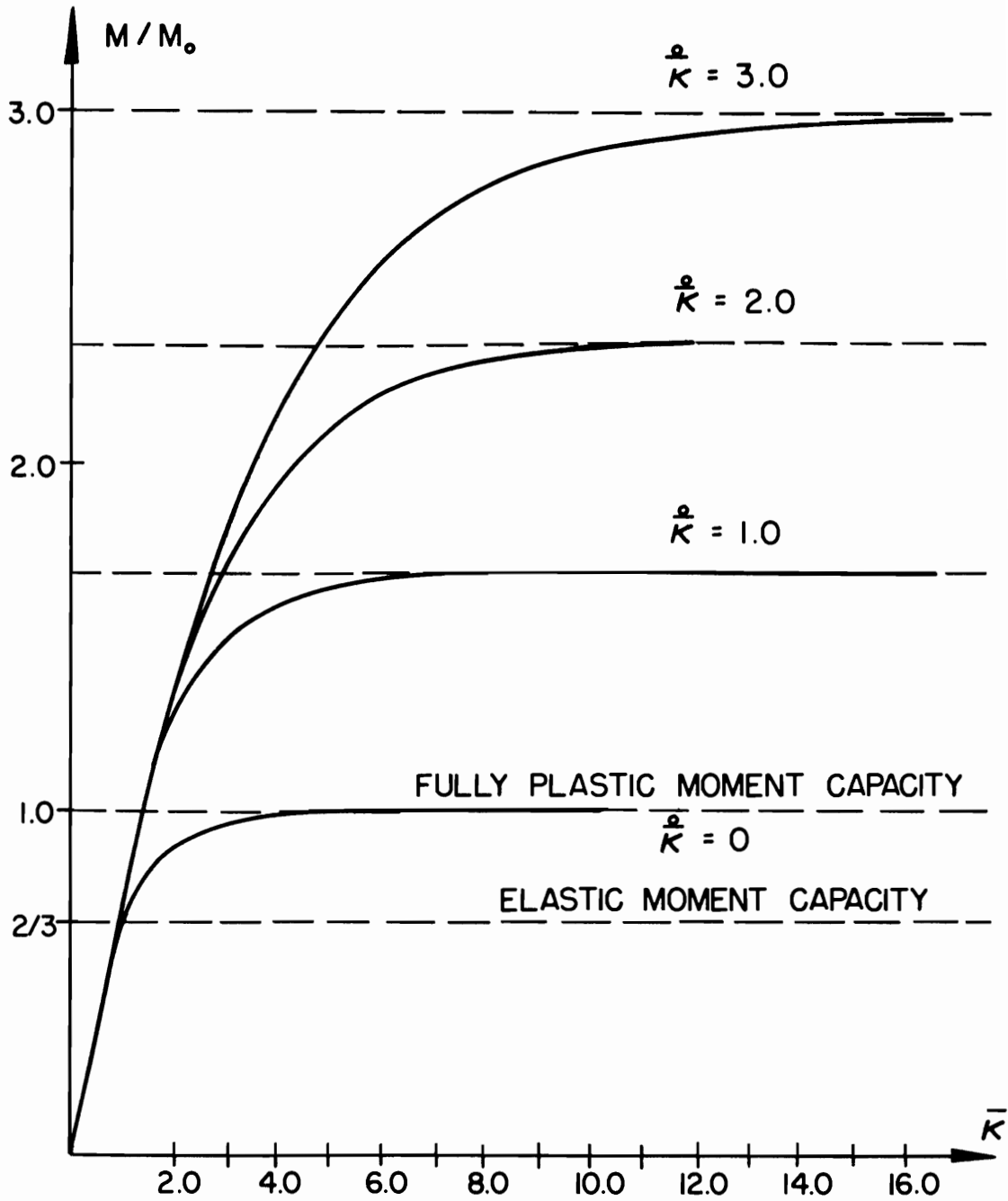


FIG. 4·1·2 MOMENT CURVATURE RELATION FOR VISCO PLASTIC MATERIAL

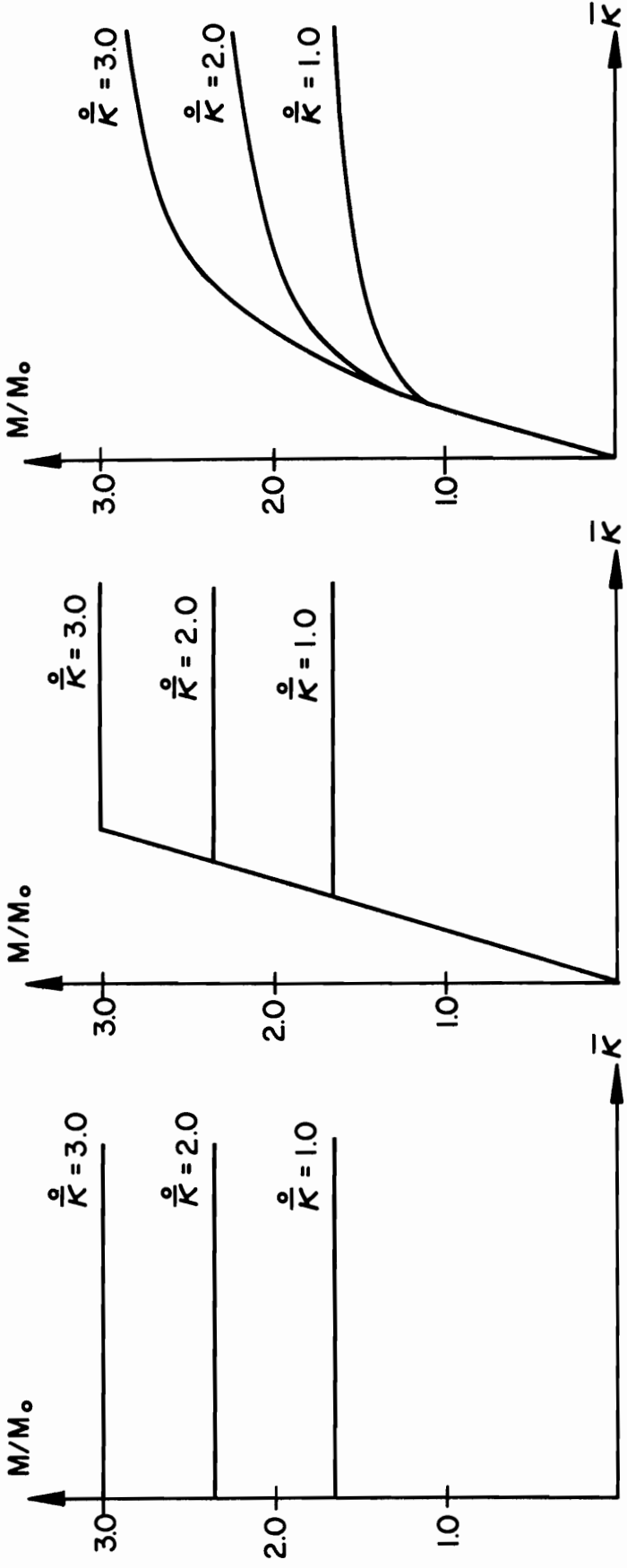


FIG. 4·1·3 DIFFERENT APPROXIMATION FOR THE MOMENT CURVATURE RELATION

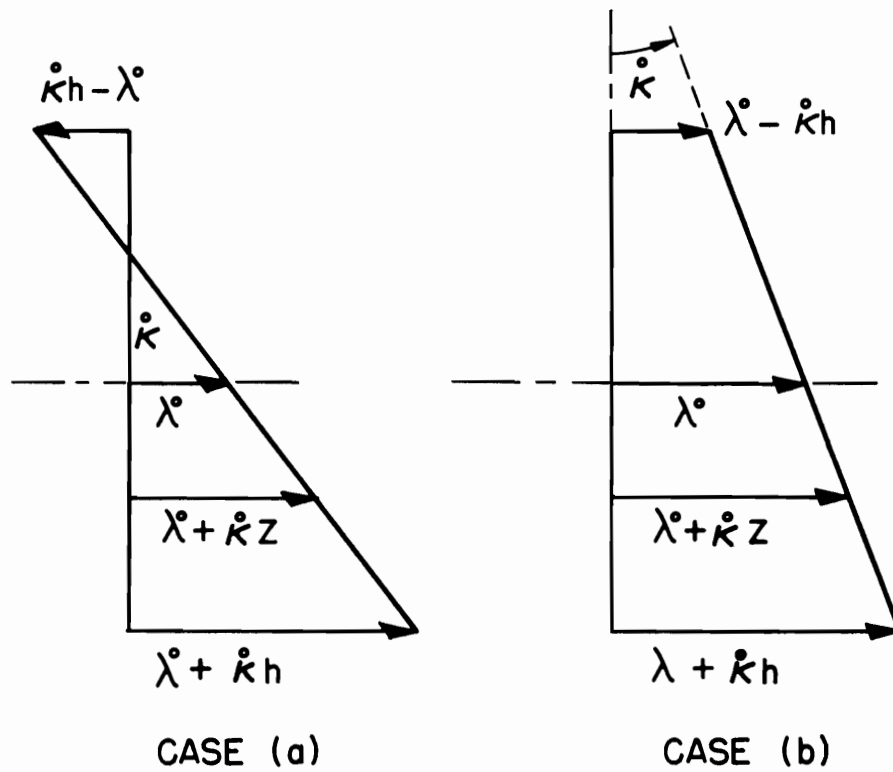
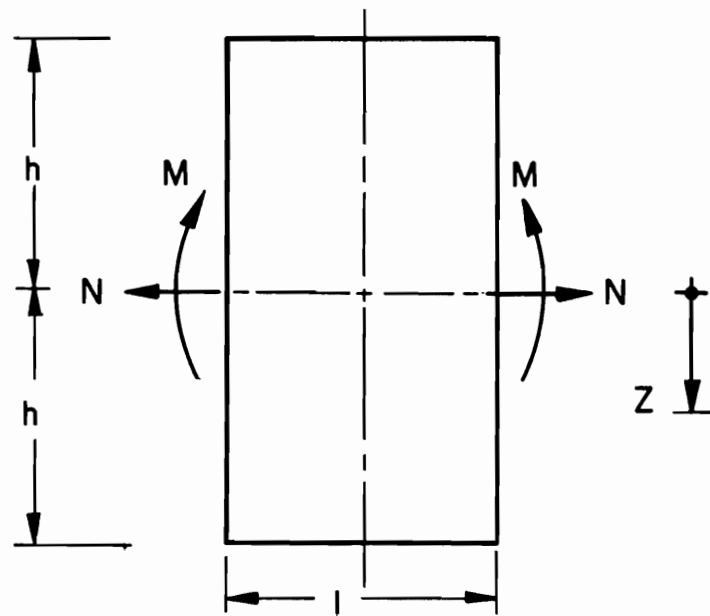


FIG. 4.1.4 STRAIN RATE DISTRIBUTION OVER THE CROSS SECTION

CASE (a)

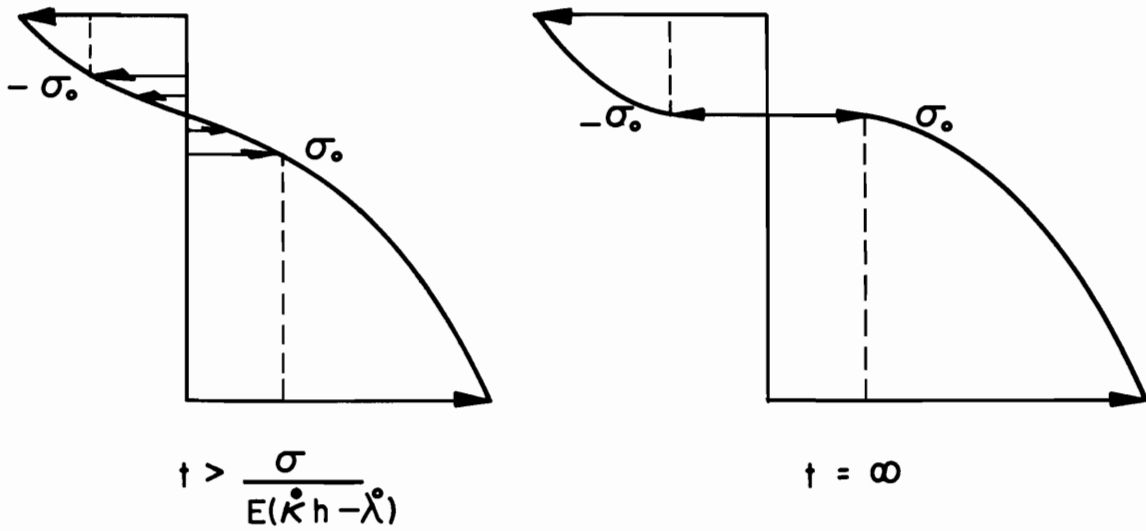
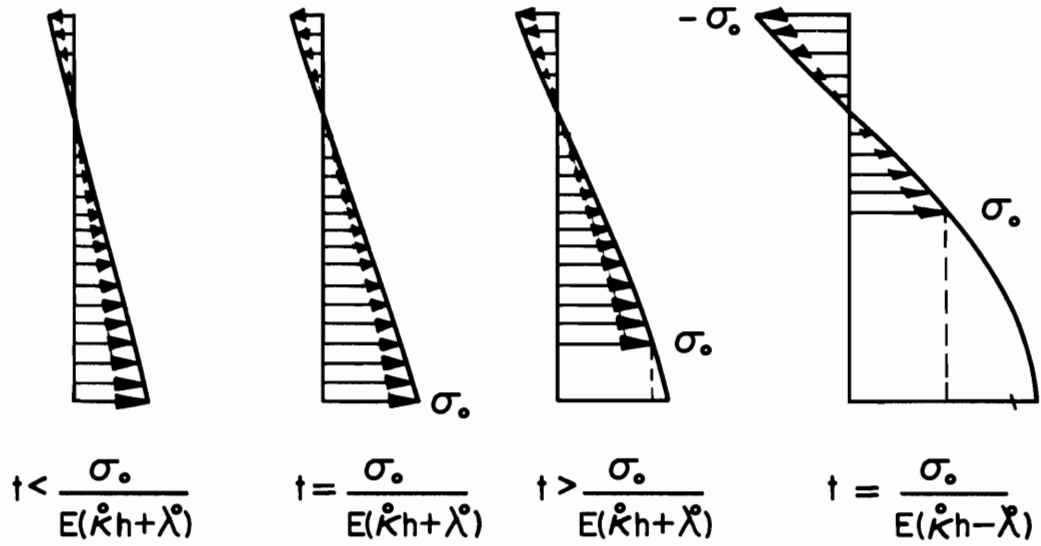


FIG. 4·1·5 STRESS DISTRIBUTION OVER THE CROSS-SECTION FOR COMBINED BENDING AND AXIAL FORCE

CASE (b)

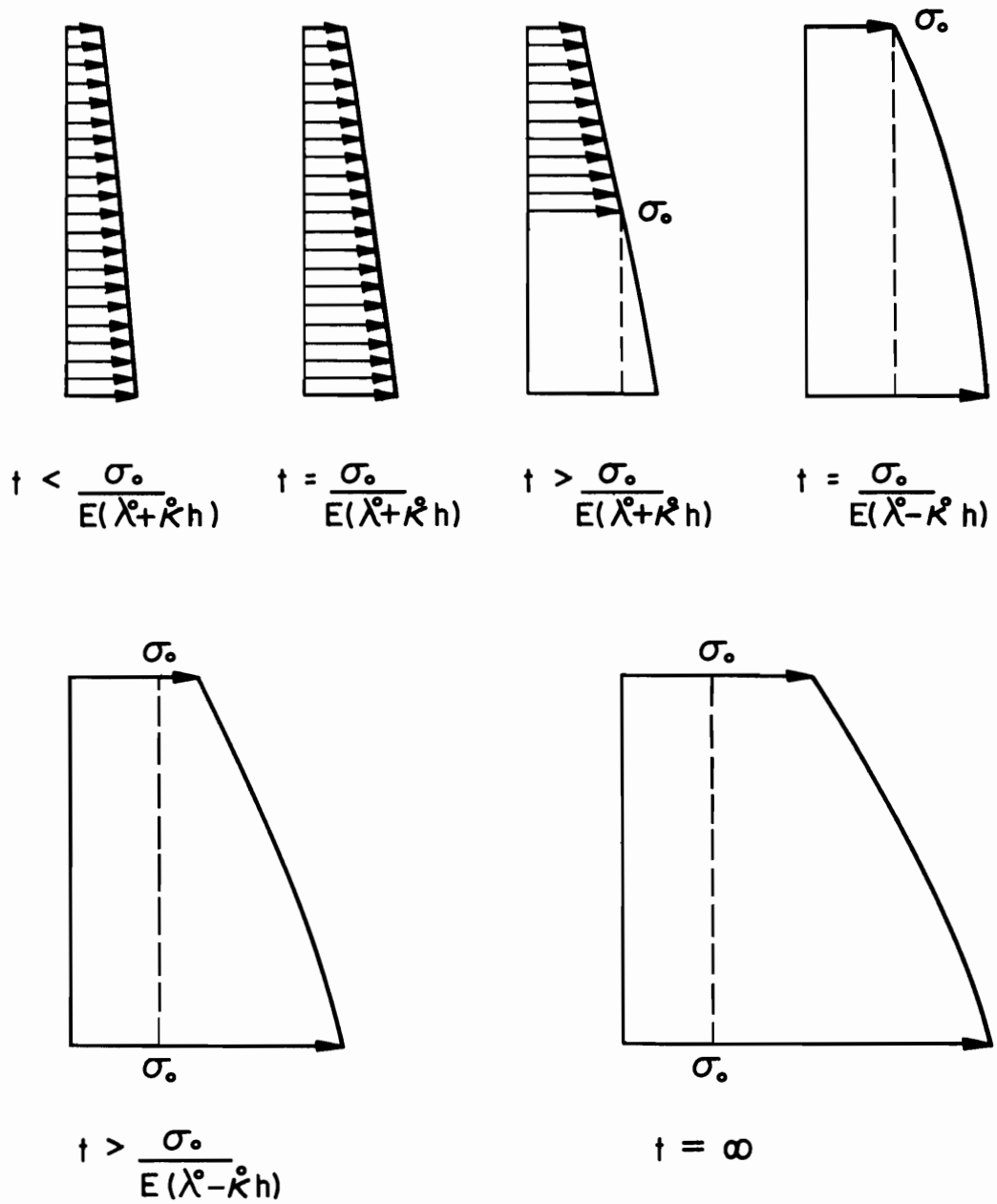


FIG. 4·1·6 STRESS DISTRIBUTION OVER THE CROSS-SECTION FOR COMBINED BENDING AND AXIAL FORCE

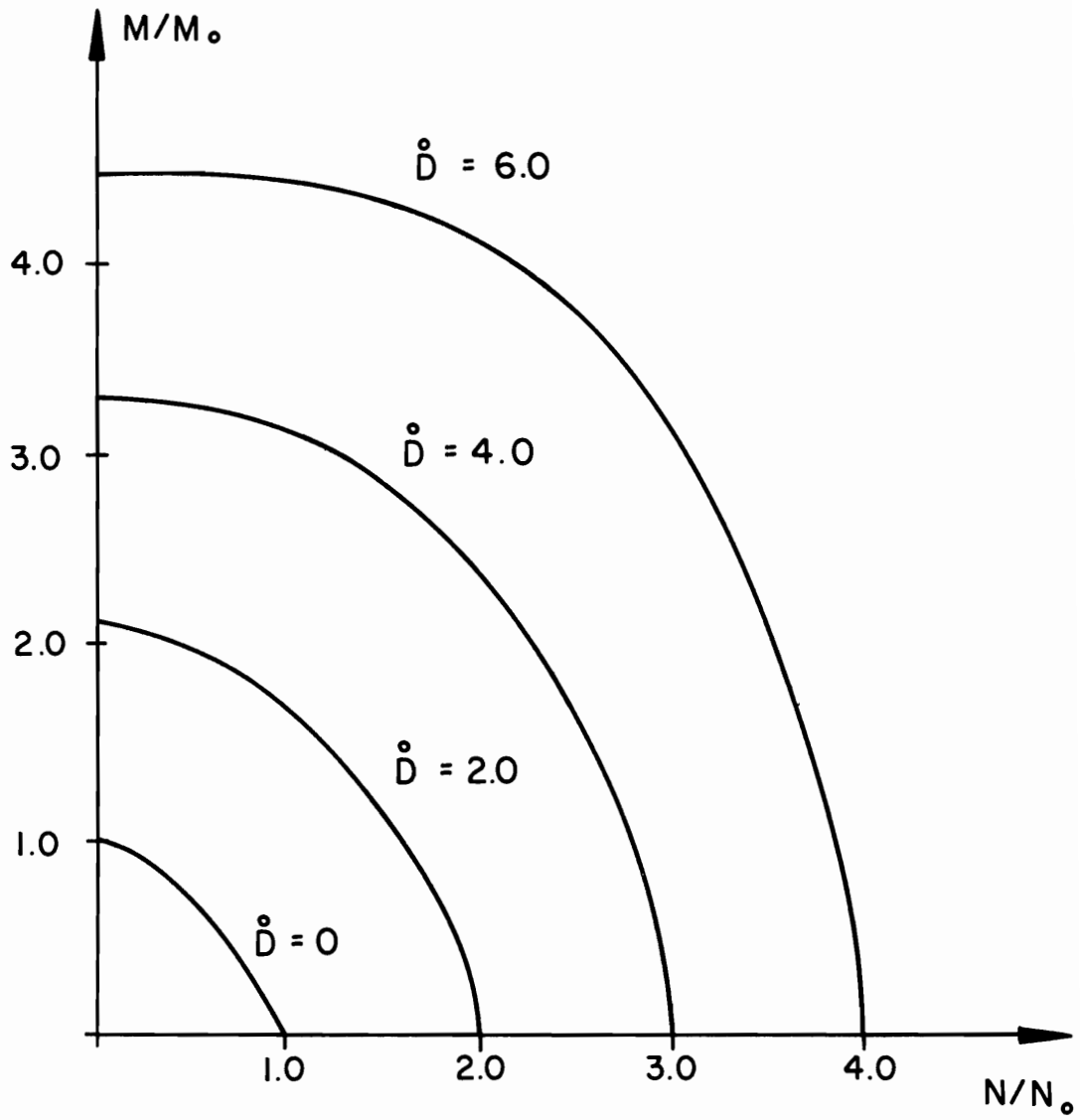


FIG. 4·1·7 DYNAMIC YIELD SURFACE FOR BENDING AND EXTENSION

4.2 Direct Methods for the Study of Impulsive Loading on Elastic Viscoplastic Beams

4.2 (i) Transformation of the Uniaxial Constitutive Equation into an Incremental Form

A constitutive equation for the viscoplastic material in the following form will be assumed

$$E\dot{\epsilon}(t) = \dot{\sigma}(t) + \frac{\sigma_0}{\tau^*} \phi\left(\frac{\sigma(t)}{\sigma_0} \pm 1\right) \quad (4.2.1)$$

This constitutive equation is a differential equation which relates strain rate, stress rate and stress. For the purpose of this study, an incremental form of this equation is more useful. Integrating equation (4.2.1) between the limits t and $t + \Delta t$ will give

$$E\Delta\epsilon = \Delta\sigma + \int_t^{t+\Delta t} \frac{\sigma_0}{\tau^*} \phi\left(\frac{\sigma(T)}{\sigma_0} \pm 1\right) dT \quad (4.2.2)$$

where

$$\Delta\epsilon = \epsilon(t + \Delta t) - \epsilon(t)$$

$$\Delta\sigma = \sigma(t + \Delta t) - \sigma(t)$$

$\Delta\epsilon$: is the increase in strain over the increment of time Δt .

$\Delta\sigma$: is the increase in stress over the increment of time Δt .

The integration in the right hand side of equation (4.2.2) is due to the viscoplastic character of the material. It is clear that it will be equal to 0, if the stress is still below the elastic limit, and this will lead to Hooke's Law

$$E\Delta\epsilon = \Delta\sigma \quad \text{if } |\sigma| < \sigma_0$$

If the integration on the right hand side is divided by E , the elastic modulus of the material, it will give the viscoplastic component of the increase in strain over the increment of time Δt . To be able to evaluate this integral the quantity under the integral sign will be expanded in a Taylor series as follows

$$\begin{aligned}
 \frac{\sigma_0}{\tau^*} \phi\left(\frac{\sigma(T)}{\sigma_0} \pm 1\right) &= \frac{\sigma_0}{\tau^*} \phi\left(\frac{\sigma(t)}{\sigma_0} \pm 1\right) \\
 &+ \frac{1}{\tau^*} \phi'\left(\frac{\sigma(t)}{\sigma_0} \pm 1\right) \dot{\sigma}(t)(T - t) \\
 &+ \frac{1}{2\tau^*} \phi''\left(\frac{\sigma(t)}{\sigma_0} \pm 1\right) \ddot{\sigma}(t)(T - t)^2 \\
 &+ \frac{1}{2\tau^* \sigma_0} \phi'''\left(\frac{\sigma(t)}{\sigma_0} \pm 1\right) \dot{\sigma}(t)^2 (T - t)^2 \\
 &+ \dots
 \end{aligned} \tag{4.2.3}$$

Also, if we expand $\sigma(t + \Delta t)$ into a Taylor series we get

$$\sigma(t + \Delta t) = \sigma(t) + \dot{\sigma}(t)\Delta t + \ddot{\sigma}(t) \frac{\Delta t^2}{2} + \dots$$

or

$$\dot{\sigma}(t) = \frac{\Delta\sigma}{\Delta t} - \ddot{\sigma}(t) \frac{\Delta t}{2} - \dots \tag{4.2.4}$$

Substituting the above results (4.2.4) in the expansion of $\phi\left(\frac{\sigma(T)}{\sigma_0} \pm 1\right)$ will give

$$\begin{aligned}
\frac{\sigma_0}{\tau^*} \phi\left(\frac{\sigma(T)}{\sigma_0} \pm 1\right) &= \frac{\sigma_0}{\tau^*} \phi\left(\frac{\sigma(t)}{\sigma_0} \pm 1\right) \\
&+ \frac{1}{\tau^*} \phi'\left(\frac{\sigma(t)}{\sigma_0} \pm 1\right) \frac{\Delta\sigma}{\Delta t} (T - t) \\
&- \frac{1}{\tau^*} \phi'\left(\frac{\sigma(t)}{\sigma_0} \pm 1\right) \frac{\ddot{\sigma}(t)}{2} \Delta t (T - t) \\
&+ \frac{1}{\tau^*} \phi'\left(\frac{\sigma^* t}{\sigma_0} \pm 1\right) \ddot{\sigma}(t) (T - t)^2 \\
&+ \frac{1}{2\tau^* \sigma_0} \phi''\left(\frac{\sigma(t)}{\sigma_0} \pm 1\right) \frac{\Delta\sigma^2}{\Delta t^2} (T - t)^2 \\
&+ \frac{1}{2\tau^* \sigma_0} \phi''\left(\frac{\sigma(t)}{\sigma_0} \pm 1\right) \frac{\ddot{\sigma}(t)^2}{4} \Delta t^2 (T - t)^2 \\
&- \frac{1}{2\tau^* \sigma_0} \phi''\left(\frac{\sigma(t)}{\sigma_0} \pm 1\right) \Delta\sigma \ddot{\sigma}(t) (T - t)^2 \\
&+ \dots
\end{aligned} \tag{4.2.5}$$

Now integrating this expression (4.2.5) between the two limits t and $t + \Delta t$ will give

$$\begin{aligned}
\int_t^{t+\Delta t} \frac{\sigma_0}{\tau^*} \phi\left(\frac{\sigma(T)}{\sigma_0} \pm 1\right) dT &= \frac{\sigma_0}{\tau^*} \phi\left(\frac{\sigma(t)}{\sigma_0} \pm 1\right) \Delta t \\
&+ \frac{1}{2\tau^*} \phi'\left(\frac{\sigma(t)}{\sigma_0} \pm 1\right) \Delta\sigma \Delta t \\
&+ \frac{1}{6\tau^* \sigma_0} \phi''\left(\frac{\sigma(t)}{\sigma_0} \pm 1\right) \Delta\sigma^2 \Delta t \\
&- \frac{1}{12\tau^*} \phi'\left(\frac{\sigma(t)}{\sigma_0} \pm 1\right) \ddot{\sigma}(t) \Delta t^3 \\
&- \frac{1}{6\tau^* \sigma_0} \phi''\left(\frac{\sigma(t)}{\sigma_0} \pm 1\right) \ddot{\sigma}(t) \Delta\sigma \Delta t^3 \\
&+ \frac{1}{24\tau^* \sigma_0} \phi''\left(\frac{\sigma(t)}{\sigma_0} \pm 1\right) \ddot{\sigma}(t)^2 \Delta t^5 \\
&+ \dots
\end{aligned} \tag{4.2.6}$$

As an approximation of this integral the first two terms will be chosen, therefore

$$\int_t^{t+\Delta t} \frac{\sigma_0}{\tau^*} \phi\left(\frac{\sigma(T)}{\sigma_0} \pm 1\right) dT = \frac{\sigma_0}{\tau^*} \phi\left(\frac{\sigma(t)}{\sigma_0} \pm 1\right) \Delta t$$

(4.2.7)

$$+ \frac{1}{2\tau^*} \phi'\left(\frac{\sigma(t)}{\sigma_0} \pm 1\right) \Delta\sigma \Delta t + \dots$$

The error involved in this expression is of the same magnitude as the absolute value of the rest of the terms in the expansion (4.2.6).

Substituting the above result in equation (4.2.2) gives

$$E\Delta\varepsilon = \left(1 + \frac{\Delta t}{2\tau^*} \phi'\left(\frac{\sigma(t)}{\sigma_0} \pm 1\right)\right) \Delta\sigma + \frac{\sigma_0}{\tau^*} \phi\left(\frac{\sigma(t)}{\sigma_0} \pm 1\right) \Delta t$$

or

$$\frac{E\Delta\varepsilon}{1 + \frac{\Delta t}{2\tau^*} \phi'\left(\frac{\sigma(t)}{\sigma_0} \pm 1\right)} = \Delta\sigma + \frac{\frac{\sigma_0}{\tau^*} \phi\left(\frac{\sigma(t)}{\sigma_0} \pm 1\right) \Delta t}{1 + \frac{\Delta t}{2\tau^*} \phi'\left(\frac{\sigma(t)}{\sigma_0} \pm 1\right)}$$

(4.2.8)

if we call

$$\alpha = \frac{1}{1 + \frac{\Delta t}{2\tau^*} \phi'\left(\frac{\sigma(t)}{\sigma_0} \pm 1\right)}$$

(4.2.9)

$$\Delta\sigma' = \frac{\frac{\sigma_0}{\tau^*} \phi\left(\frac{\sigma(t)}{\sigma_0} \pm 1\right) \Delta t}{1 + \frac{\Delta t}{2\tau^*} \phi'\left(\frac{\sigma(t)}{\sigma_0} \pm 1\right)}$$

then equation (4.2.8) will be

$$\alpha E\Delta\varepsilon = \Delta\sigma + \Delta\sigma'$$

(4.2.10)

Equation (4.2.10) is the incremental form of the constitutive equation (4.2.1). The two coefficients α and $\Delta\sigma'$ will change from one increment to the other according to equation (4.2.9) but will stay constant during each increment.

It should be mentioned here that an incremental formulation of the constitutive equation (4.2.1) where the coefficient α is always equal to 1.0 is possible. However, it was found that the coefficient α helps in the convergence of the numerical solution. This is due mainly to the fact that the tangent modulus of the viscoplastic material relaxes with time from its initial elastic value until it reaches the zero value.

To improve the approximation assumed here, an iteration scheme within each increment could be used. After obtaining a solution to the problem using the incremental constitutive equation (4.2.10) the increase in stress $\Delta\sigma$ will be determined. Using this as a starting point again, a new value for α and $\Delta\sigma'$, for the same increment, is calculated in the following way

$$\alpha = \frac{1}{1 + \frac{\Delta t}{2\tau^*} \phi' \left(\frac{\sigma(t) + \Delta\sigma/2}{\sigma_0} \pm 1 \right)}$$

(4.2.11)

$$\Delta\sigma' = \frac{\frac{\sigma_0}{\tau^*} \phi \left(\frac{\sigma(t)}{\sigma_0} \pm 1 \right) \Delta t}{1 + \frac{\Delta t}{2\tau^*} \phi' \left(\frac{\sigma(t) + \Delta\sigma/2}{\sigma_0} \pm 1 \right)}$$

and the procedure is repeated many times.

We should mention here that the unloading criteria associated with (4.2.10) are the following

(1) for tensile stresses, $\sigma \geq 0$

$$\sigma > \sigma_0, \quad \text{for loading} \quad \text{i.e.} \quad \dot{\epsilon}^{VP} > 0 \quad (4.2.12)$$

$$\sigma \leq \sigma_0, \quad \text{for unloading} \quad \text{i.e.} \quad \dot{\epsilon}^{VP} = 0$$

(2) for compression stresses, $\sigma \leq \sigma_0$

$$\sigma < -\sigma_0, \quad \text{for loading} \quad \text{i.e.} \quad \dot{\epsilon}^{VP} < 0 \quad (4.2.13)$$

$$\sigma > -\sigma_0, \quad \text{for unloading} \quad \text{i.e.} \quad \dot{\epsilon}^{VP} = 0$$

However, if the load is removed instantaneously, i.e., $\dot{\sigma} = -\infty$ in the case of tensile stresses, or $\dot{\sigma} = +\infty$ in the case of compression stresses, the unloading will follow Hooke's Law immediately.

It is clear that this incremental procedure could be applied to other types of constitutive equations for viscoplastic material with slight modification. It could also handle very easily the case where strain hardening exists. It could also be applied to the multi-axial constitutive equation.

4.2 (ii) Incremental Constitutive Equation for a Beam of Rectangular Section

Assuming plane sections remain plane, the incremental increase in strain at any level in the cross section will be

$$\Delta \epsilon = \frac{\Delta \lambda}{\Delta x} + \frac{\Delta \psi}{\Delta x} z \quad (4.2.14)$$

if we call

$$\frac{\Delta \lambda}{\Delta x} = \Delta \epsilon_m$$

$$\frac{\Delta \psi}{\Delta x} = - \Delta \kappa$$

Where $\Delta \epsilon_m$ is the increase in strain of the center line of the cross section, $\Delta \kappa$ is the increase in curvature of the cross section.

therefore

$$\Delta \epsilon = \langle 1 \quad -z \rangle \begin{Bmatrix} \Delta \epsilon_m \\ \Delta \kappa \end{Bmatrix} \quad (4.2.15)$$

We now apply at the cross-section virtual displacements $\overline{\Delta \lambda}$ and $\overline{\Delta \kappa}$ and use the principle of virtual work, which states that for any body in equilibrium, the work done by the external forces during a virtual displacement will be equal to the work done by the internal forces, or

$$W_E = W_I$$

where W_E is the work done by the bending moment and axial force in the cross section, and W_I is the work done by the stresses during the same virtual displacements. Therefore

$$\langle \overline{\Delta\lambda} \quad \overline{\Delta\psi} \rangle \begin{Bmatrix} \Delta N \\ \Delta M \end{Bmatrix} = \int_{-h/2}^{h/2} b \overline{\Delta\epsilon}^T \Delta\sigma \, dz \cdot \Delta x \quad (4.2.16)$$

If we substitute (4.2.10) and (4.2.15) into (4.2.16) we get

$$\begin{Bmatrix} \Delta N \\ \Delta M \end{Bmatrix} = b \int_{-h/2}^{h/2} \langle 1 \quad z \rangle^T \alpha E \langle 1 \quad -z \rangle \begin{Bmatrix} \Delta\epsilon_m \\ \Delta\kappa \end{Bmatrix} dz \\ - b \int_{-h/2}^{h/2} \langle 1 \quad z \rangle^T \Delta\sigma' \, dz$$

or

$$\begin{Bmatrix} \Delta N \\ \Delta M \end{Bmatrix} = \begin{bmatrix} EA' & -ES' \\ ES' & -EI' \end{bmatrix} \begin{Bmatrix} \Delta\epsilon_m \\ \Delta\kappa \end{Bmatrix} - \begin{Bmatrix} \Delta N' \\ \Delta M' \end{Bmatrix} \quad (4.2.17)$$

which in matrix notation takes the form

$$\{\Delta S\} = [k]\{\Delta v\} - \{\Delta S'\} \quad (4.2.18)$$

where

$$A' = \int_{-h}^h b \alpha \, dz \\ S' = \int_{-h/2}^{h/2} b \alpha z \, dz \\ I' = \int_{-h/2}^{h/2} b \alpha z^2 \, dz \quad (4.2.19)$$

$$\Delta N' = \int_{-h/2}^{h/2} b \Delta \sigma' dz$$

$$\Delta M' = \int_{-h/2}^{h/2} b \Delta \sigma' z dz$$

$$[k] = \begin{bmatrix} EA' & -ES' \\ ES' & -EI' \end{bmatrix}$$

$$\{\Delta v\} = \begin{Bmatrix} \Delta \epsilon_m \\ \Delta \kappa \end{Bmatrix}$$

$$\{\Delta S\} = \begin{Bmatrix} \Delta N \\ \Delta M \end{Bmatrix}$$

$$\{\Delta S'\} = \begin{Bmatrix} \Delta N' \\ \Delta M' \end{Bmatrix}$$

Equation (4.2.17) is the generalized incremental constitutive equation. The coefficients of this equation are changing with time, and they have to be calculated at the beginning of each increment. It can be shown that if the stresses everywhere in the cross section were below the yield stress, then (4.2.17) reduces to the well known result

$$\begin{Bmatrix} \Delta N \\ \Delta M \end{Bmatrix} = \begin{bmatrix} EA & 0 \\ 0 & -EI \end{bmatrix} \begin{Bmatrix} \Delta \epsilon_m \\ \Delta \kappa \end{Bmatrix}$$

We should mention here that a similar incremental relation could be obtained directly from the generalized constitutive relation which was developed in Section 4.1 (ii).

4.2 (iii) Dynamic Equilibrium Equations for Beam Element in Incremental Form

Consider a beam element (I), figure 4.2.1, which is at an arbitrary position X. This position will be considered as an initial position. The material of the beam will be assumed to be concentrated in the center line. It behaves according to the generalized constitutive equation (4.2.17). This element will be referred to two coordinate systems, the first is global one X_0 , and the second is a local one X. Suppose now that the element (I) is moved to a new position \bar{X} . This position will be referred again to a global coordinate X_0 and a local one \bar{X} . Therefore a point (P) in the element (I) will move to a new position (\bar{P}). The displacement vector of point (P) referred to the coordinate system X is

$$\{\Delta r\} = \begin{Bmatrix} \Delta w \\ \Delta \theta \\ \Delta u \end{Bmatrix}$$

and to the coordinate system X_0 is

$$\{\Delta r_0\} = \begin{Bmatrix} \Delta w_0 \\ \Delta \theta_0 \\ \Delta u_0 \end{Bmatrix}$$

The relation between $\{\Delta r\}$ and $\{\Delta r_0\}$ could be established in terms of the rotation ψ of the X-coordinate system with respect to the X_0 -coordinate system.

$$\begin{Bmatrix} \Delta w \\ \Delta \theta \\ \Delta u \end{Bmatrix} = \begin{bmatrix} \cos \psi & 0 & -\sin \psi \\ 0 & 1 & 0 \\ \sin \psi & 0 & \cos \psi \end{bmatrix} \begin{Bmatrix} \Delta w_0 \\ \Delta \theta_0 \\ \Delta u_0 \end{Bmatrix} \quad (4.2.20)$$

or

$$\{\Delta r\} = [Q] \{\Delta r_0\}$$

now let:

$\{\Delta r^i\}$ and $\{\Delta r^j\}$ be the increase in the nodal displacements vectors between position X and position \bar{X} , referred to the X-coordinate system.

$\{R^i\}$, and $\{R^j\}$ are the nodal forces vectors at position X referred to the X-coordinate system.

$\{R^i + \Delta R^i\}$, and $\{R^j + \Delta R^j\}$ are the nodal forces vectors at position \bar{X} referred to the X-coordinate system.

$\{F\}$ is the body force vector at position X measured per unit length of the X-coordinate system.

$\{F + \Delta F\}$ is the body force vector at position \bar{X} referred to and measured per unit length of the X-coordinate system.

$\{S\}$ are the internal forces at position X referred to and measured per unit length of the X-coordinate system.

$\{S + \Delta S\}$ are the internal forces at position \bar{X} measured per unit length of the X-coordinate system.

$\{\Delta v\}$ is the increase in the internal displacements from position X to position \bar{X} referred to the X-coordinate system. $\{\Delta v\}$ can be obtained in terms of the component of the position vector $\{\Delta r\}$ in the following way

$$\{\Delta v\} = \begin{Bmatrix} \Delta \epsilon_m \\ \Delta \kappa \end{Bmatrix}$$

But $\Delta \epsilon_m$ and $\Delta \kappa$ can be expressed in terms of Δv and Δu as follows

$$\Delta \epsilon = \frac{\partial \Delta u}{\partial x} + \frac{1}{2} \left(\frac{\partial \Delta u}{\partial x} \right)^2 + \frac{1}{2} \left(\frac{\partial \Delta w}{\partial x} \right)^2$$

and (4.2.21)

$$\Delta \kappa = \frac{\partial^2 \Delta w}{\partial x^2}$$

Equation (4.2.21) can be considered as generalized strain displacement relation. The first part of equation (4.2.21) is the well known Lagrangian strain. Therefore $\{\Delta v\}$ can be considered as having two components; a linear one, $\{\Delta v\}_L$, and a nonlinear one, $\{\Delta v\}_{NL}$

$$\{\Delta v\}_L = \begin{Bmatrix} \frac{\partial \Delta u}{\partial x} \\ \frac{\partial^2 \Delta w}{\partial x^2} \end{Bmatrix} \quad (4.2.22)$$

$$\{\Delta v\}_{NL} = \begin{bmatrix} \frac{1}{2} \left(\frac{\partial \Delta u}{\partial x} \right)^2 + \frac{1}{2} \left(\frac{\partial \Delta w}{\partial x} \right)^2 \\ 0 \end{bmatrix}$$

then

$$\{\Delta v\} = \{\Delta v\}_L + \{\Delta v\}_{NL} \quad (4.2.23)$$

From the above definitions we are able to write an expression for the virtual work at positions X and \bar{X} . Since all forces at X are in equilibrium, we give the system a virtual displacement $\delta\{\Delta r\}$ during which the work done by the external forces will be equal to the work done by the internal forces.

That is

$$\delta \begin{Bmatrix} \Delta r^i \\ \Delta r^j \end{Bmatrix}^T \begin{Bmatrix} R^i \\ R^j \end{Bmatrix} + \int_0^L \delta\{\Delta r\}^T \{F\} dx = \int_0^L \delta\{\Delta v_{NL}\}^T \{S\} dx \quad (4.2.24)$$

L : is the length of the element (I) in position X .

The expression of virtual work at position \bar{X} is obtained by giving the system again a virtual displacement $\delta\{\Delta r\}$ and setting the external work done equal to the internal work done, or:

$$\begin{aligned} \delta \begin{Bmatrix} \Delta r^i \\ \Delta r^j \end{Bmatrix}^T \begin{Bmatrix} \Delta R^i + R^i \\ \Delta R^j + R^j \end{Bmatrix} + \int_0^L \delta\{\Delta r\}^T \{F + \Delta F\} dx \\ = \int_0^L \delta\{\Delta v\}^T \{S + \Delta S\} dx \end{aligned} \quad (4.2.25)$$

Now, subtracting equation (4.2.24) from equation (4.2.25) we get the incremental virtual work relation

$$\begin{aligned} \delta \begin{Bmatrix} \Delta r^i \\ \Delta r^j \end{Bmatrix}^T \begin{Bmatrix} \Delta R^i \\ \Delta R^j \end{Bmatrix} + \int_0^L \delta\{\Delta r\}^T \{\Delta F\} dx \\ = \int_0^L \delta\{\Delta v_{NL}\}^T \{S\} dx + \int_0^L \delta\{\Delta v\}^T \{\Delta S\} dx \end{aligned} \quad (4.2.26)$$

To develop the dynamic equilibrium equations we assume that the position vector $\{\Delta r\}$ could be expressed in terms of the incremental displacements vectors of the nodal points $\{\Delta r^i\}$ and $\{\Delta r^j\}$ in the following way

$$\{\Delta r\} = \begin{Bmatrix} \Delta w \\ \Delta \theta \\ \Delta u \end{Bmatrix} = \begin{bmatrix} \langle \phi w \rangle \\ \langle \phi' w \rangle \\ \langle \phi u \rangle \end{bmatrix} \begin{Bmatrix} \Delta r^i \\ \Delta r^j \end{Bmatrix} \quad (4.2.27)$$

where $\langle \phi w \rangle$ and $\langle \phi u \rangle$ are called interpolation functions. They are chosen in such a way as to insure compatibility between the adjacent elements, and they include the rigid body motion and uniform straining modes. For the purpose of our problem, they are chosen in the following way

$\langle \phi w \rangle$ is a third degree polynomial function which is obtained by releasing one at a time the degrees of freedom of a fixed end beam while keeping the others fixed.

$\langle \phi u \rangle$ is a linear function.

The forms of $\langle \phi w \rangle$ and $\langle \phi u \rangle$ are as follows

$$\langle \phi w \rangle^T = \begin{Bmatrix} \xi_1^2(3 - 2\xi_1) \\ \xi_1^2\xi_2L \\ 0 \\ \xi_2^2(3 - 2\xi_2) \\ -\xi_1\xi_2^2L \\ 0 \end{Bmatrix} \quad (4.2.28)$$

and

$$\langle \phi u \rangle^T = \begin{Bmatrix} 0 \\ 0 \\ \xi_1 \\ 0 \\ 0 \\ \xi_2 \end{Bmatrix} \quad \begin{array}{l} (4.2.28) \\ (\text{cont.}) \end{array}$$

where $\xi_1 = 1 - \frac{x}{L}$, $\xi_2 = \frac{x}{L}$.

After establishing the interpolation functions we can proceed to express the incremental internal displacement $\{\Delta v\}$ in terms of the nodal displacements vectors in the following way

Substituting (4.2.27) in (4.2.22) and taking the variation of the results will give

$$\delta\{\Delta v_L\} = \delta \begin{bmatrix} \langle \phi 'u \rangle \\ \langle \phi ''w \rangle \end{bmatrix} \delta \begin{Bmatrix} \Delta r^i \\ \Delta r^j \end{Bmatrix}$$

and

(4.2.29)

$$\delta\{\Delta v_{NL}\} = \begin{Bmatrix} \Delta r^i \\ \Delta r^j \end{Bmatrix}^T \begin{bmatrix} \langle \phi 'u \rangle^T \langle \phi 'u \rangle + \langle \phi 'w \rangle^T \langle \phi 'w \rangle \\ \underline{0} \end{bmatrix} \delta \begin{Bmatrix} \Delta r^i \\ \Delta r^j \end{Bmatrix}$$

Now, substituting the incremental constitutive equation (4.2.18) and (4.2.29) into (4.2.26), after some operations we get

$$\begin{aligned}
\begin{Bmatrix} \Delta R^i \\ \Delta R^j \end{Bmatrix} + \int_0^L \begin{bmatrix} \langle \phi w \rangle \\ \langle \phi' w \rangle \\ \langle \phi u \rangle \end{bmatrix}^T \{\Delta F\} dx = & \left(\int_0^L [\langle \phi' u \rangle^T \langle \phi' u \rangle \right. \\
& \left. + \langle \phi' w \rangle \langle \phi' w \rangle] (N - \Delta N') dx \right) \begin{Bmatrix} \Delta r^i \\ \Delta r^j \end{Bmatrix} \\
& + \left(\int_0^L \begin{bmatrix} \langle \phi' u \rangle \\ \langle \phi'' w \rangle \end{bmatrix}^T [k] \begin{bmatrix} \langle \phi' u \rangle \\ \langle \phi'' w \rangle \end{bmatrix} dx \right) \begin{Bmatrix} \Delta r^i \\ \Delta r^j \end{Bmatrix} \\
& - \int_0^L \begin{bmatrix} \langle \phi' u \rangle \\ \langle \phi'' w \rangle \end{bmatrix}^T \{\Delta S'\} dx + O(\Delta r)^2
\end{aligned} \tag{4.2.30}$$

All higher order terms in (4.2.30) were dropped because they are small in comparison to the remaining terms.

The only term which still has to be defined in (4.2.30) is the inertia term. Applying D'Alembert's principle, the increment inertia force vector $\{\Delta F\}$ is given by

$$\{\Delta F\} = - \rho [Q^T]^{-1} \begin{bmatrix} A & & \\ & I & \\ & & A \end{bmatrix} \begin{Bmatrix} \Delta \ddot{w}_0 \\ \Delta \ddot{\theta}_0 \\ \Delta \ddot{u}_0 \end{Bmatrix} \tag{4.2.31}$$

ρ : is the mass per unit volume at position X.

As for the position vector $\{\Delta r\}$, the inertia vector $\{\Delta \ddot{r}_0\}$ may be

expressed in terms of the nodal inertia vectors $\{\Delta\ddot{r}_0^i\}$ and $\{\Delta\ddot{r}_0^j\}$ using the same interpolation functions, or

$$\{\Delta F\} = -\rho [Q^T]^{-1} \begin{bmatrix} A & & \\ & I & \\ & & A \end{bmatrix} [Q^T] \begin{bmatrix} \langle \phi w \rangle \\ \langle \phi' w \rangle \\ \langle \phi u \rangle \end{bmatrix} \begin{bmatrix} Q & 0 \\ 0 & Q \end{bmatrix} \begin{Bmatrix} \Delta\ddot{r}_0^i \\ \Delta\ddot{r}_0^j \end{Bmatrix} \quad (4.2.32)$$

or

$$\{\Delta F\} = -\rho \begin{bmatrix} A & & \\ & I & \\ & & A \end{bmatrix} \begin{bmatrix} \langle \phi w \rangle \\ \langle \phi' w \rangle \\ \langle \phi u \rangle \end{bmatrix} \begin{bmatrix} Q & 0 \\ 0 & Q \end{bmatrix} \begin{Bmatrix} \Delta\ddot{r}_0^i \\ \Delta\ddot{r}_0^j \end{Bmatrix} \quad (4.2.33)$$

Equation (4.2.30) is expressed in the coordinate system X. However, in order to be able to assemble all the elements together, later, the dynamic equilibrium equations of each element should be referred to a global coordinate system X_0 . Carrying out a coordinate transformation on (4.2.30) and substituting (4.2.33) in (4.2.30) will give

$$\begin{Bmatrix} \Delta R_0^i \\ \Delta R_0^j \end{Bmatrix} = [M] \begin{Bmatrix} \Delta\ddot{r}_0^i \\ \Delta\ddot{r}_0^j \end{Bmatrix} + [K] \begin{Bmatrix} \Delta r_0^i \\ \Delta r_0^j \end{Bmatrix} - \begin{Bmatrix} \Delta R_0'^i \\ \Delta R_0'^j \end{Bmatrix} \quad (4.2.34)$$

Equation (4.2.34) is the incremental dynamic equilibrium equation of element (I) referred to the global coordinate system X_0 . The terms which appear in this equation are defined as follows

1. The applied loads

$$\begin{Bmatrix} \Delta R_O^i \\ \Delta R_O^j \end{Bmatrix}$$

which are the incremental nodal forces.

2. The mass matrix [M]

$$[M] = \begin{bmatrix} Q^T & 0 \\ 0 & Q^T \end{bmatrix} \left(\int_0^L \begin{bmatrix} \langle \phi_w \rangle \\ \langle \phi'_w \rangle \\ \langle \phi_u \rangle \end{bmatrix}^T \rho \begin{bmatrix} A & & \\ & I & \\ & & A \end{bmatrix} \begin{bmatrix} \langle \phi_w \rangle \\ \langle \phi'_w \rangle \\ \langle \phi_u \rangle \end{bmatrix} dx \right) \begin{bmatrix} Q & 0 \\ 0 & Q \end{bmatrix} \quad (4.2.35)$$

This mass matrix is called the consistent mass matrix. It includes the effect of the rotational inertia of the cross section as well as its mass. It could be substituted by a lumped mass matrix, where the mass of the element is assumed to be concentrated at the nodal points. It could also be replaced by a diagonal matrix, obtained by diagonalizing the consistent mass matrix itself. Both approaches have been used extensively in many problems. They offer great simplicity. However, for the purpose of this study the original consistent mass will be used to be able to include directly the rotational inertia.

3. The element global stiffness matrix [K]

$$[K] = \begin{bmatrix} Q^T & 0 \\ 0 & Q^T \end{bmatrix} [[K1] + [K2]] \begin{bmatrix} Q & 0 \\ 0 & Q \end{bmatrix} \quad (4.2.36)$$

where $[K1]$ is the elastic viscoplastic element stiffness matrix and $[K2]$ is the geometric stiffness matrix.

Both of these matrices are referred to the local coordinate system, and they are as follows

$$[K1] = \int_0^L \begin{bmatrix} \langle \phi' u \rangle \\ \langle \phi'' w \rangle \end{bmatrix}^T [K] \begin{bmatrix} \langle \phi' u \rangle \\ \langle \phi'' w \rangle \end{bmatrix} dx \quad (4.2.37)$$

$$[K2] = \int_0^L [\langle \phi' u \rangle^T \langle \phi' u \rangle + \langle \phi'' w \rangle^T \langle \phi'' w \rangle] (N - \Delta N') dx$$

The stiffness matrix $[K1]$ is the usual elastic stiffness if the stresses anywhere in the element were less than the static yield stress. But if the stress in some points of the element exceeds the static yield stress, this will have an effect on $[K1]$ and it will be reduced.

The stiffness matrix $[K2]$ is due mainly to the change in geometry of the element between position X and position \bar{X} . It is of a second order in comparison to $[K1]$.

4. The viscoplastic loads

$$\begin{Bmatrix} \Delta R_O^i \\ \Delta R_O^j \end{Bmatrix} = \begin{bmatrix} Q^T & 0 \\ 0 & Q^T \end{bmatrix} \int_0^L \begin{bmatrix} \langle \phi' u \rangle \\ \langle \phi'' w \rangle \end{bmatrix}^T \{\Delta S'\} dx \quad (4.2.32)$$

These viscoplastic loads will be equal to zero if the stresses everywhere in the element were below the static yield stress. They are due to the viscoplastic character of the material which is clear in the constitutive equation (4.2.10). They came from the coefficient ($\Delta\sigma'$) in the constitutive equation, which is defined in equation (4.2.11). They amount to adding an extra load in the nodal points of the element.

The procedures for the solution of the beam problem:

In order to be able to solve the problem of impact on a beam, some preliminary details are needed. First, the beam will be divided into a number of elements, with the number depending on the particular problem. The geometry of each element is defined with respect to a global system of coordinates. Each individual element will have a certain length L , will be straight, and will have a uniform rectangular cross section. The length, the cross section, and the orientation of the element could be different from one element to the other. The material properties of each element have to be specified. The boundary condition at each nodal point has to be specified also, as for example, a fixed boundary or a free boundary has to be specified.

The loads which are applied to the beam impulsively have to be specified as increments of loads over a short period of time, which is the duration of the impulse. The loads will be applied only at the nodal points. They could be either vertical, horizontal or bending forces. At the end of the impulse time the applied loads will be zero. Also the point at which we want to terminate the solution to the problem has to be specified, and the total number of time increments needed to do so should be specified. Concentrated masses and their moments of

inertia may be added at the nodal points, and they have to be specified. Once all the above is done, it is possible then to proceed with the actual solution of the problem.

Using a direct stiffness approach, the incremental dynamic equilibrium equations are assembled in the following way

$$\{\Delta R\}_B = [M]_B \{\Delta \ddot{r}\}_B + [K]_B \{\Delta r\}_B - \{\Delta R'\}_B \quad (4.2.39)$$

where:

$[M]_B$: is the mass matrix of the whole beam

$[K]_B$: is the stiffness matrix of the whole beam

$\{\Delta R\}_B$: is the incremental applied load vector for all the nodal points

$\{\Delta \ddot{r}\}_B$: is the incremental acceleration vector for all the nodal points

$\{\Delta r\}_B$: is the incremental displacement vector for all the nodal points

$\{\Delta R'\}$: is the viscoplastic load vector for all the nodal points.

In order to solve equation (4.2.39), the incremental acceleration vector $\{\Delta \ddot{r}\}_B$ has to be expressed in terms of the incremental displacement vector $\{\Delta r\}_B$. The approximate procedure used for that is as follows.

The vector $\{r(t + \Delta t)\}_B$, which is the total displacement vector, is expanded into a Taylor expansion, giving

$$\{r(t + \Delta t)\}_B = \{r(t)\}_B + \{\dot{r}(t)\}_B \Delta t + \{\ddot{r}(t)\}_B \frac{\Delta t^2}{2} + \{\dddot{r}(t)\}_B \frac{\Delta t^3}{6} + \dots \quad (4.2.40)$$

Assuming that the expansion is terminated after Δt^3 and substituting the following, for the rate of acceleration vector $\{\ddot{\mathbf{r}}(t)\}_B$,

$$\{\ddot{\mathbf{r}}(t)\}_B = \frac{\{\Delta\ddot{\mathbf{r}}\}_B}{\Delta t}$$

into (4.2.40) gives

$$\{\Delta\ddot{\mathbf{r}}\}_B = \frac{6}{\Delta t^2} \{\Delta\mathbf{r}\}_B - \frac{6}{\Delta t} \{\dot{\mathbf{r}}(t)\}_B - 3\{\ddot{\mathbf{r}}(t)\}_B \quad (4.2.41)$$

giving the incremental acceleration vector in terms of the incremental displacement vector and the velocity and acceleration vector at the beginning of the time increment. The velocity and acceleration vectors at the end of the time increment are easily obtained in terms of the incremental displacement vector $\{\Delta\mathbf{r}\}_B$.

$$\{\dot{\mathbf{r}}(t + \Delta t)\}_B = \frac{3}{\Delta t} \{\Delta\mathbf{r}\}_B - 2\{\dot{\mathbf{r}}(t)\}_B - .5\{\ddot{\mathbf{r}}(t)\}_B \Delta t \quad (4.2.42)$$

and

$$\{\ddot{\mathbf{r}}(t + \Delta t)\}_B = \frac{6}{\Delta t^2} \{\Delta\mathbf{r}\}_B - \frac{6}{\Delta t} \{\dot{\mathbf{r}}(t)\}_B - 3\{\ddot{\mathbf{r}}(t)\}_B \quad (4.2.43)$$

The above approximate procedure is equivalent to assuming the acceleration vector to be linear over the time increment Δt . This procedure could be improved by using an iteration scheme within each increment similar to the one which was suggested for the constitutive equation (4.2.10).

Substituting equation (4.2.41) into (4.2.39) gives the following

$$\begin{aligned} \{\Delta R\}_B + \{\Delta R'\}_B + \frac{6}{\Delta t^2} [M]_B \{\dot{r}(t)\}_B + 3[M]_B \{\ddot{r}(t)\}_B \\ = [K]_B \{\Delta r\}_B + \frac{6}{\Delta t^2} [M]_B \{\Delta r\}_B \end{aligned}$$

or

$$\{\Delta R^*\}_B = [K^*]_B \{\Delta r\}_B \quad (4.2.44)$$

where $\{\Delta R^*\}_B$, $[K^*]_B$ is defined as follows

$$\{\Delta R^*\}_B = \{\Delta R\}_B + \{\Delta R'\}_B + \frac{6}{\Delta t} [M]_B \{\dot{r}(t)\}_B + 3[M]_B \{\ddot{r}(t)\}_B \quad (4.2.45)$$

and

$$[K^*]_B = [K]_B + \frac{6}{\Delta t^2} [M]_B$$

Now equation (4.2.44) is transformed into a system of a linear simultaneous algebraic equation which could be solved using any of the many schemes available for that purpose.

Once equation (4.2.44) is solved, a back substitution procedure is carried out until the incremental increase in stresses, strains, axial force, etc. are determined. An iteration procedure within each time increment could be carried out to improve the accuracy of the solution and its convergence once the values of all the unknowns of the problem are determined at the end of the time increment. The same procedure is repeated for the new increment with the new values obtained at the end of the previous increment taken as initial values for the new increment. However, before it is possible to do so, some of the variables of the

problem should be referred to the new local coordinate system obtained at the end of the previous increment. A new length, a new orientation, and a new mass per unit length of the element should be used in developing the incremental dynamic equilibrium equations. Also, the internal forces $\{S + \Delta S\}$ obtained at the end of the time increment should be measured per unit length of the new position.

A computer program was developed using the procedure presented here and was used to solve some numerical examples.

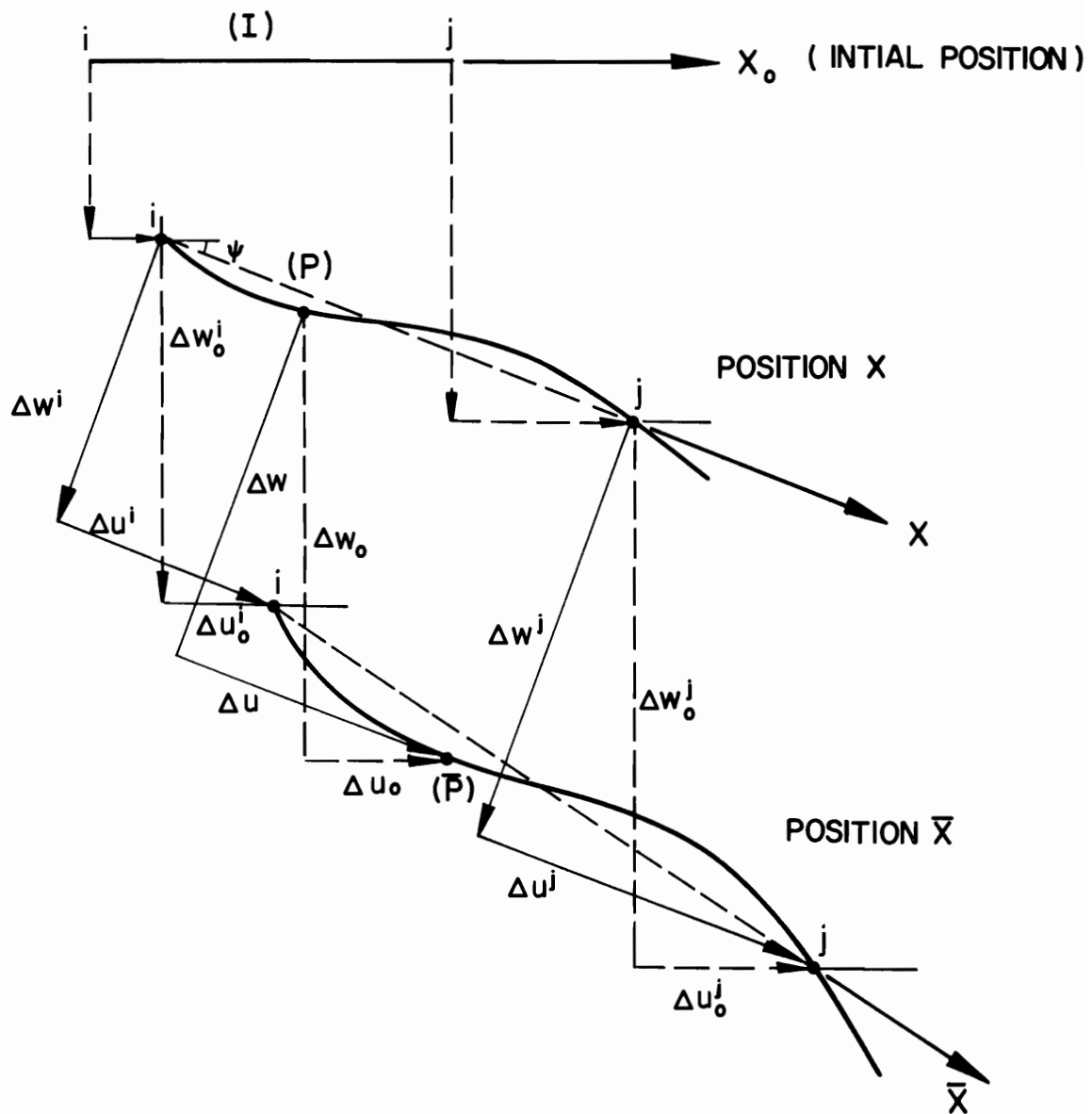


FIG. 4.2.1 INCREMENTAL DISPLACEMENT OF A BEAM ELEMENT

4.3 Numerical Examples of Impulsive Loading Problems in Elastic Visco-plastic Beams

In order to evaluate the method of solution which was developed in this chapter, some numerical examples have been treated. Two of these examples are chosen from a paper by Bodner and Symonds [4.1]. In the paper the authors presented the results of impulsive loading tests which were conducted on cantilever beams with varying tip mass. The third example is one of a cantilever without a tip mass, the purpose of which is to investigate the solution in the absence of a tip mass and show its stability.

The constitutive equation which will be used for the numerical examples is one modified from that used by Bodner and Symonds [4.1] for mild steel

$$E\dot{\epsilon} = \dot{\sigma} + 40 \cdot E \left(\frac{\sigma}{\sigma_0} \pm 1 \right)^5 \quad (4.3.1)$$

Example (1): A cantilever beam with a tip mass, figure 4.3.1

Length of beam	$L = 14.0''$
Height of beam	$H = .177''$
Width of beam	$B = .644''$
Modulus of Elasticity	$E = 30 \times 10^6 \text{ lb./in.}^2$
Yield Stress	$\sigma_0 = 29,000 \text{ lb./in.}^2$
Mass/unit volume	$\rho_0 = .000736 \text{ lb. sec.}^2/\text{in.}^4$
Tip mass	$= .00381 \text{ lb. sec.}^2/\text{in.}$
Impulse at tip	$= .975 \text{ lb. sec.}$
Duration of impulse	$= .001 \text{ sec.}$

Number of increments during the impulse period = 10

The time increment Δt for the rest of the solution = .001 sec.

The beam was divided into 14 elements. Each element has a length of 1".

Final configuration of the beam corresponding to zero velocity of the tip is shown in figure 4.3.2. A plot of the displacements of the tip are shown in figure 4.3.3.

Example (2): A cantilever beam with a tip mass, figure 4.3.1

Length of beam $L = 4.34"$

Height of beam $H = .053"$

Width of beam $B = .312"$

Modulus of elasticity $E = 30 \times 10^6 \text{ lb./in.}^2$

Yield stress $\sigma_0 = 44,000 \text{ lb./in.}^2$

Mass/unit volume $\rho_0 = .000736 \text{ lb./in.}^3$

Tip mass = .000030 lb./in.

Impulse at the tip = .031 lb. sec.

Duration of the impulse = .0001 sec.

Number of increments during the impulse time = 10

The time increment Δt for the rest of the solution = .0002475 sec.

The beam was divided into 10 elements. Each has a length of .434".

Final configuration is shown in figure 4.3.4. The displacements of the tip mass are shown in figure 4.3.5.

Example (3): A cantilever beam without a tip mass, figure 4.3.1.

Length of beam	$L = 14.0''$
Height of beam	$H = .177''$
Width of beam	$B = .644''$
Modulus of elasticity	$E = 30 \times 10^6 \text{ lb./in.}^2$
Yield stress	$\sigma_0 = 29,000 \text{ lb.in.}^2$
Mass/unit volume	$\rho_0 = .000736 \text{ lb./sec.}^2/\text{in.}^4$
Impulse at the tip	$= .075 \text{ lb. sec}$
Duration of impulse	$= .001 \text{ sec.}$
Number of increments during the impulse time	$= 10$
The time increment for the rest of the solution	$= .0001 \text{ sec.}$

The beam was divided into 14 elements each, with a length of 1".

Final configuration is shown in figure 4.3.6. The displacements of the free end are shown in figures 4.3.7.

Discussion of the results:

Comparing the results obtained here for example (1) and (2) with those obtained by Bodner and Symonds [4.1], shows a good agreement between the theory and their experiments. The damage angle which is predicted here is very close to what the experiments showed.

In example (1) the ratio of the tip mass to the beam mass was (3.33), while in example (2), the ratio was (.56) and for example (3) there was no tip mass. This covers a wide range of tip mass to beam mass ratios, and all the solutions obtained were stable. The beam with the large tip mass behaved mainly like a rigid body with a very slight change in curvature across the beam except near the base, where there

was a major change in curvature. In case of example (3), some change in curvature was noticed all over the beam and even near the tip. This is due mainly to the absence of a tip mass which tends to dominate and affect the configuration of the beam considerably. In all the three examples the vertical velocity of the tip was increased during the impulse time and reached its peak at the end of the impulse time, and started to decrease until it reached zero. A similar behavior was noticed for the horizontal velocity except that it reached its maximum value somewhat later than the vertical velocity.

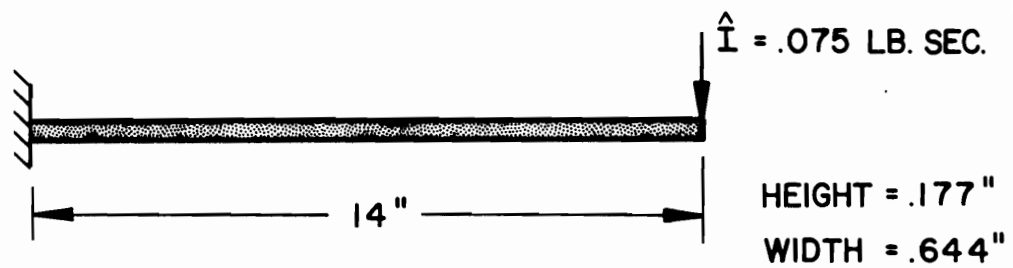
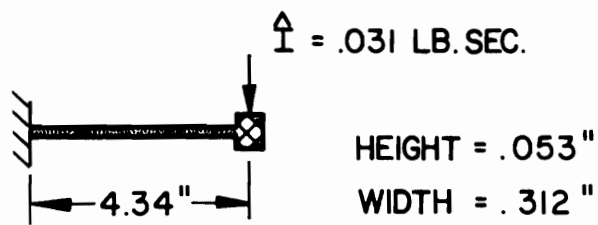
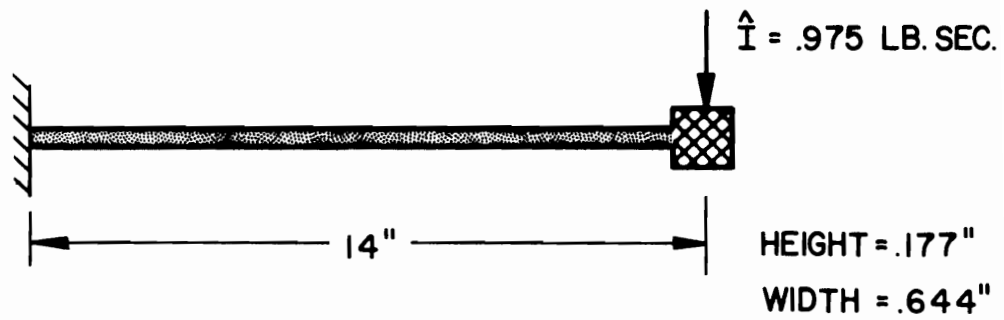
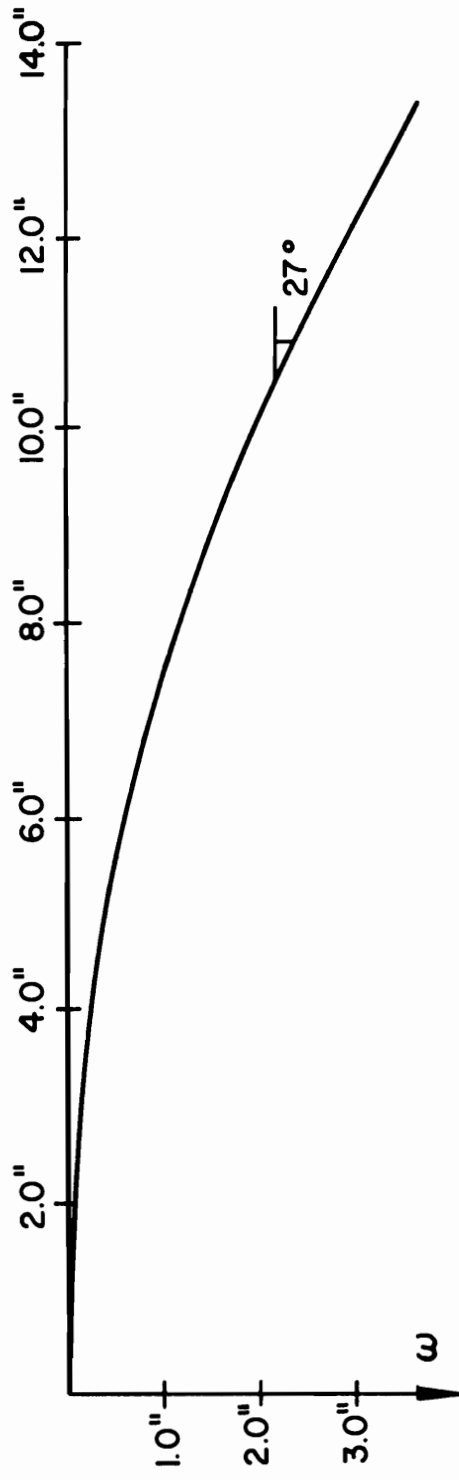


FIG. 4-3-1 CANTILEVER BEAMS GEOMETRY



EXPERIMENTAL DAMAGE = 24°
 ANGLE (4.1)

FIG. 4·3·2 FINAL CONFIGURATION OF EXAMPLE (I)

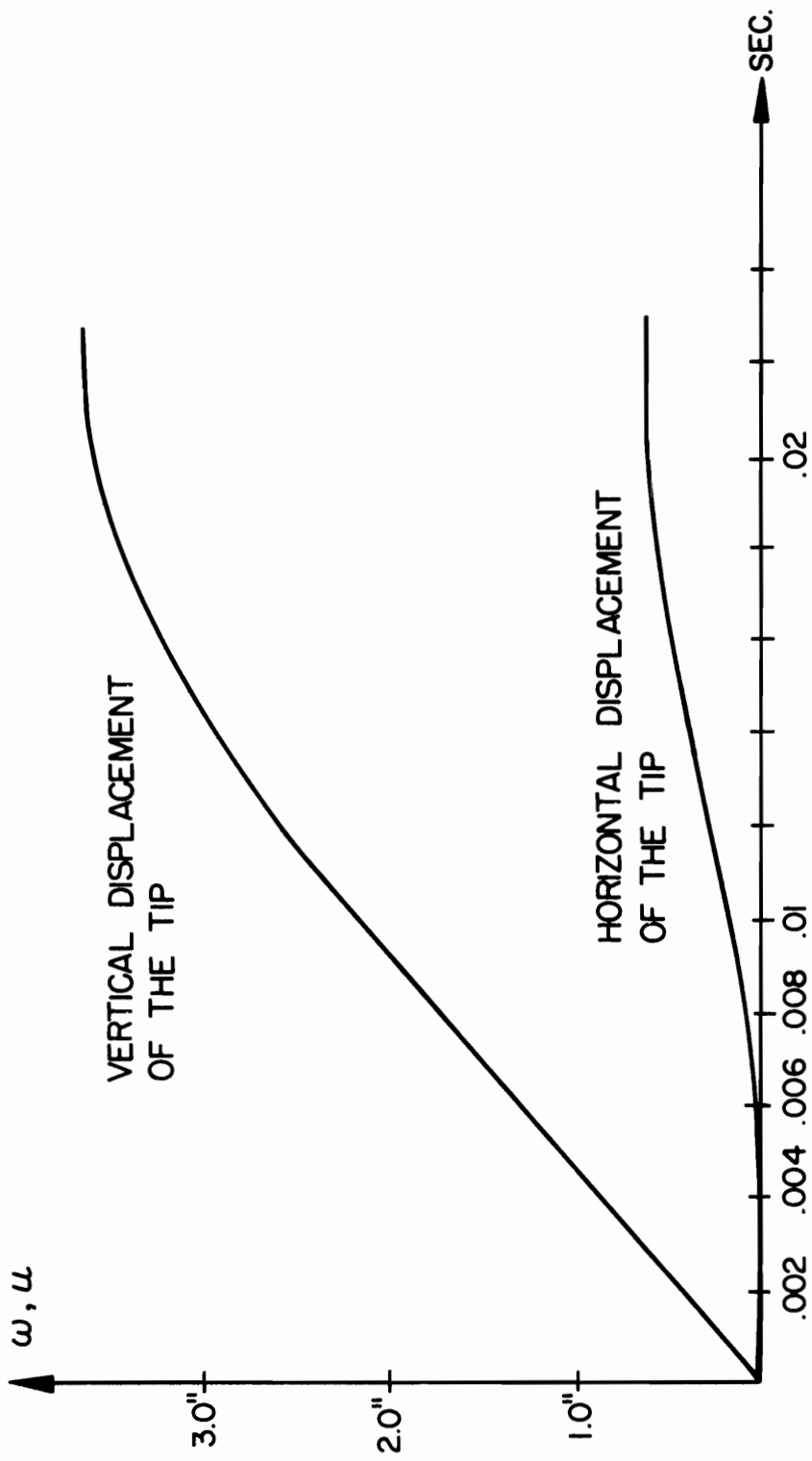


FIG. 4 · 3 · 3 DISPLACEMENT OF THE TIP, EXAMPLE (1)

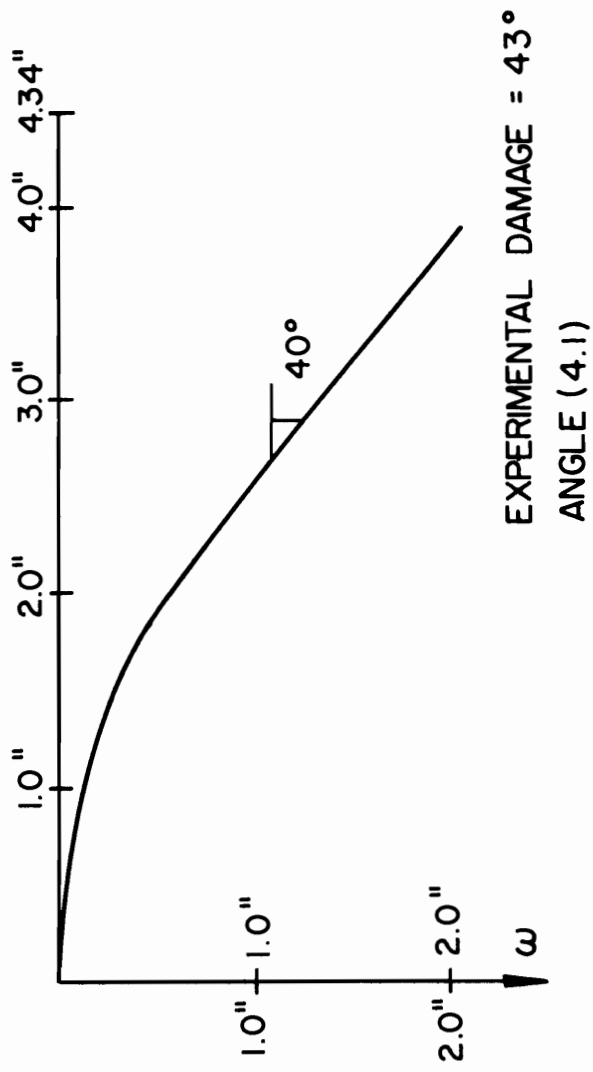


FIG. 4·3·4 FINAL CONFIGURATION OF EXAMPLE (2)

- (2.18) J. J. Gilman, *J. Applied Physics*, Vol. 36, 3195, (1965).
- (2.19) W. G. Johnston, *J. Applied Physics*, Vol. 3B, 2716, (1962).
- (2.20) P. Perzyna, *Quart. Appl. Math.*, Vol. 20, 321, (1963).
- (2.21) N. Cristescu, *Dynamic Plasticity*, North-Holland, Amsterdam, (1967).
- (2.22) J. W. Craggs, *Inter. J. Eng. Science*, Vol. 3, 21-26, (1965).
- (2.23) B. Hopkinson, *Proc. Roy. Soc., London*, Vol. 74, 498, (1904).
- (2.24) D. S. Clark and D. S. Wood, *Procs, ASTM*, Vol. 50, 717, (1949).
- (2.25) J. D. Campbell and K. J. Marsh, *Phil. Mag.* Vol. 7, 933, (1962).
- (2.26) J. M. Krafft and A. M. Sullivan, *Trans. Amer. Soc. Metals*, Vol. 51, 643, (1952).

References for Section 3.

- (3.1) J. M. Kelly, *Int. J. Sol. St.*, Vol. 3, 191, 1967.
- (3.2) E. H. Lee and P. S. Symonds, "Large Plastic Deformations of Beams under Transverse Impact," *J. Appl. Mech.*, Vol. 19, p. 308, (1952).
- (3.3) P. S. Symonds, "Large Plastic Deformations of Beams under Blast Type Loading," *Procs, Second U.S. National Congress of Applied Mechanics*, Ann Arbor, Michigan, p. 505, (1956).
- (3.4) M. G. Salvadori and F. DiMaggio, "On the Development of Plastic Hinges in Rigid-Plastic Beams," *Quart. Appl. Math.*, Vol. 11, p. 223, (1953).
- (3.5) J. A. Seiler and P. S. Symonds, "Plastic Deformation in Beams under Distributed Dynamic Loads," *J. Appl. Phys.*, Vol. 25, p. 556, (1954).
- (3.6) H. G. Hopkins, "On the Behavior of Infinitely Long Rigid-Plastic Beams under Transverse Concentrated Load," *J. Mech. Phys. Solids*, Vol. 4, p. 38, (1955).
- (3.7) M. F. Controy, "The Plastic Deformation of Built-in Beams due to Distributed Dynamic Loading," *J. Appl. Mech.*, Vol. 31, p. 507, (1964).
- (3.8) S. R. Bodner and P. S. Symonds, "Experimental and Theoretical Investigation of the Plastic Deformation of Cantilever Beams Subjected to Impulsive Loadings," *J. Appl. Mech.*, Vol. 29, p. 719, (1962).

- (3.9) P. S. Symonds, "Survey of Methods of Analysis for Plastic Deformation of Structures under Dynamic Loading," Brown University, BU/NSRDC/1-67, (1967).
- (3.10) J. M. Kelly, "Vehicle-barrier impact by rigid-plastic analysis submitted to Procs. ASCE (1968).
- (3.11) W. Goldsmith, IMPACT, Arnold, London, (1960).
- (3.12) P. S. Symonds, "Survey of methods of analysis for plastic deformation of structures under dynamic loading," Brown University, BU/NSRDC/1-67, (1967).
- (3.13) T. Y. Thomas, "The general theory of compatibility conditions," Int. J. Engng. Sci., Vol. 4, 207-233, (1966).
- (3.14) G. Eason and R. T. Shield, "Dynamic loading of rigid plastic cylindrical shells," J. Mech. Phys. Solids, Vol. 4, 56-71, (1956).
- (3.15) P. S. Symonds and T. J. Mantel, "Impulsive Loading of Plastic Beams with Axial Constraints," J. of Mech. and Phys. of Solids, Vol. 6 (1958).
- (3.16) W. Prager, "The General Theory of Limit Design," Proceedings of 8th International Congress of Applied Mechanics. Vol. 2 Istanbul, Turkey, (1952).
- (3.17) D. C. Drucker, "The Effect of Shear on the Plastic Bending of Beams," JAM Vol. 23, No. 4, Trans. ASME Vol. 78, (1956).
- (3.18) P. S. Symonds, "Survey of Methods of Analysis for Plastic Deformation of Structures under Dynamic Loadings," Brown University Report, BU/NSRDC/1-67.
- (3.19) T. Nonaka and P. S. Symonds, "Effects of Shear on a Rigid Plastic Beam under Blast-Type Loading," Brown University Report, NSF GK 1013.
- (3.20) B. G. Neal, "The Effect of Shear and Normal Forces on the Fully Plastic Moment of a Beam of Rectangular Cross Section," JAM Vol. 28, No. 2, Trans. ASME Vol. 83 Series E, (1961).
- (3.21) T. Nonaka, "Some Interaction Effects in a Problem of Plastic Beam Dynamics," Part 3. Experimental Study, JAM Vol. 35, No. 4, Trans. ASME, Vol. 90, (1968)

References for Section 4.

- (4.1) S. R. Bodner and P. S. Symonds, "Experimental and Theoretical Investigation of the Plastic Deformations of Cantilever Beams Subjected to Impulsive Loading," J. Appl. Mech., Vol. 29, Trans., ASME, 82, Series E., pp. 719-728, 1962.